NASA/TM–1998–104606, Vol. 14

Technical Report Series on Global Modeling and Data Assimilation

Max J. Suarez, Editor

Volume 14

A Comparison of GEOS Assimilated Data with FIFE Observations

Michael G. Bosilovich and Siegfried D. Schubert

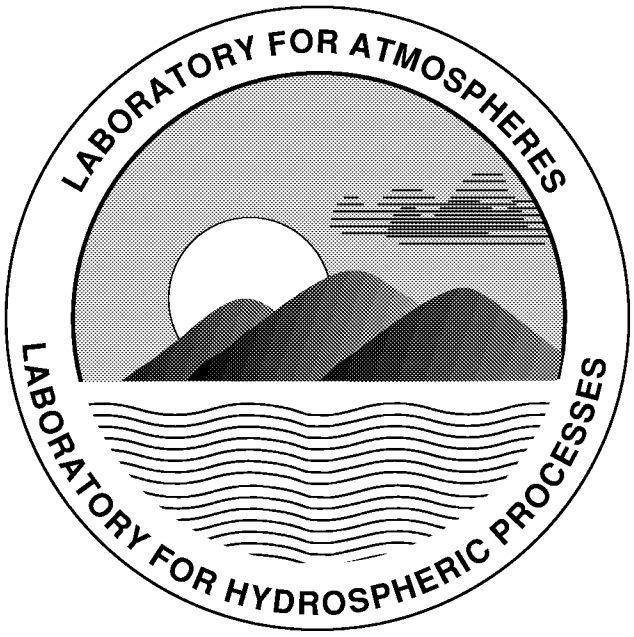

DATA ASSIMILATION OFFICE

August 1998

The NASA STI Program Office ... in Profile

Since its founding, NASA has been dedicated to the advancement of aeronautics and space science. The NASA Scientific and Technical Information (STI) Program Office plays a key part in helping NASA maintain this important role.

The NASA STI Program Office is operated by Langley Research Center, the lead center for NASA's scientific and technical information. The NASA STI Program Office provides access to the NASA STI Database, the largest collection of aeronautical and space science STI in the world. The Program Office is also NASA's institutional mechanism for disseminating the results of its research and development activities. These results are published by NASA in the NASA STI Report Series, which includes the following report types:

- TECHNICAL PUBLICATION. Reports of completed research or a major significant phase of research that present the results of NASA programs and include extensive data or theoretical analysis. Includes compilations of significant scientific and technical data and information deemed to be of continuing reference value. NASA's counterpart of peer-reviewed formal professional papers but has less stringent limitations on manuscript length and extent of graphic presentations.
- TECHNICAL MEMORANDUM. Scientific and technical findings that are preliminary or of specialized interest, e.g., quick release reports, working papers, and bibliographies that contain minimal annotation. Does not contain extensive analysis.
- CONTRACTOR REPORT. Scientific and technical findings by NASA-sponsored contractors and grantees.
- CONFERENCE PUBLICATION. Collected papers from scientific and technical conferences, symposia, seminars, or other meetings sponsored or cosponsored by NASA.
- SPECIAL PUBLICATION. Scientific, technical, or historical information from NASA programs, projects, and mission, often concerned with subjects having substantial public interest.
- TECHNICAL TRANSLATION. English-language translations of foreign scientific and technical material pertinent to NASA's mission.

Specialized services that complement the STI Program Office's diverse offerings include creating custom thesauri, building customized databases, organizing and publishing research results . . . even providing videos.

For more information about the NASA STI Program Office, see the following:

- Access the NASA STI Program Home Page at http://www.sti.nasa.gov/STI-homepage.html
- E-mail your question via the Internet to help@sti.nasa.gov
- Fax your question to the NASA Access Help Desk at (301) 621-0134
- Telephone the NASA Access Help Desk at (301) 621-0390
- Write to:
  NASA Access Help Desk
  NASA Center for AeroSpace Information
  7121 Standard Drive
  Hanover, MD 21076-1320

NASA/TM–1998–104606, Vol. 14

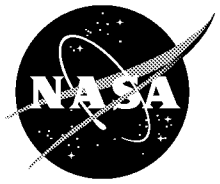

Technical Report Series on Global Modeling and Data Assimilation

Max J. Suarez, Editor
Goddard Space Flight Center, Greenbelt, Maryland

Volume 14

A Comparison of GEOS Assimilated Data with FIFE Observations

Michael G. Bosilovich, Universities Space Research Association, Greenbelt, Maryland; and
Siegfried D. Schubert, Goddard Space Flight Center, Greenbelt, Maryland

National Aeronautics and
Space Administration

Goddard Space Flight Center
Greenbelt, Maryland 20771

August 1998

Available from:

NASA Center for AeroSpace Information
7121 Standard Drive
Hanover, MD 21076-1320
Price Code: A17

National Technical Information Service
5285 Port Royal Road
Springfield, VA 22161
Price Code: A10

Abstract

First ISLSCP Field Experiment (FIFE) observations have been used to validate the near-surface properties of various versions of the Goddard Earth Observing System (GEOS) Data Assimilation System. The site-averaged FIFE data set extends from May 1987 through November 1989, allowing the investigation of several time scales, including the annual cycle, daily means and diurnal cycles. Furthermore, the development of the daytime convective planetary boundary layer is presented for several days. Monthly variations of the surface energy budget during the summer of 1988 demonstrate the affect of the prescribed surface soil wetness boundary conditions. GEOS data comes from the first frozen version of the assimilation system (GEOS-1 DAS) and two experimental versions of GEOS (v. 2.0 and 2.1) with substantially greater vertical resolution and other changes that influence the boundary layer.

Two issues must be carefully considered when interpreting the results of this study. First, the GCM grid space area is much larger than the FIFE site area. This could lead to differences in local boundary conditions, such as albedo, surface roughness and soil wetness that lead to differences between the assimilation data and observations. Secondly, the results may depend on the regional climate and may not apply to all regions of the globe.

Results indicate several potential systematic problems in the surface properties of GEOS. First, the surface layer specific humidity is generally too large, especially during the daytime. This occurs even in cases where the latent heat flux is slightly underestimated (eg. July 1988). This results in a lifted condensation level that is too low to the surface compared with observations. While the large latent heating in some cases contributes to the specific humidity bias, the PBL is likely not entraining enough dry free atmosphere.

The PBL and surface analysis has identified two factors that affect the development of the assimilated mixed layer. First, the surface sensible heat flux is consistently underestimated between 12 and 15 UTC. The lack of heat from the surface allows the stable surface layer to stay in place longer than observed. Second, the observed profiles indicate that the surface layer stability is too strong in the assimilation system or may include an elevated stable layer. The stable layer could be related to the slightly cooler surface temperatures, and too much net upward longwave radiation. As these factors are overcome by the diurnal heating of the surface, the GEOS 2.1 PBL can develop quickly, but too late in the diurnal period to catch up with observations.

This report provides a baseline for future versions of the GEOS data assimilation system that will incorporate a state-of-the-art land surface parameterization. Several suggestions are proposed to improve the generality of future comparisons. These include the use of more diverse field experiment observations and an estimate of gridpoint heterogeneity from the new land surface parameterization.

Contents

List of Figures

List of Tables

1 Introduction and Background

The surface of the Earth directly affects the weather and climate. Hence, improved representation of the surface boundary in atmospheric numerical models can positively affect the simulation (or assimilation) of the weather and climate.

Recent studies (eg. Betts et al. 1993, 1996 and 1998) have compared point field experiment data with global reanalysis data. These studies have shown strengths and weaknesses in the reanalysis systems and have contributed to the improvement of the surface physical parameterizations. Here, the output from several recent versions of the Goddard Earth Observing System (GEOS) Data Assimilation System (DAS) is validated against surface and Planetary Boundary Layer (PBL) observations from the First ISLSCP (International Satellite Land Surface Climatology Project) Field Experiment (FIFE, Sellers et al. 1988). This exercise represents an important step in the evolution of the GEOS DAS, and a benchmark for the incorporation of a detailed Land Surface Model (LSM, Koster and Suarez 1996).

Betts et al.(1993) used the FIFE observational data to validate the European Center for Medium-range Weather Forecasting (ECMWF) global atmospheric numerical model. Since then, both the ECMWF and National Centers for Environmental Prediction (NCEP) reanalyzed data were also compared to the FIFE observations (Betts et al. 1996, 1998). In this section, we describe the GEOS DAS and FIFE observations, summarize the results of the previous comparison studies, and outline the methodology of this comparison.

1.1 GEOS DAS

The GEOS-1 DAS has produced a multi-year global atmospheric data set for use in climate and weather studies (Schubert et al. 1993). The GEOS-1 General Circulation Model (GCM) is described by Takacs et al. (1994) and Molod et al. (1996). Pfaendtner et al. (1995) document the analysis system. While these data have proven valuable in many research projects, the system evolves to address new and different problems. An important component of the GEOS DAS evolution concerns the incorporation of detailed land surface processes. All the GEOS data presented in this note were generated with the same simplified land surface parameterization (Takacs et al. 1994 and Schubert et al. 1995) revisited below.

The surface temperature and soil wetness representations in the GEOS system are most important to this discussion. An energy balance determines the ground temperature of a bulk layer. The layer's heat capacity recognizes the diurnal oscillation and the influence of soil wetness (details in the DAO ATBD, 1996). A simple model specifies the monthly mean soil wetness offline. The model uses monthly mean observations of precipitation and temperature as input (Schemm et al. 1992). The advantage of this method is that the

specified soil wetness provides repeatable and fixed forcing (with respect to atmospheric interactions) at the surface, analogous to the use of specified sea surface temperatures. The modeled precipitation may be biased, but the bias does not feed back into the atmospheric system. The lack of interaction between the surface and atmosphere, however, introduces error into the hydrology budget, because the long term integration of evaporation no longer depends on the modeled precipitation.

The PBL and its diurnal oscillation interact with the surface. Helfand and Labraga (1988) discuss the details of the PBL turbulence parameterization. In short, the turbulence is modeled by a Mellor and Yamada level 2.5 closure. In addition to the standard prognostic variables, the turbulent kinetic energy (TKE) is also predicted. The vertical turbulent fluxes of momentum, moisture, and heat are diagnosed from mean vertical gradients and diffusion coefficients. Similarity theory provides the surface boundary values of the fluxes and diffusion coefficients. Roughness length also characterizes the surface. Sellers and Dorman (1989) data specify the annually varying surface roughness (see also, Molod et al. 1994 and Helfand and Schubert 1995). Additionally, the atmospheric surface layer parameterization includes a viscous sub-layer above the roughness elements.

GEOS 2.0 was developed as a baseline for GEOS-3 (the system to support EOS AM-1). Scientific improvements were implemented in GEOS 2.0 to correct some deficiencies in GEOS-1 (Schubert et al. 1996). GCM improvements included the tuning of cloud parameterizations, gravity wave drag, new surface albedo and higher vertical extent and resolution (through the stratosphere and roughly double the grid points in the PBL). See Table 1 for the PBL vertical levels. The OI analysis system (Bloom et al. 1996) was replaced by the physical-space statistical analysis system (PSAS) which allows the flexibility to incorporate non-state variables and eliminates the need for data selection (Cohn et al. 1998, DAO ATBD 1996).

The validation of GEOS 2.0 indicated a drastic increase of daytime precipitation during the summer, especially over the central United States. Several modifications to the GCM (in GEOS 2.1) have partially ameliorated this problem. First, a variable sub-cloud layer was added. The height of the sub-cloud layer is specified at one level below a critical level. The critical level is determined by the lowest level where turbulent kinetic energy (TKE) is 10% of the maximum TKE in the PBL. Secondly, a relative humidity criteria was implemented in the convective precipitation parameterization. The criteria permits convective adjustment only when the relative humidity exceeds 85%. In addition, some changes in the radiation parameterization were implemented. Shortwave radiation was invoked more frequently (every one hour instead of every three). Also, the longwave radiation was modified to incorporate the effects of surface temperature changes that occur between radiation time steps.

Table 1: Lowest 13 vertical sigma levels and the corresponding pressure of GEOS-1 DAS and GEOS 2.x, assuming a surface pressure in the FIFE regions of 963 mb.

	GEOS-1		GEOS 2.x	
Level	σ	p (mb)	σ	p (mb)
1	0.993935	957.22	0.998548	961.60
2	0.971300	935.64	0.994248	957.46
3	0.929925	896.21	0.987150	950.62
4	0.874137	843.05	0.977200	941.04
5	0.807833	779.86	0.964250	928.57
6	0.734480	709.95	0.948115	913.03
7	0.657114	636.23	0.928565	894.20
8	0.578389	561.20	0.905322	871.82
9	0.500500	486.97	0.878157	845.66
10	0.424750	414.78	0.846935	815.60
11	0.352000	345.45	0.811635	781.60
12	0.283750	280.41	0.772457	743.87
13	0.222750	222.28	0.729920	702.91

1.2 FIFE Observations

The main purpose of FIFE was to develop remote sensing algorithms of the land surface and PBL. To accomplish this task, the FIFE scientists made comprehensive observations of the surface properties, meteorology and energy balance. The resulting data set has helped develop detailed parameterizations of the surface processes, and, more recently, has validated the surface properties of data assimilation systems (Betts et al. 1996, 1998).

The FIFE data archived on CD-ROM is used in this study (Sellers et al. 1988, Strebel et al. 1994, and Betts and Ball 1998). The FIFE site is located in Manhattan, Kansas (approximately 39.05° N, 96.53° W). The surface in-situ observations consist of approximately 20 - 30 meteorological and energy flux stations. Some observations are available continuously from May 1987 through November 1989. The flux measurements, however, were taken only during summer. Intensive Field Campaigns (IFCs) are periods of more extensive of data collection. Four IFCs in 1987 encompassed various stages of vegetation growth (see Sellers et al. 1992 for details).

During IFCs, the PBL was observed with radiosonde balloons, but observation were restricted to mostly clear sky conditions during the daytime. Also, balloon launches were at

irregular time intervals. The current study uses radiosonde observations analyzed to 5 mb pressure levels (Strebel et al. 1994). The FIFE surface meteorological and energy observations have been site-averaged and quality checked by Betts and Ball (1998). These data include standard deviations of the site-average at each time period. Betts and Ball (1998) provide a detailed description of the data and the quality checking. The Appendix of the present report gives information on further processing of the data.

1.3 Methodology

While the GEOS GCM represents the atmosphere on a global $2° \times 2.5°$ grid, the FIFE site represents essentially a point measurement within the entire globe. The GEOS DAS data used in the comparison comes from a nearby grid point (38°N, 97.5°W). The present GCM grid does not include sub-grid scale surface heterogeneity, such as variations in the vegetation cover. Within the FIFE site, a variety of vegetation cover and topography exists. As Betts et al. (1993, 1996, 1998) point out, the goal of such a study is not to search for exact agreement between the model and observations, but to identify potential systematic biases in the DAS.

The standard deviation of the site-average is included in the analysis when available. These data are interpreted as a representation of FIFE site heterogeneity and the realistic range of values given the geographical region and prevailing synoptic weather. Hence, GEOS DAS data outside the bounds of the observed heterogeneity may indicate a model bias. To evaluate the choice of gridpoint, a brief comparison of the four closest model grid points will also be presented.

Two issues must be carefully considered when interpreting the results of this study. First, the GCM grid space area is much larger than the FIFE site area. This could lead to differences in local boundary conditions, such as albedo, surface roughness and soil wetness that lead to differences between the assimilation data and observations. Secondly, the results may depend on the regional climate and may not apply to all regions of the globe.

2 Results

The Betts and Ball (1998) site-averaged FIFE dataset report observations at 30 minute intervals (centered on 15 and 45 minutes past the hour). The data were processed to monthly means and 3 hour backward mean (see the Appendix) for comparison to GEOS standard output format. The Appendix describes the processed data in more detail.

All GEOS data are from assimilation experiments, as opposed to simulation experiments which implement only the GCM. This is a crucial point, because we will be comparing

observations to the GEOS gridpoint data. GEOS-1 refers to the first frozen GEOS DAS (Schubert et al. 1993). GEOS 2.0 was intended to be the baseline system for future development of the GEOS system that will support EOS. Validation of this system indicated several significant problems, and prompted a focused development effort (called the "reconciliation" experiment) to fix the most severe problems. The validated reconciliation system is identified by GEOS 2.1. At the time of this writing, GEOS 2.1 is the most recent validated system.

The present comparison covers various time scales. The seasonal cycle is examined in terms of monthly means for the FIFE period. Only the GEOS-1 seasonal cycle is compared to FIFE because assimilations with the more recent GEOS versions have, to date, been limited to no more than a season. The analysis focuses on FIFE's IFC2 for daily variations and mean diurnal cycle. Likewise, the diurnal evolution of the convective PBL is presented during IFC2. Lastly, monthly variations of the surface energy balance are examined during the summer of 1988 (chosen because the validation effort of GEOS 2.0 and 2.1 coincide here).

When available, the standard deviations of the FIFE site-average will be included. This can be interpreted as a representation of heterogeneity and the observed variability of the observations. This should provide a range of acceptable values for the GEOS comparison. Of course, the results presented for FIFE should not be applied generally across the globe. GEOS variability around the FIFE site (at the grid point level) will also be investigated.

2.1 Seasonal Cycle

While the GEOS-1 reanalysis encompasses the entire FIFE period, the experimental GEOS 2.0 and 2.1 systems reanalyzed only several months for special periods. Figure 1 compares monthly mean GEOS-1 surface variables for the entire period of FIFE (May 1987 - November 1989). The mean FIFE elevation (410 $\pm$ 29 m) was approximately 30 m lower than the GEOS-1 DAS grid point (439 m) during the summer of 1987. This causes the difference in surface pressure during 1987 and 1988. The mean altitude of FIFE sites increases in 1989 to 420 $\pm$ 28 m due to a lower number (and some shifting) of stations. Despite the mean difference of the model and observed surface pressure, the assimilation follows the observed time series quite well.

GEOS-1 2 meter (2 m) and 10 meter (10 m) winds were averaged together (linearly) to compare with the FIFE 5.4 meter wind speed (Fig. 1b). The GEOS wind speeds consistently underestimate the observed monthly mean. This may indicate surface roughness length that is biased high. The variability of the wind speed within the FIFE site is very large, but the GEOS winds still tend to be small.

The GEOS-1 temperature follows the observations reasonably well. The most notable dif-

ferences occur in winter, when the model is too cold (documented by Schubert et al. 1995), and a smaller bias in July 1988 when the model is too warm (Fig. 1c). A more substantial problem occurs in the surface layer specific humidity (Fig. 1d). Spring, Fall and especially Summer specific humidity are greatly overestimated (3 - 4 g kg^{-1}). The difference repeats regularly in each of the three years. The implications of this bias and its interaction with the PBL will be discussed in the following sections.

Figure 2a shows the general overestimation of net incoming shortwave radiation by GEOS. The GEOS-1 albedo varies annually (0.09 in July to 0.10 in January) for this grid point. The FIFE site albedo, determined by the incoming and reflected shortwave radiation (Fig. 2c, and Betts and Ball 1998), is approximately 0.18 during the summertime, and larger in the winter. In general, GEOS-1 overestimates net upward longwave radiation with the largest differences occurring in winter (Fig. 2b). Note that the April and May 1988 FIFE radiation observations have some bias (see the Appendix). The minimal representation of snow (snow occurs when the surface temperature is less than zero) in the GEOS-1 system may contribute to this overestimate, which likely affects the aforementioned surface temperature biases (Fig. 1c).

The GEOS precipitation shows some general inter-annual variations that parallel the observations (Fig. 2d). For example, the 1988 summer precipitation tends to be lower than the 1989 precipitation. The average GEOS precipitation for the entire period exceeds the FIFE observations by 0.43 mm day^{-1}. The monthly differences, however, can be near 3 mm day^{-1} for June and July 1987 and May 1989. In general, the spring and summer precipitation is overestimated, especially May, June, and July while fall precipitation is slightly underestimated (Fig. 3) compared to the FIFE site. The NOAA precipitation is almost always less than the GEOS for this time period.

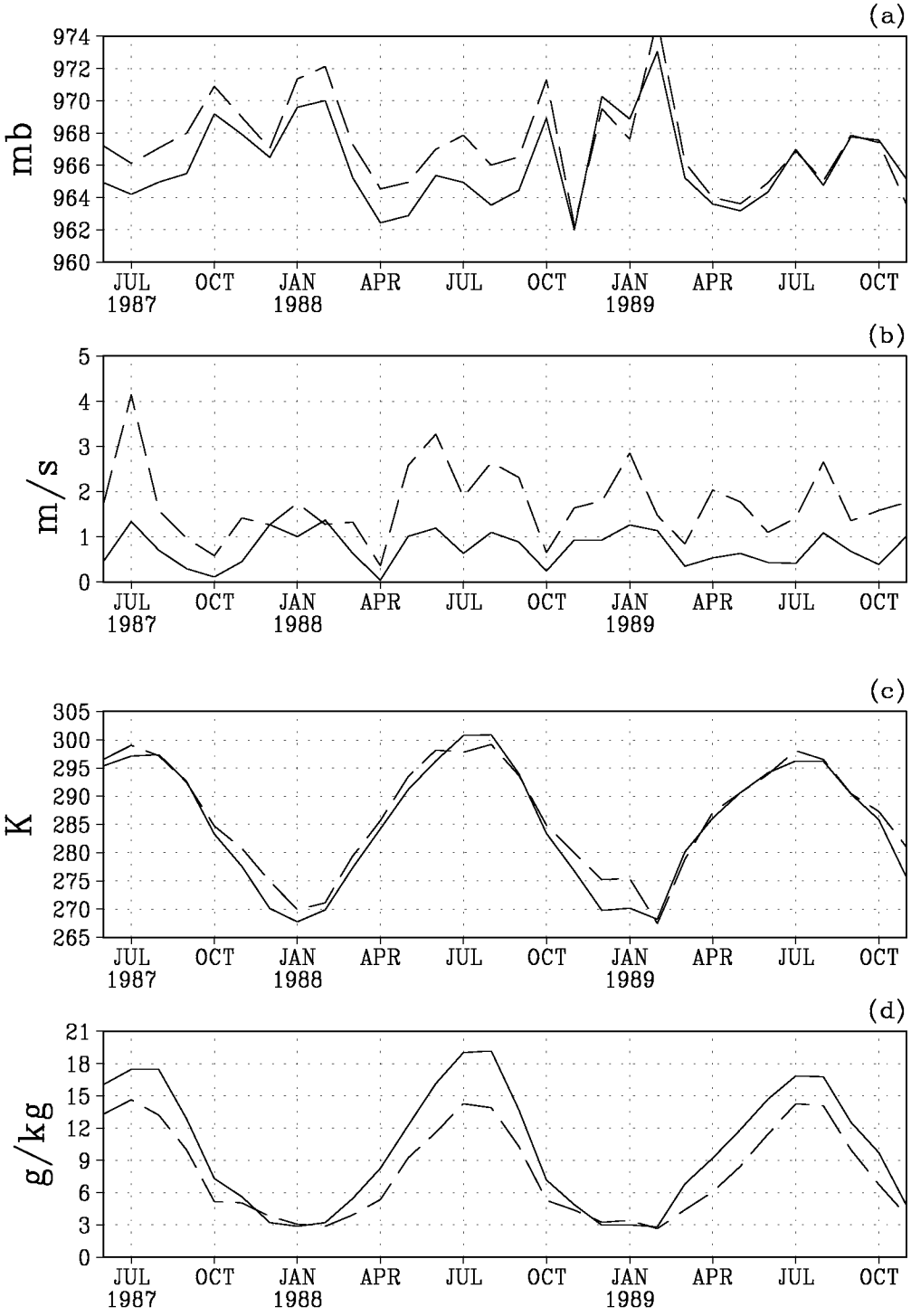

Figure 1: Monthly mean GEOS-1 (solid line) surface variables compared with FIFE (dashed line), (a) surface presure, (b) wind speed, (c) 2m air temperature, and (d) 2 m specific humidity.

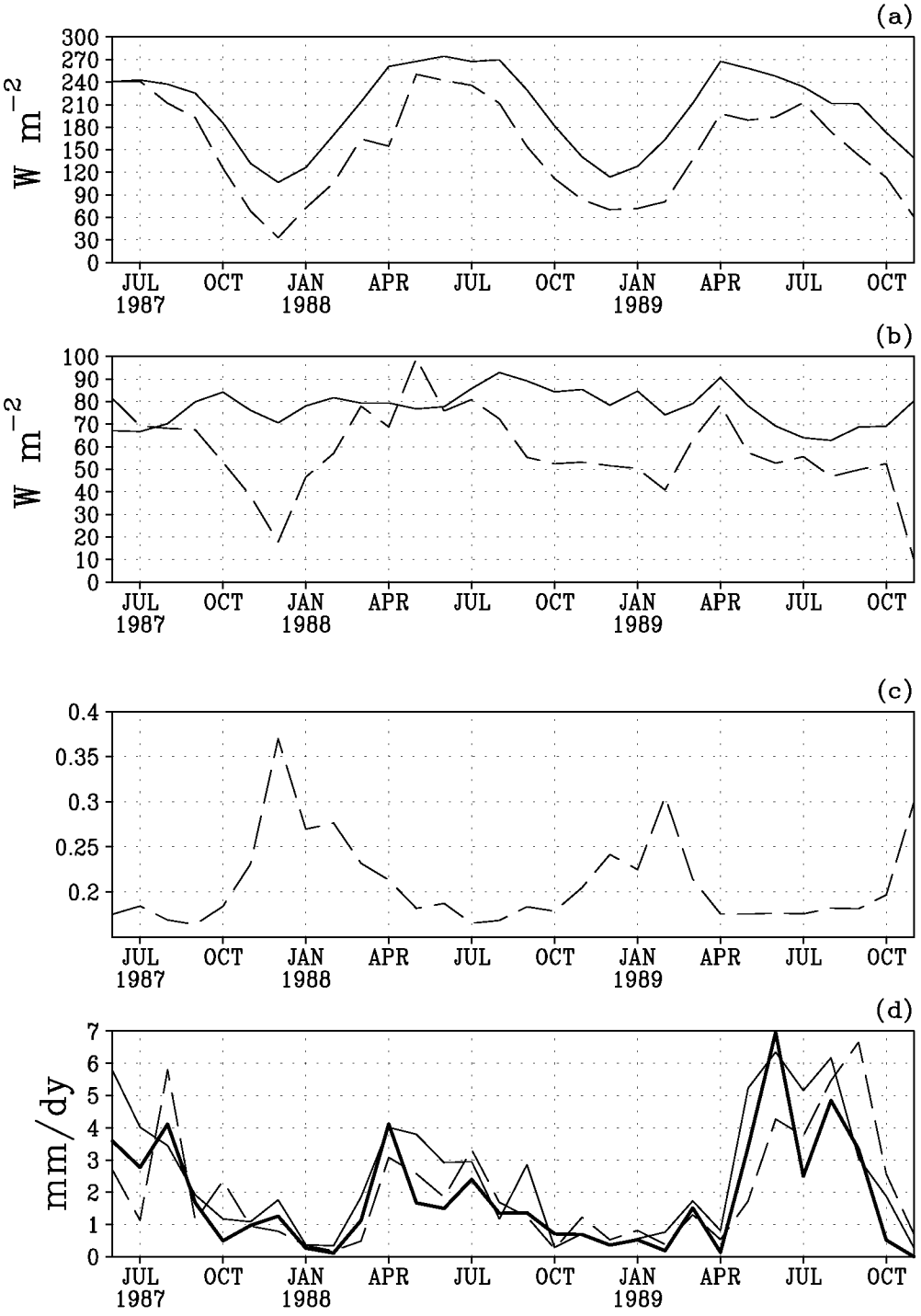

Figure 2: Monthly mean GEOS-1 (solid line) surface variables compared with FIFE (dashed line), (a) net downward shortwave radiation, (b) net upward longwave radiation, (c) FIFE surface albedo ($R_s{}^{\uparrow}/R_s{}^{\downarrow}$), and (d) precipitation (with NOAA precipitation in the bold solid line).

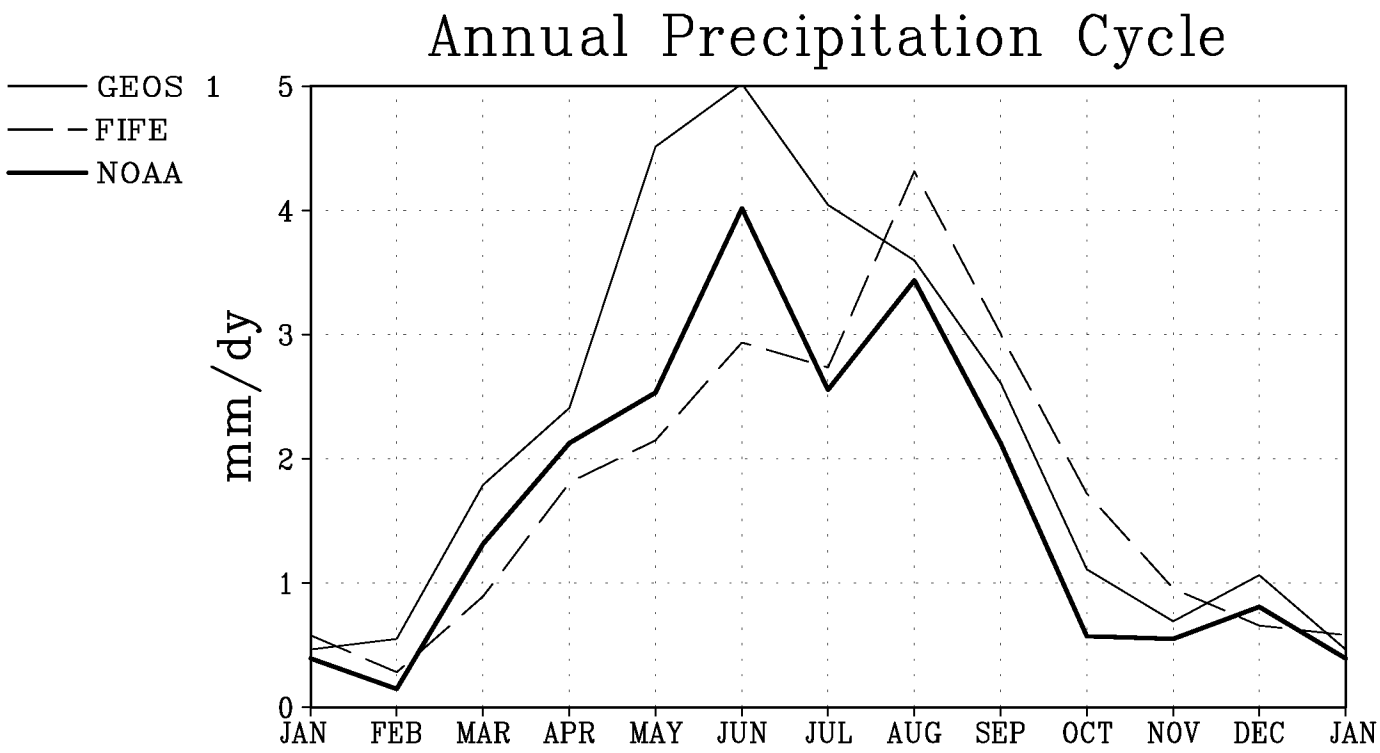

Figure 3: Mean annual cycle of precipitation for GEOS-1 DAS (solid line), FIFE (dashed line), and NOAA (Higgins et al. 1996, bold line) for May 1987 - Nov 1989.

2.2 Surface Daily Mean

Currently, GEOS 2.0 and 2.1 data assimilations exist for only a fraction of the time period covered by GEOS-1. All the assimilation systems have data that overlap in time with a special observing period during FIFE. In order to examine higher frequency variations and the diurnal cycle, we focus on FIFE's second Intensive Field Campaign (IFC2). The IFCs concentrated the observational effort into two week periods. IFC2 began on June 24, 1987 and lasted until July 11, 1987. In this section, we examine the daily variation of the FIFE observations compared with assimilated data generated with GEOS-1, 2.0 and 2.1.

GEOS data is taken from the grid point 38° N and 97.5° W. While the comparison at any of the four surrounding grid points may provide similar results (Betts et al. 1996, 1998), the FIFE site-average surface pressure and altitude above sea level compare most favorably to this grid point. Aside from a mean bias (probably due to the difference in altitude of approximately 30 m), the GEOS assimilation surface pressure parallels the observations (Fig. 4a).

Similarly, the daily variations in 2 m temperature follow the observations reasonably well (Fig. 4b). While the GEOS values generally do not stay within the observed horizontal standard deviations, there does not seem to be any significant biases in the daily mean temperature. The GEOS assimilations, however, show less day-to-day variability than FIFE observations. GEOS 2.1 tends to be the warmest assimilation. Most noticeably, the GEOS-1 and 2.0 are cold toward the end of the period and all the assimilations are warm on July 1.

Some of the fluctuations in the daily mean temperature and the differences between model and observation relate (in part) to the radiational heating at the surface (Fig. 5). The observed cold temperature on July 1 correspond to the reduction of daytime insolation by clouds. GEOS, on the other hand, has less clouds (Fig. 6b), more insolation, and more net upward longwave radiation, at this time. Some of the overestimate of net upward longwave radiation may be compensated for by the overestimate of net downward shortwave radiation.

Some similarities between model and observed cloud fields are evident. The cloudy period at the end of June is an example. In general, the assimilations seem to have more cloud cover than the observations, especially GEOS 2.0 (Fig. 6b). Large variations in the observed cloud cover seem to correlate with net upward longwave radiation, but this seems less clear in GEOS. Overall, the models coupling between clouds, radiation and surface temperature is internally consistent, and compares favorably with observations, with the exception that the observed day-to-day variations tend to be larger than in the assimilations.

Daily mean precipitation is presented in Figure 6a. The GEOS assimilations consistently show more precipitation than FIFE observations. The large differences are probably not too surprising given that the FIFE observations are taken over a 15×15 km area, while the

GEOS data represent $2° \times 2.5°$. We have already identified the summer of 1987 as having large precipitation in the GEOS-1 annual cycle. Also, the GCM grid representation of the convective scale precipitation may have deficiencies. NOAA precipitation data (Higgins et al. 1996) that has been averaged to the GEOS grid, indicate three days with heavy precipitation. The GEOS assimilations, especially GEOS 2.0 and 2.1, have more days with heavy precipitation. The precipitation time series' must be interpreted cautiously. Even at the $2° \times 2.5°$ resolution, in both the model and observation, the variability between neighboring grid points or stations can be very large.

For the IFC2 period, the GEOS assimilations show reasonable partitioning of sensible and latent heat fluxes, with latent heat being generally larger than sensible (Fig. 7). GEOS latent heat does tend to be biased higher than the observed daily mean. On July 1, when clouds were underestimated, both turbulent heat fluxes are overestimated in the GEOS data.

Similar to the monthly mean comparison, GEOS daily mean specific humidity is overestimated (Fig. 8a). Daily mean differences can be more than 3 g kg^{-1}. These differences seem too large to be simply resolved by the difference in altitude of the model and observations, as evidenced by the relatively small area standard deviations. While it might be simple to ascribe the large specific humidity to the high latent heat, Betts et al. (1996) results indicate that the NCEP high specific humidity bias is related to inadequate PBL top entrainment of dry (free-atmosphere) air and low mixed layer depth. The PBL interactions in GEOS are investigated later in this chapter.

Near surface wind speeds also appear strongly biased. GEOS seems to systematically underestimate the daily mean wind speed (Fig. 8b). The roughness length for GEOS-1 is 51 cm, and for GEOS 2.0 and 2.1 it is 19.5 cm. While this may explain why GEOS-1 winds are slightly less than GEOS 2.0 and 2.1, the differences between observation and all GEOS output are too large. Betts and Beljaars (1993) estimate the FIFE site roughness length for momentum to be 19 cm and for heat to be 1.2 cm.

In the daily mean, the differences between the three assimilation systems seem to be generally small at the surface, compared to the difference between any one model and the observations. This likely relates to the prescription of soil water, its lack of interaction with precipitation, and the strong control that soil water has on the surface energy balance.

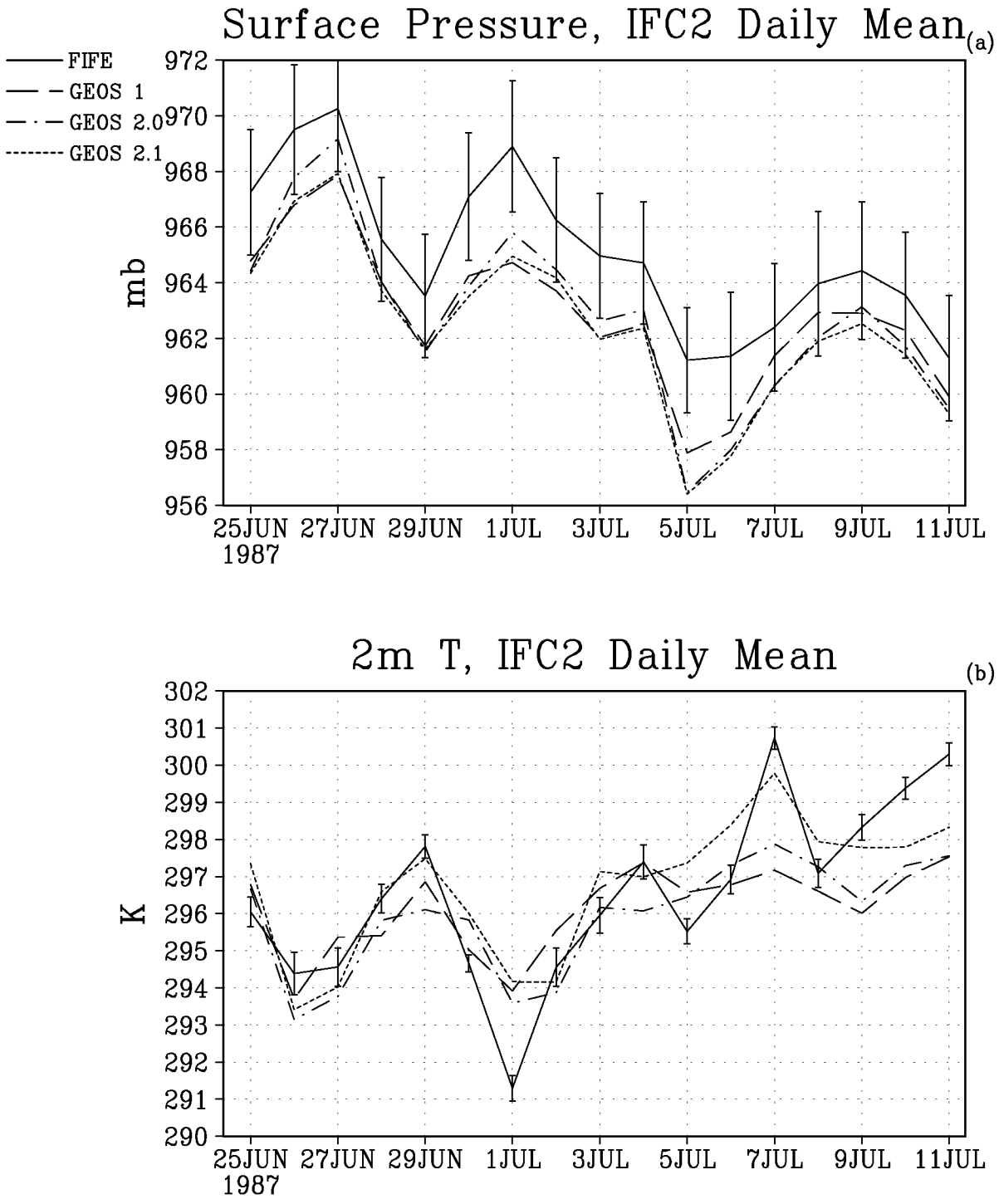

Figure 4: FIFE IFC2 daily mean comparison to GEOS assimilations for (a) surface pressure and (b) air temperature at 2m.

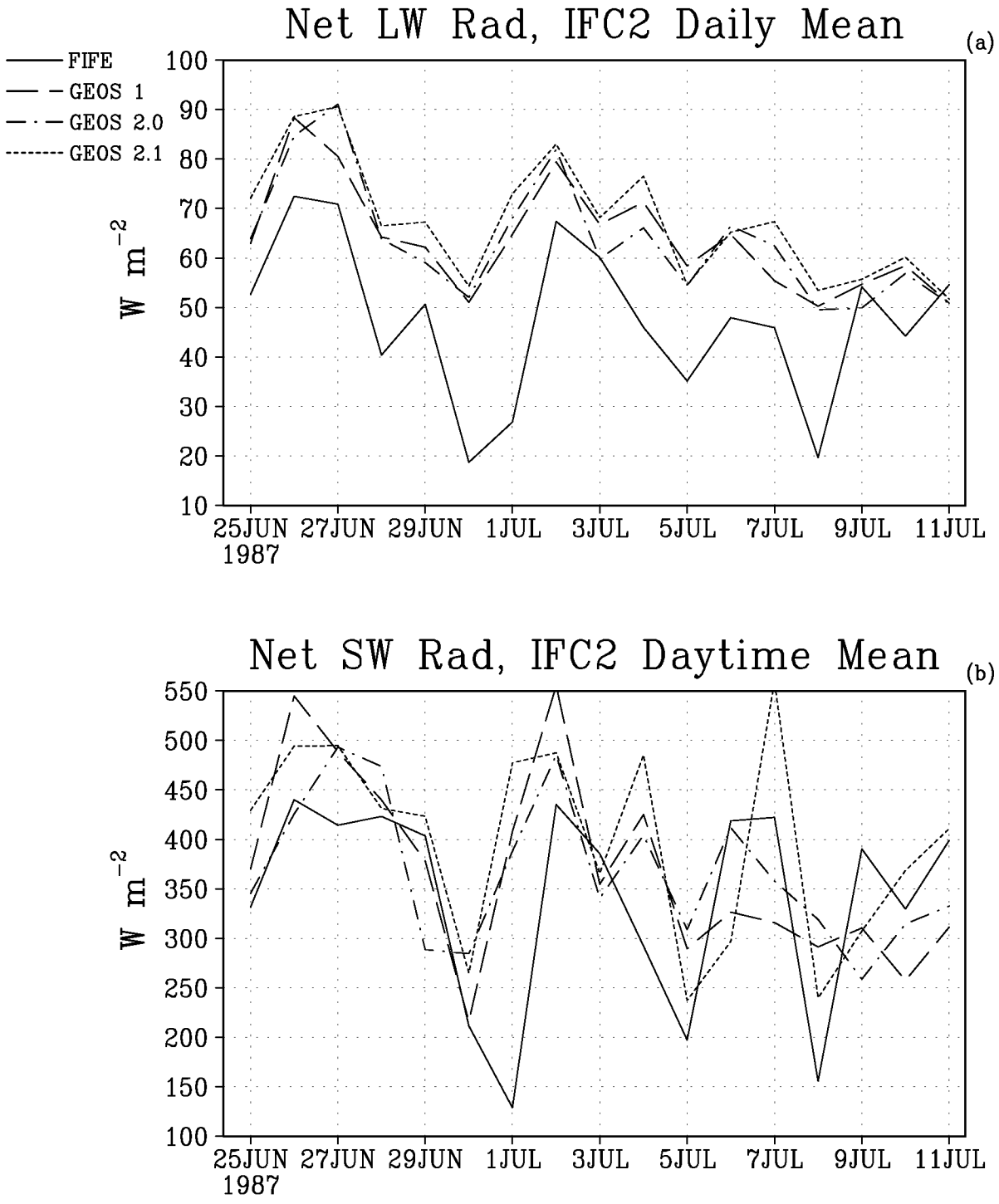

Figure 5: FIFE IFC2 daily mean comparison to GEOS assimilations for (a) net upward longwave radiation and (b) net downward shortwave radiation.

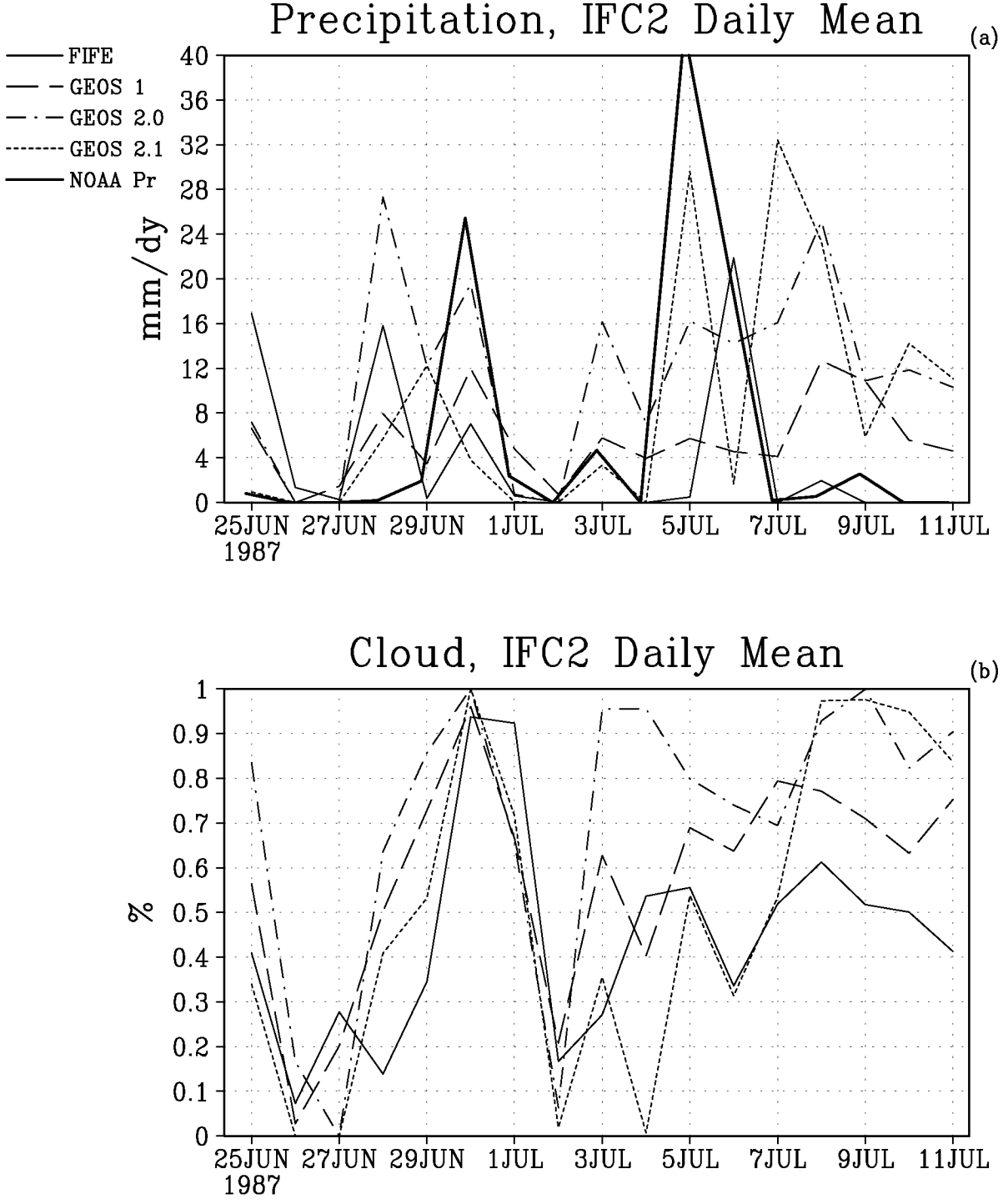

Figure 6: FIFE IFC2 daily mean comparison to GEOS assimilations for (a) total precipitation (with NOAA observations) and (b) cloud fraction.

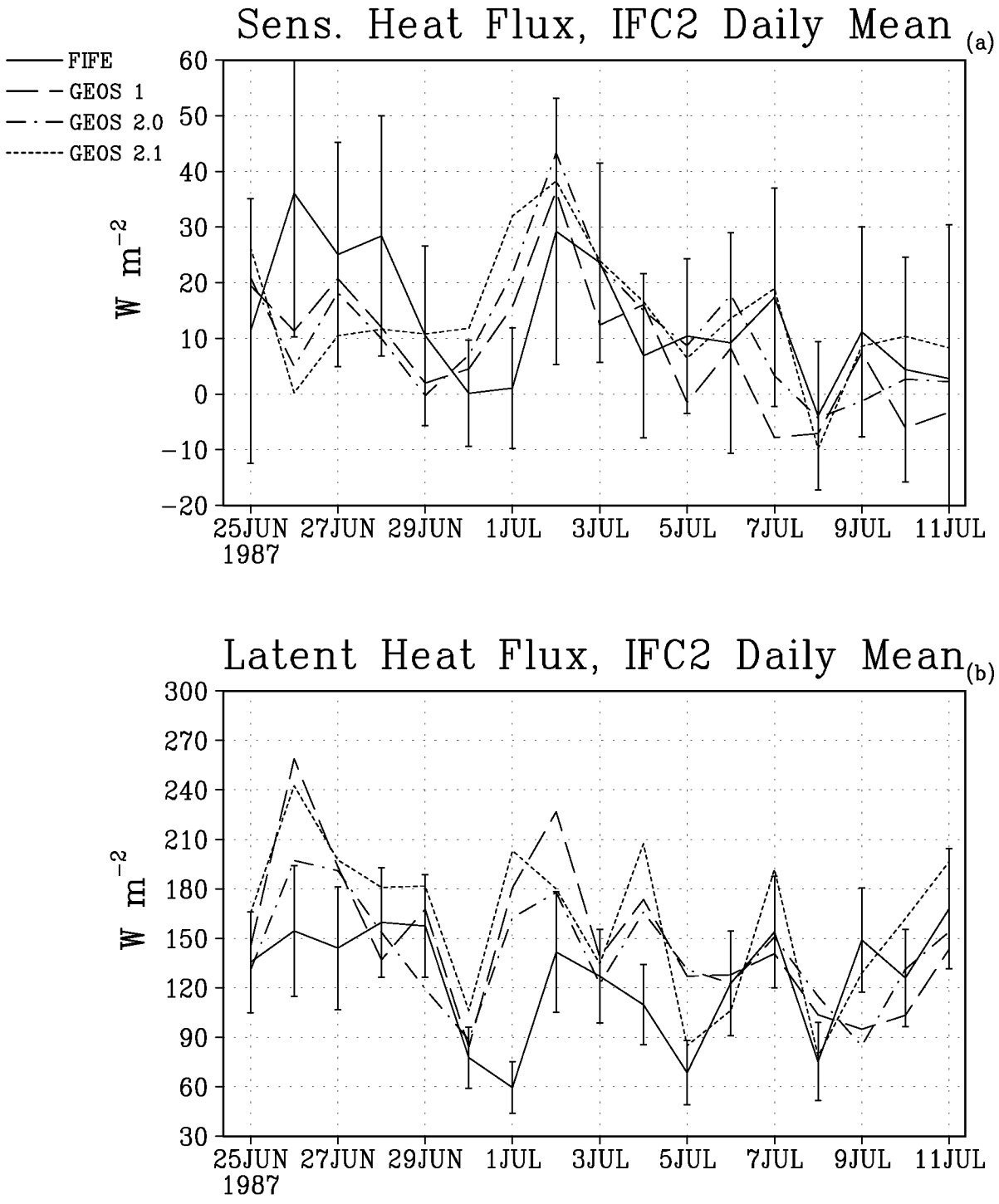

Figure 7: FIFE IFC2 daily mean comparison to GEOS assimilations for (a) sensible heat flux and (b) latent heat flux.

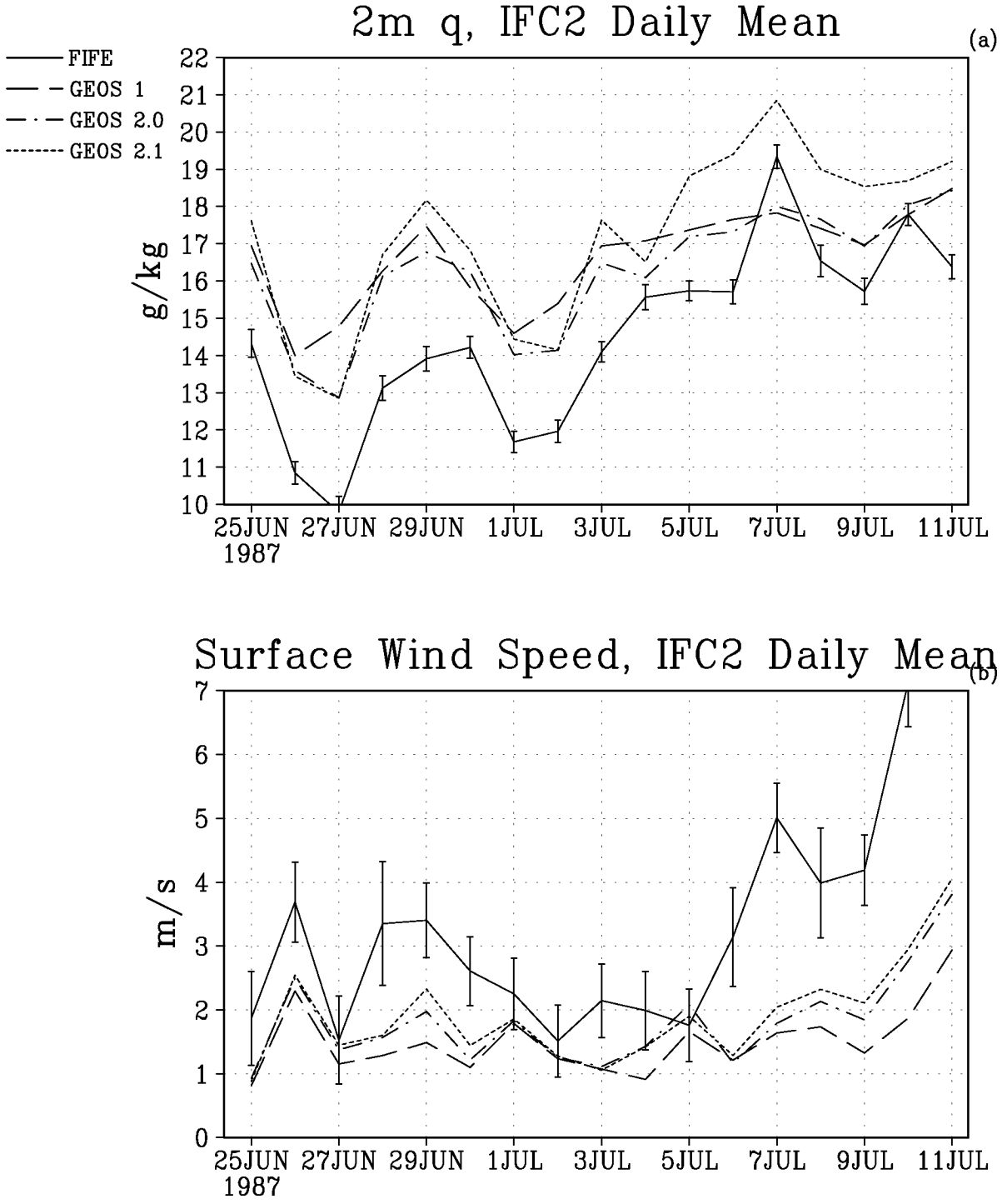

Figure 8: FIFE IFC2 daily mean comparison to GEOS assimilations for (a) specific humidity at 2m and (b) wind speed. FIFE winds were measured at 5.4 m, GEOS winds are the linear average of 2 m and 10 m levels.

2.3 Diurnal Cycle

While the daily mean time series' provide some information on DAS surface representation, the investigation of the diurnal cycle is also important. Here, we examine the mean diurnal cycle for the FIFE IFC2 period.

FIFE observed surface pressure varies about 2 mb for the average diurnal cycle (Fig. 9a). The GEOS assimilations seem to vary slightly less, and there may be a phase difference compared to observations. The near surface atmospheric temperature minimum of GEOS-1 and GEOS 2.0 tends to be too cold ($\tilde{}$1 K), even less than the lowest standard deviation (Fig. 9b). GEOS 2.1 seems to be cool at night and a little warm during the day, but represents the diurnal cycle (highs and lows) very well.

Recent changes in the radiation parameterization seem to have improved the phase of the GEOS 2.1 net upward longwave radiation diurnal cycle (Fig. 10a). GEOS 2.1 longwave radiation biases are fairly uniform throughout the diurnal period ($\tilde{}$20 W m^{-2}). The biases are likely related to the downward radiation from the atmosphere because near surface temperatures seem to be reasonable (1 K difference in temperature does not lead to 20 W m^{-2} differences in upward terrestrial radiation). As discussed earlier, the net downward shortwave radiation is overestimated, but the diurnal phase in GEOS 2.0 and 2.1 seems improved over GEOS-1 (Fig. 10b).

Schubert et al. (1995) identify the diurnal oscillation of precipitation in the United States as being overestimated in GEOS-1 DAS. GEOS 2.0 was found to have an even stronger diurnal oscillation than GEOS-1 DAS (a primary factor in the modifications to GEOS 2.1). For the FIFE case, the NOAA observed precipitation (Fig. 11a) shows a strong maximum at 15 UTC (NOAA observed precipitation comes from Higgins et al. (1996) at the grid point that matches the GEOS data). Care must be taken when comparing the model and observed diurnal precipitation. This maximum is primarily the result of one very strong event. The GEOS system, on the other hand, tends to overestimate the number of significant events.

Figure 11b indicates that GEOS 2.1 produces the least amount of cloud during the FIFE IFC2. None of the assimilation systems, however, reproduce the observed diurnal cycle of clouds. The observations indicate a noticeable diurnal cycle of cloudiness. Low level clouds that top the developing convective PBL would have a diurnal cycle. The GEOS 2.0 and 2.1 vertical distribution of clouds, however, indicate very little low cloud and mostly high cloud (Fig. 12), and Molod et al. (1996) show that GEOS-1 DAS has too little low cloud. GEOS-1 also shows too much high cloud (Pickering et al. 1995; Allen et al. 1997). Significant differences in the vertical distribution of clouds could have detrimental effects on the surface radiation.

The sensible heat flux at the surface is reproduced quite well by the GEOS 2.1 assimilation (Fig. 13a). GEOS-1 sensible heat is too low in the late afternoon. At night, the downward

sensible heat is reproduced by each assimilation. Latent heat fluxes in the assimilation systems are overestimated during the daytime, which was to be expected, given the daily mean analysis. GEOS 2.1 produces more latent heat than GEOS 2.0 (Fig. 13b). The mean observed nocturnal latent heat flux is slightly positive. GEOS, however, shows some slightly negative values. Note that GEOS 2.0 and 2.1 underestimate both sensible and latent heat at the 15 UTC period.

The net surface heating (H_g) is defined by,

$$H_g = R_n - H_s - LE,$$

where R_n is the net radiation, H_s is the sensible heat flux and LE is the latent heat of evaporation. Figure 14a shows GEOS surface heating is particularly strong at 15 UTC. The heat capacity of the soil may be larger than observed leading to the differences. Note the small temperature change between 12 and 15 UTC despite the strong heating (Fig. 14b). Turbulent fluxes are small until the surface layer warms and becomes more thermodynamically unstable. The phase lag of surface heating is a common problem of bulk surface heat budget models. The phase lag of surface temperature in the ECMWF and NCEP models was related to thick soil layers (Betts. et al. 1993 and 1997).

As in the previous analyses, the surface layer specific humidity bias is quite apparent (Fig. 15a). The bias maximizes during the daytime coinciding with the diurnal cycle of the latent heat. While the specific humidity bias may be partly related to the latent heat bias, at least one other factor is identified later in this paper. The specific humidity bias most likely affects the lifted condensation level (LCL) in the GEOS system. The LCL identifies the level at which parcels lifted from the surface begin to condense water vapor. In GEOS, there are few low clouds considering the low LCL and the specific humidity bias.

In summary, this analysis demonstrates several shortcomings in the present GEOS system surface fields. In particular, the specific humidity, clouds, longwave radiation precipitation and latent heat flux all show large biases compared with the FIFE site observations. While some improvement is anticipated by incorporating a more comprehensive land surface parameterization, other parameterizations (eg. radiation, convective precipitation or cloud microphysics) may require further study and development. Consideration must also be given to the differences in albedo and the adverse effect that this will pose in the surface energy balance.

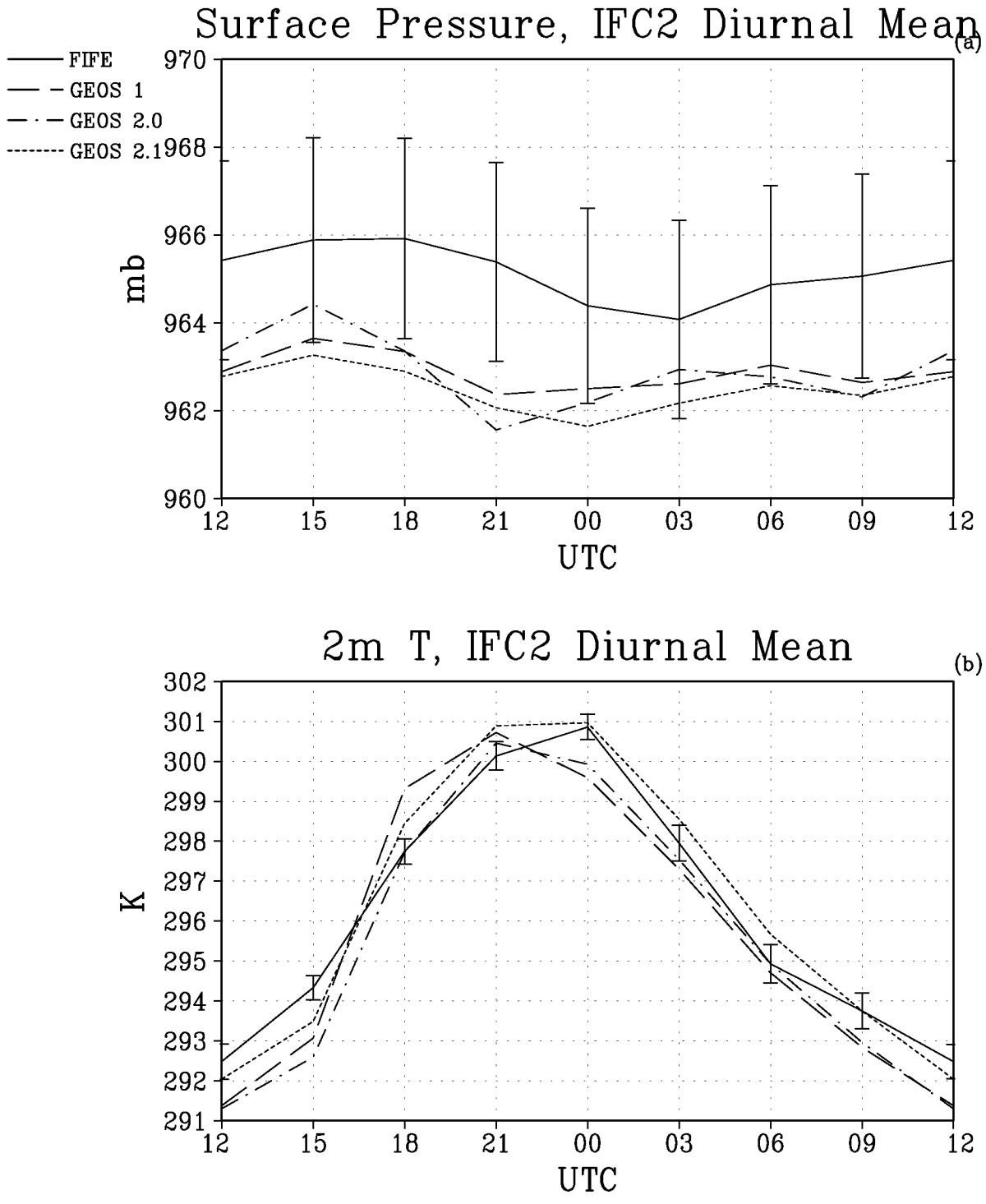

Figure 9: FIFE IFC2 mean diurnal cycle comparison to GEOS assimilations for (a) surface pressure and (b) air temperature at 2m.

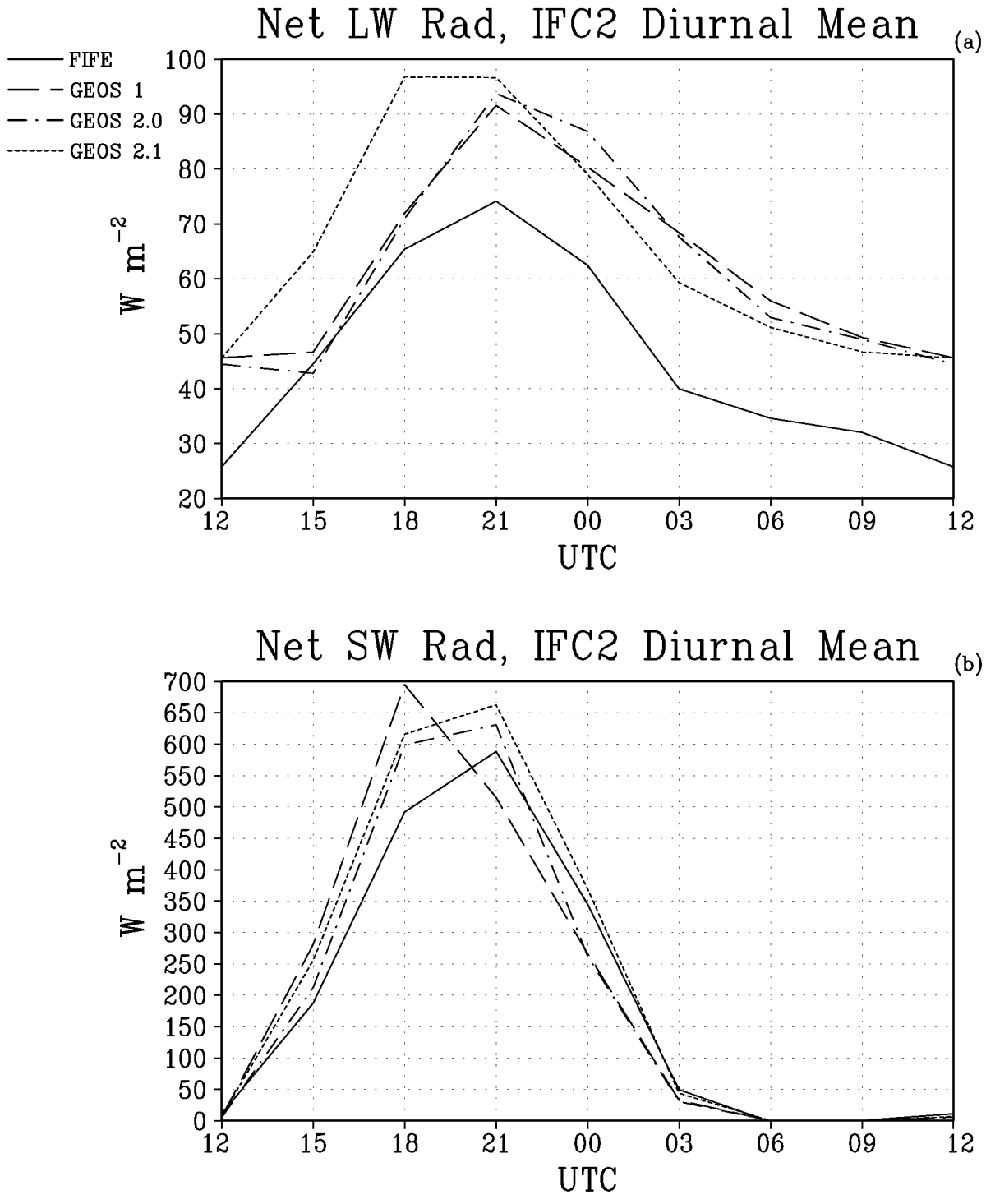

Figure 10: FIFE IFC2 mean diurnal cycle comparison to GEOS assimilations for (a) net upward longwave radiation and (b) net downward shortwave radiation.

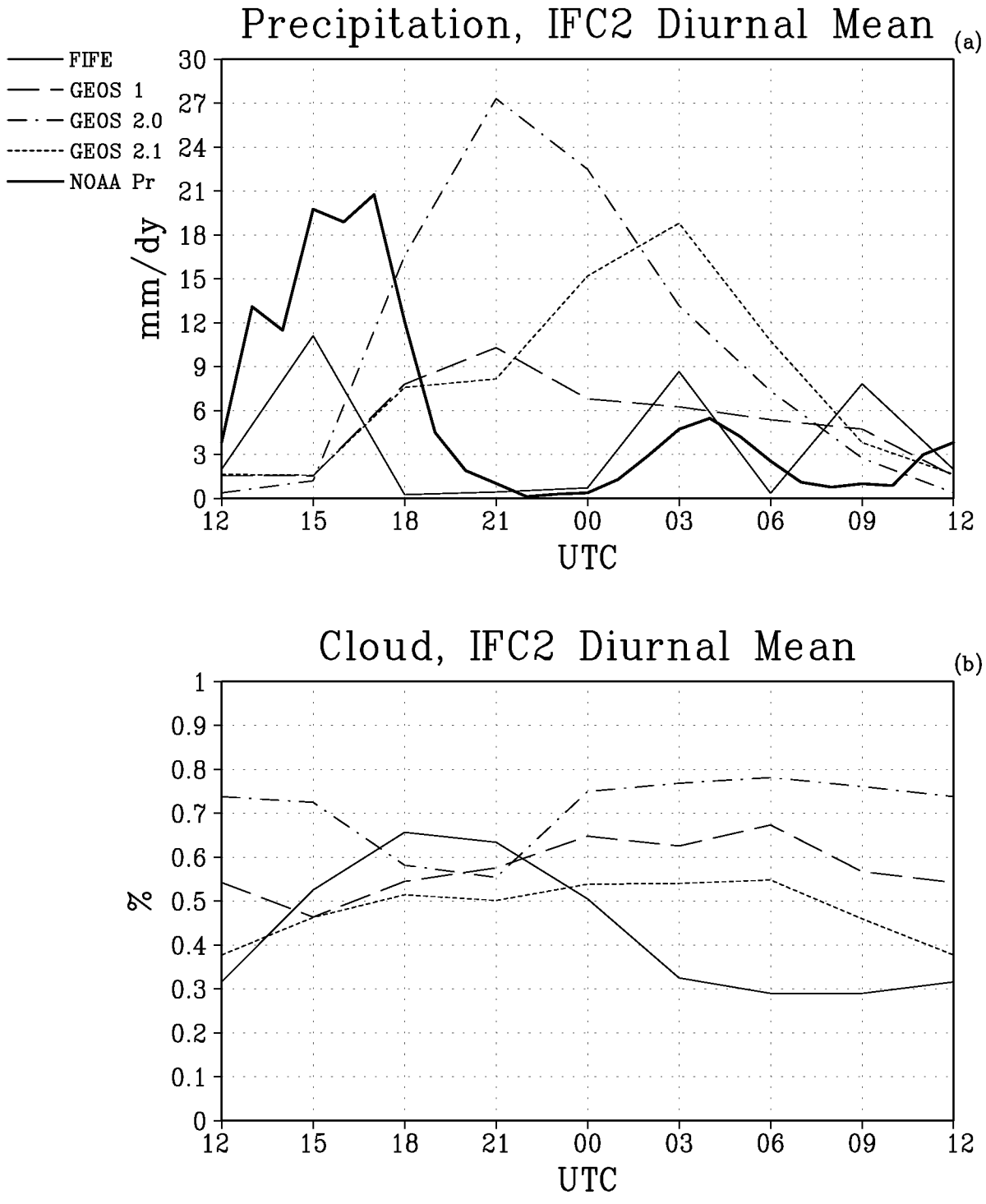

Figure 11: FIFE IFC2 mean diurnal cycle comparison to GEOS assimilations for (a) total precipitation (with NOAA observations) and (b) cloud fraction.

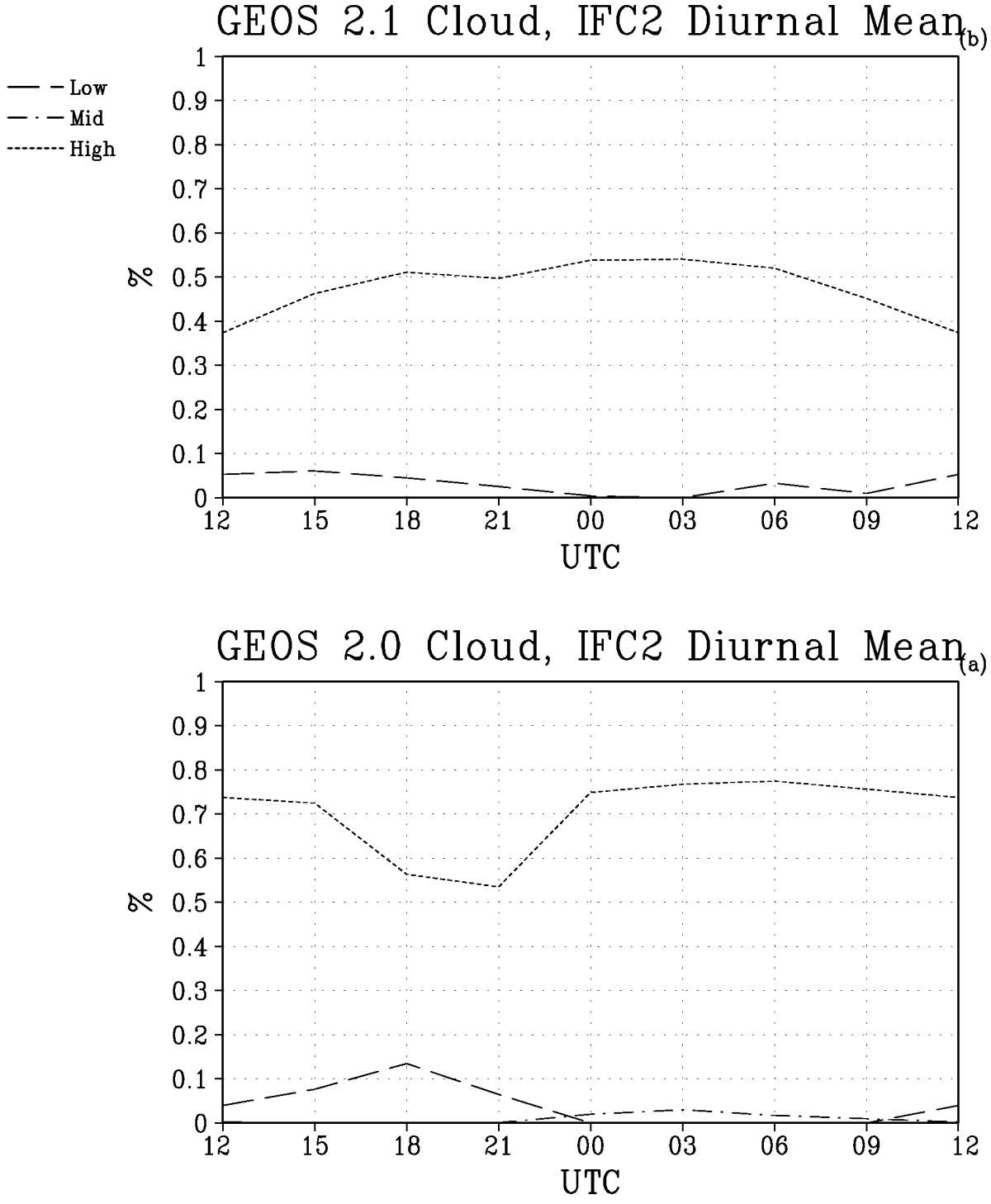

Figure 12: Vertical distribution of clouds (high, middle and low) for (a) GEOS 2.1 and (b) GEOS 2.0.

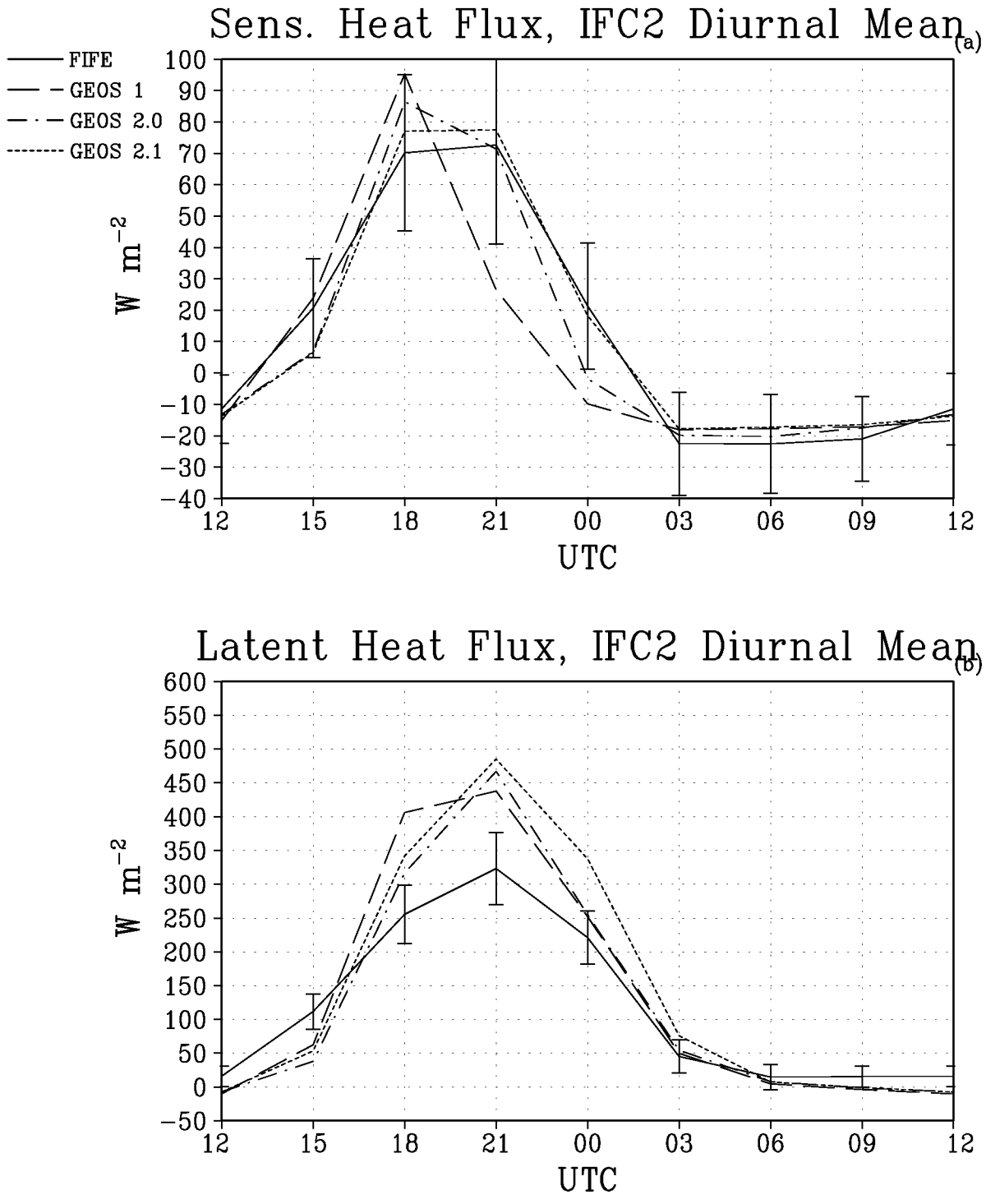

Figure 13: FIFE IFC2 mean diurnal cycle comparison to GEOS assimilations for (a) sensible heat flux and (b) latent heat flux.

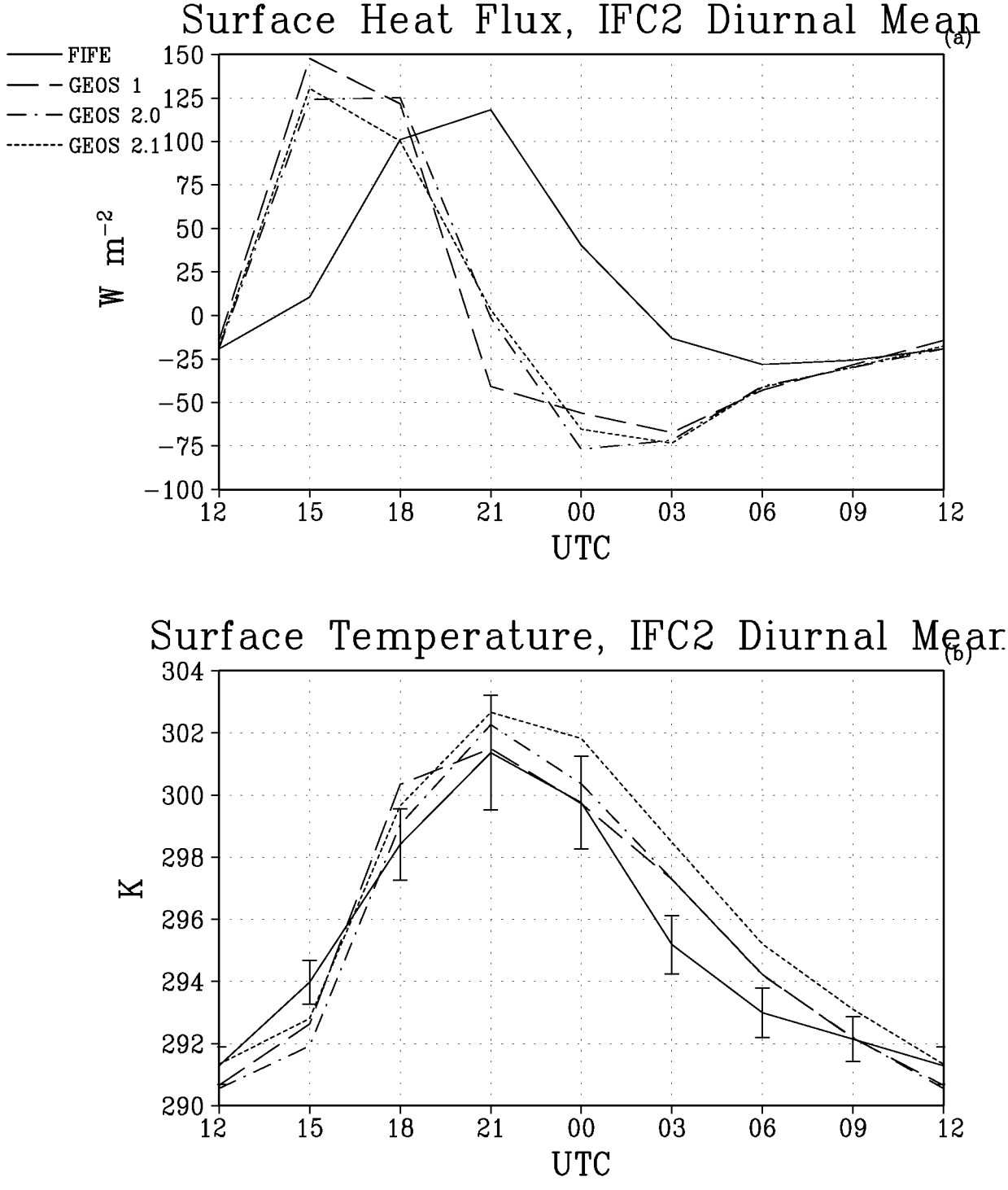

Figure 14: FIFE IFC2 mean diurnal cycle comparison to GEOS assimilations for (a) heat flux into the surface and (b) surface temperature, where FIFE surface temperature is measured by a radiometer.

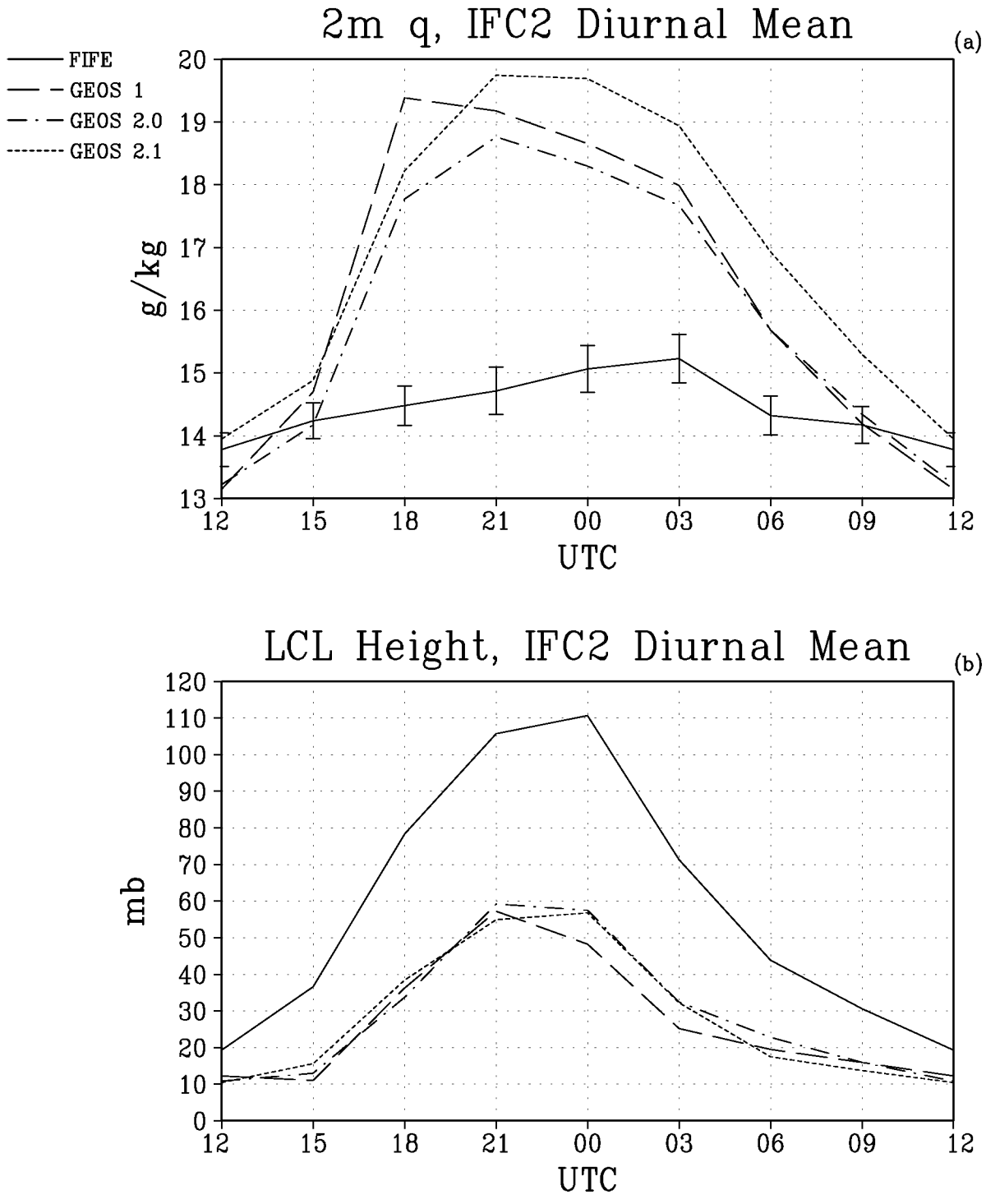

Figure 15: FIFE IFC2 mean diurnal cycle comparison to GEOS assimilations for (a) specific humidity at 2m and (b) LCL height above the surface.

2.4 Planetary Boundary Layer

Radiosonde balloon observations of the PBL were made on most days during FIFE's IFC2. Here, we present seven days of FIFE IFC2 PBL observation where the frequency of balloon launches allows the examination of the daytime part of the diurnal cycle. Two analyses of the diurnal cycle are presented. First, six hourly intervals of GEOS-1, GEOS 2.0 and GEOS 2.1 are compared to the closest time during FIFE. The standard GEOS assimilation system data are instantaneous at 12 UTC, 18 UTC, and 00 UTC. GEOS 2.1 profiles, however, are available at 3 hour intervals. Unless otherwise noted, GEOS profiles are plotted on sigma levels. The second analysis uses three hourly vertical profiles from GEOS 2.1 to examine the diurnal cycle with more temporal resolution.

The comparison of PBL observations to the GEOS assimilation systems has several difficulties. First, the observational data are not as regular nor as continuous as the surface observations. Instantaneous profiles of observation and assimilation must be compared. The FIFE PBL observations were taken at only one station, and only during clear afternoons. Horizontal heterogeneity within the FIFE site can influence local mesoscale circulations (Smith et al. 1994). Of course, the $2° \times 2.5°$ GEOS grid cannot resolve these small features. At any given time, there can be large differences between GEOS and the observations. Furthermore, the GEOS systems can have substantial differences between each other. Nonetheless, we expect that the assimilation systems profiles and diurnal variation should bear some likeness to the observations.

2.4.1 GEOS PBL Comparison with FIFE

The comparison of GEOS-1, 2.0 and 2.1 with FIFE PBL profiles of potential temperature, specific humidity and wind are presented in Figures 16 - 36. We will discuss some of the generalizations that can be seen in this comparison, rather than a description of each figure.

The GEOS potential temperature profiles at 12 UTC show more thermodynamic stability near the surface than in the observed profile. The morning of 07 JUL demonstrates this feature (Fig. 28a). Figure 37 shows that the near-surface temperature gradients are generally larger in the assimilations than the observations. The assimilations and observation are, however, closer to each other toward the end of the period.

On 10 JUL, the near surface stability seems more comparable to the observations but there is an elevated stable layer (Fig. 34a) that even persists at 18 UTC (Fig. 35a). The observed elevated stable layer appears weaker than in GEOS, and the GEOS system does not penetrate as deep into the free atmosphere. At 18 UTC, the GEOS systems' well mixed layers are consistently lower than the observed profiles. Furthermore, the GEOS 18 UTC profiles indicate a slightly unstable tilt, while the observations are closer to neutral stability.

At 00 UTC (toward the end of the day in FIFE observations), all the GEOS assimilations underestimate the depth of the mixed layer. Note that the last radiosonde balloon launch of each day can be 1 - 2 hours before 00 UTC. In general, the GEOS 2.1 assimilation produces a deeper mixed layer than GEOS-1 and GEOS 2.0 at 00 UTC. Of the seven days investigated, the GEOS 2.1 PBL is not the deepest only on 01 JUL (Fig. 21a). The diurnal evolution of the GEOS 2.1 PBL will be discussed further in the next section.

The wind and specific humidity observations tend to be noisier than the potential temperature profiles. In particular, the specific humidity is computed from measurements of wet bulb temperature. If the bulb dries or freezes, the observations are erroneous. Most specific humidity profiles show higher values than the observations in the lower part of the PBL, but this is not always true. This seems to occur more frequently in the GEOS 2.1 system despite the generally deeper late afternoon PBL. The wind profiles are difficult to draw conclusions from due to some variability in the observations and with the assimilation systems. Some profiles are quite comparable to the observations (09-10 JUL, Figs. 31 - 36). There does not seem to be a consistent low wind bias in the PBL that might explain the low surface winds (through vertical momentum transport) noted in the discussions of the surface diurnal cycles and daily means.

2.4.2 GEOS 2.1 PBL Diurnal Cycle

The GEOS 2.1 assimilation archived data at three hour intervals. This permits further investigation of some of the features of GEOS 2.1 discussed in the previous section. Specifically, the higher time resolution profiles of GEOS 2.1 are compared to all the FIFE profiles for the same days shown in the previous section (Figs. 38 - 44).

On 27 JUN (Fig. 38a and c) and 01 JUL(Fig. 39a and c), both observations and assimilation show the presence of a near-neutral residual layer above the surface stable layer at 12 UTC. Once the model mixes through the surface stable layer, the mixed layer deepens rapidly. On 27 JUN, the assimilation PBL becomes deeper than observed late in the day. The profile above the PBL on 01 JUL is more stable than 27 JUN and the entrainment and deepening of the PBL is also lessened in the assimilation.

In general, the observations clearly show that the PBL can deepen rapidly between 12 UTC and 18 UTC. GEOS 2.1 is not able to consistently reproduce this feature. However, the previous section showed that GEOS 2.1 produces the deepest (compared to the previous versions) late afternoon PBL. Here, with three hourly data we see that on five of the seven days (excluding 02 JUL, Fig. 40, and 07 JUL, fig. 42), the GEOS 2.1 PBL deepens rapidly between 18 UTC and 21 UTC. Most of these days show that the model has mixed through a very stable layer during this period. Entrainment from above this layer allows the PBL to deepen, and become drier. The IFC2 mean diurnal cycle of TKE shows the drastic increase in turbulence from 18 to 21 UTC (Fig. 45) when the surface sensible heat flux is more

comparable with observed (Fig. 13). Also, the GEOS 2.1 morning surface temperatures tend to be slightly warmer than the previous GEOS versions.

This analysis has identified two factors that affect the development of the assimilated mixed layer. First, the surface sensible heat flux is consistently underestimated between 12 and 15 UTC. The lack of heat from the surface allows the stable surface layer to stay in place longer than observed. Secondly, the observed profiles indicate that the surface layer stability is too strong in the assimilation system or may include an elevated stable layer. The stable layer could be related to the slightly cooler surface temperatures, and too much net upward longwave radiation. As these factors are overcome by the diurnal heating of the surface, the GEOS 2.1 PBL can develop quickly, but too late in the diurnal period to catch up with observations.

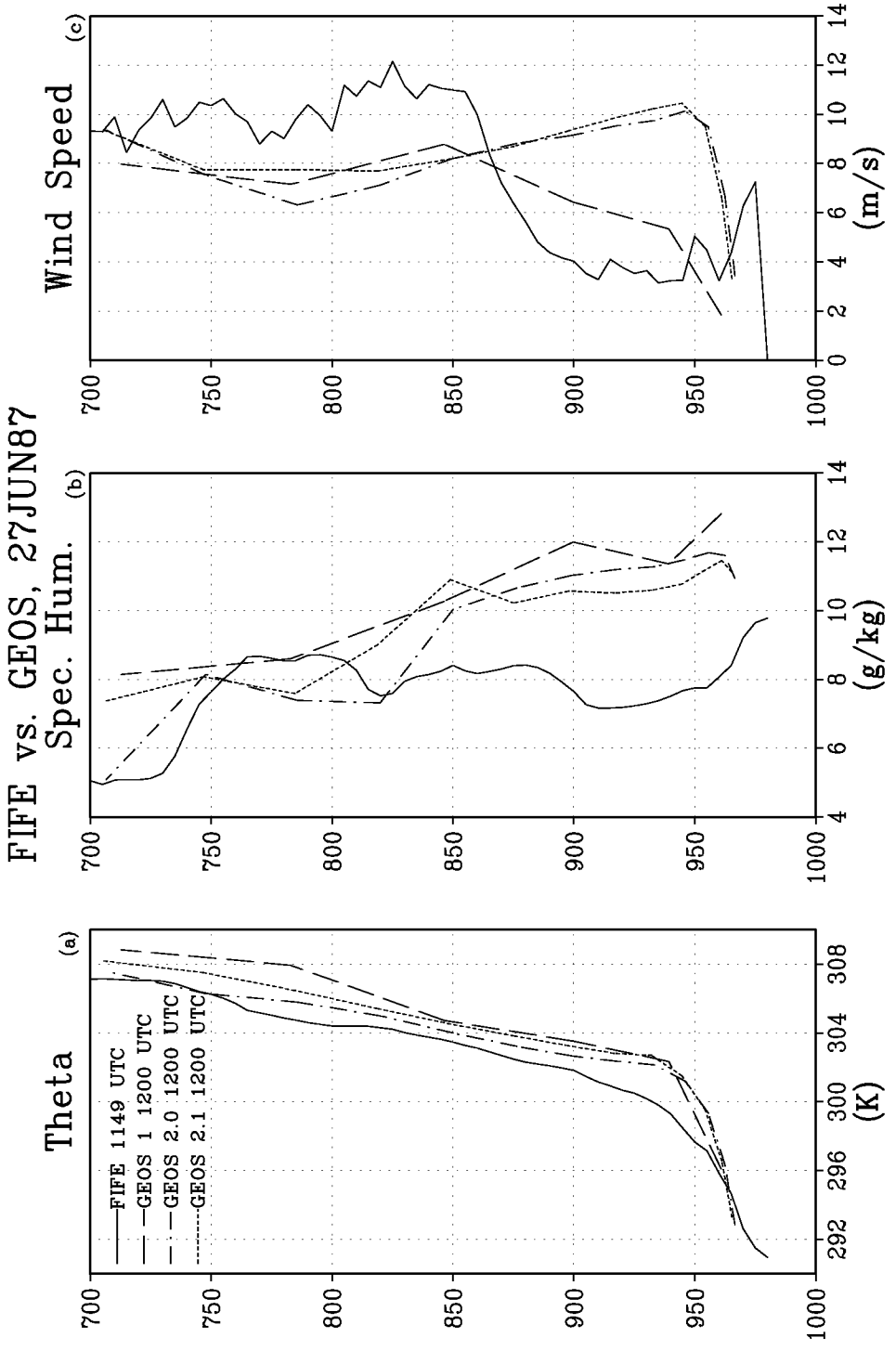

Figure 16: Vertical profiles for 12 UTC 27 JUN for FIFE PBL observations (the legend indicates launch time) and GEOS PBL profiles of (a) potential temperature, (b) specific humidity, and (c) wind velocity.

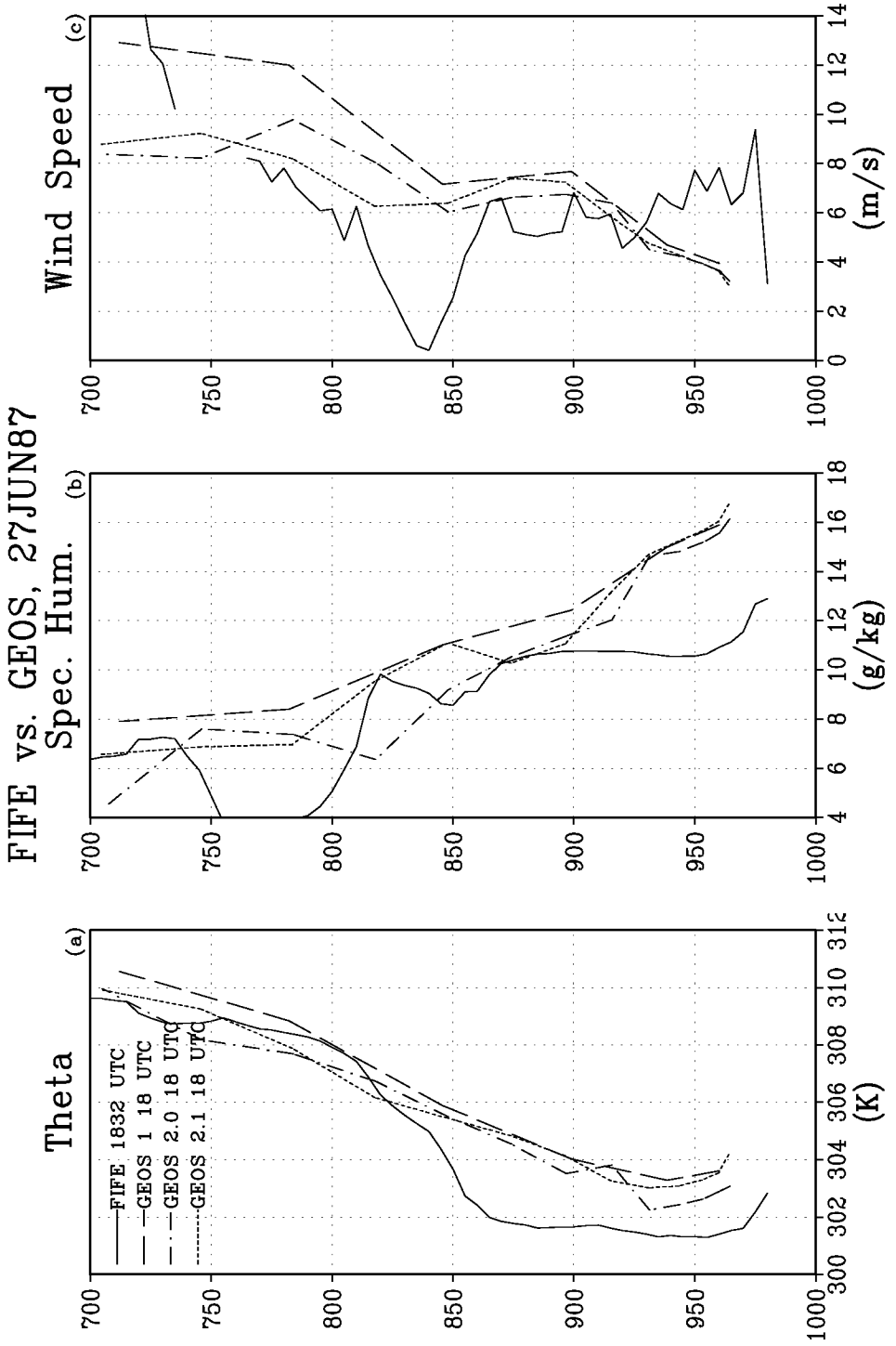

Figure 17: Vertical profiles for 18 UTC 27 JUN for FIFE PBL observations (the legend indicates launch time) and GEOS PBL profiles of (a) potential temperature, (b) specific humidity, and (c) wind velocity.

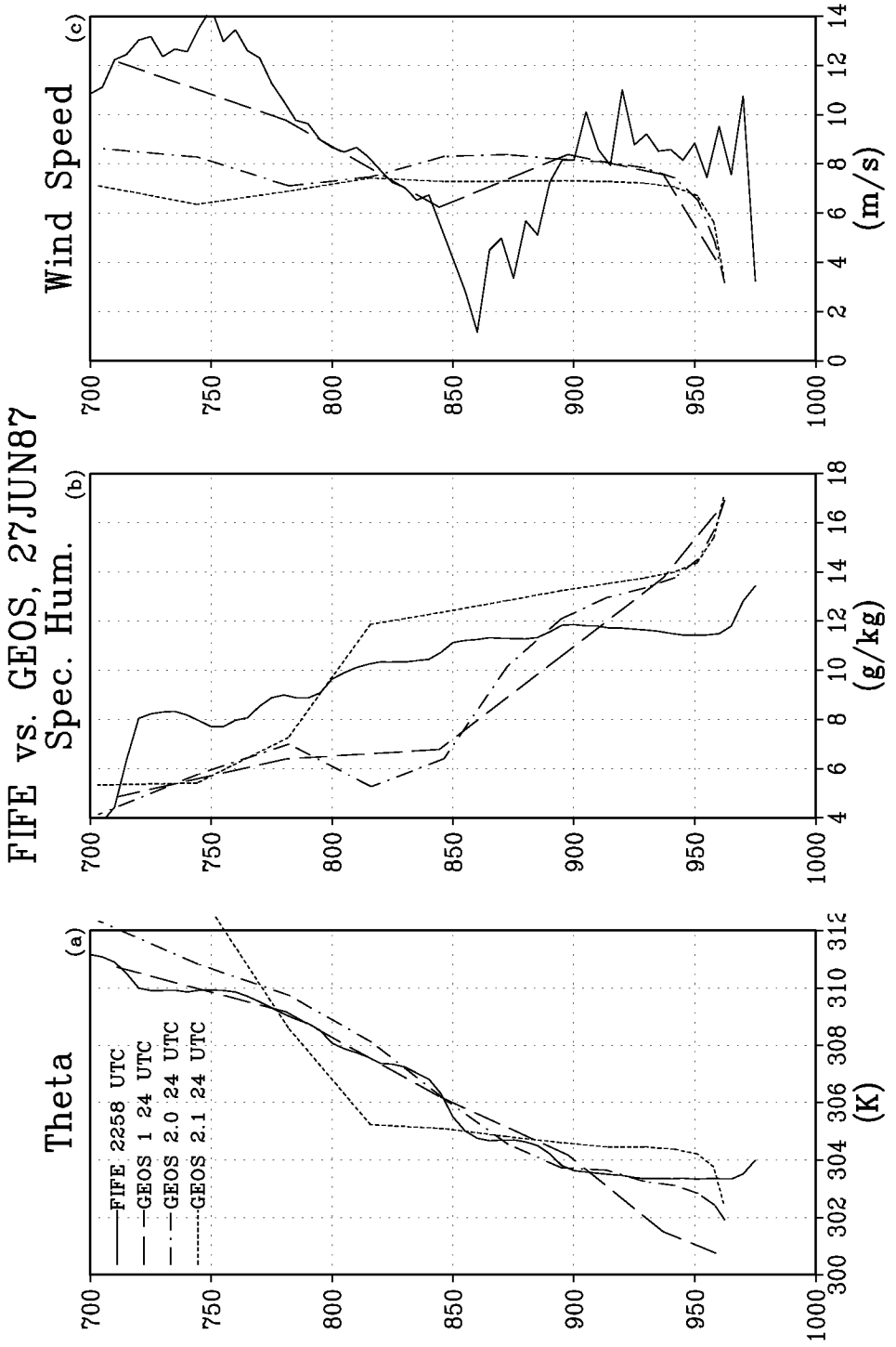

Figure 18: Vertical profiles near 00 UTC 28 JUN for FIFE PBL observations (the legend indicates launch time) and GEOS PBL profiles of (a) potential temperature, (b) specific humidity, and (c) wind velocity (note that 24 UTC equates to 00 UTC of the following day).

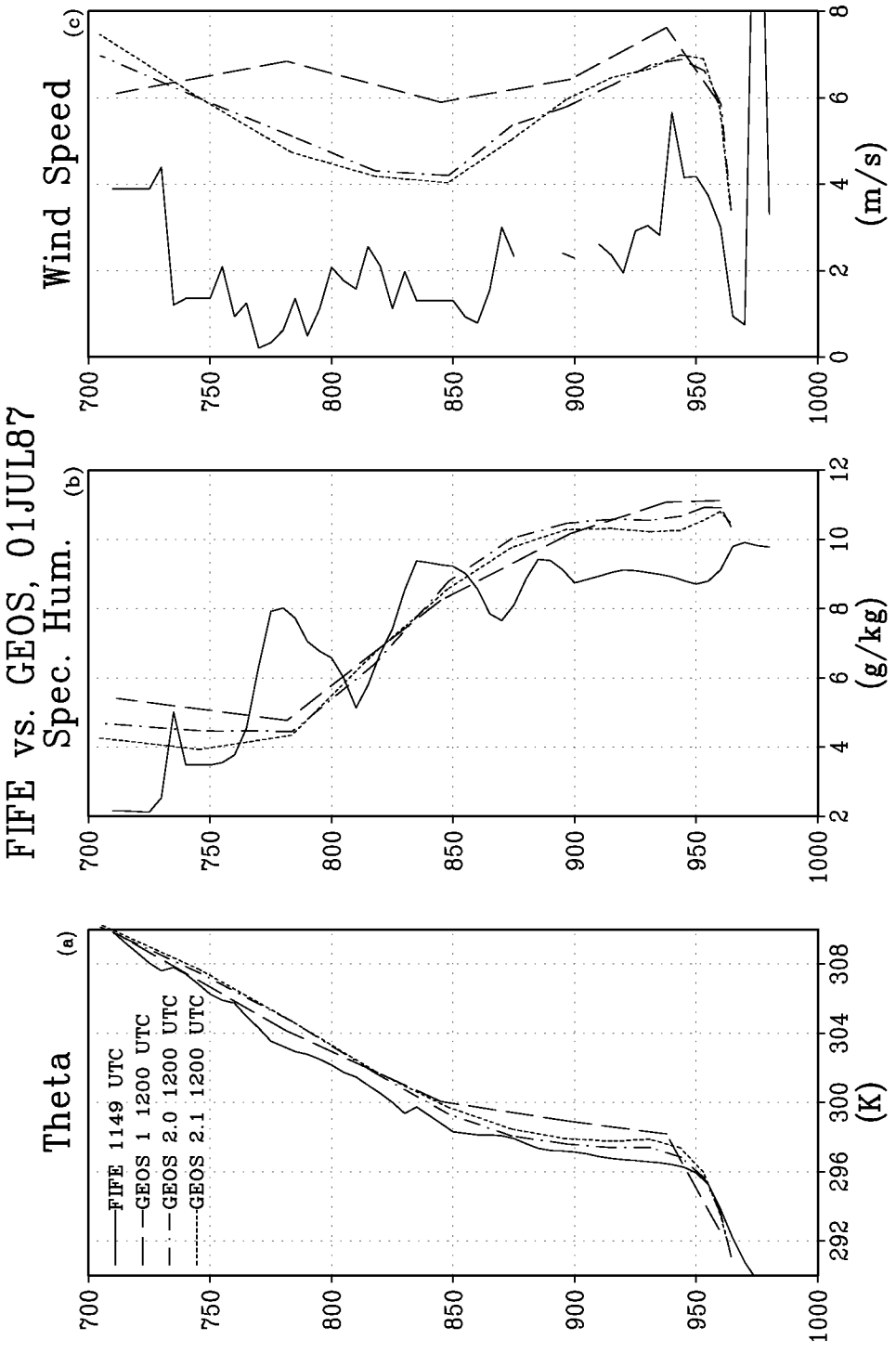

Figure 19: Vertical profiles for 12 UTC 01 JUL for FIFE PBL observations (the legend indicates launch time) and GEOS PBL profiles of (a) potential temperature, (b) specific humidity, and (c) wind velocity.

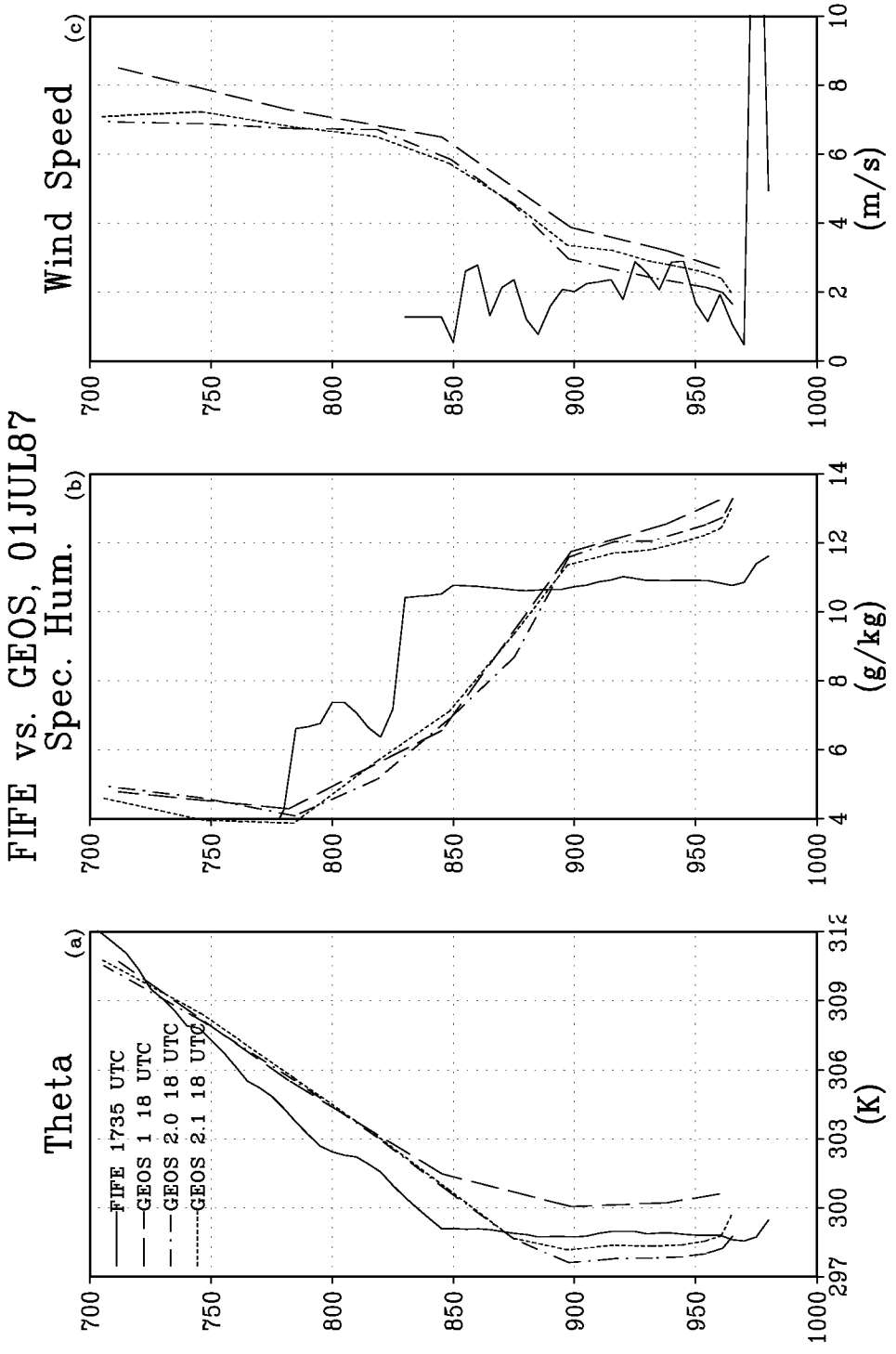

Figure 20: Vertical profiles for 18 UTC 01 JUL for FIFE PBL observations (the legend indicates launch time) and GEOS PBL profiles of (a) potential temperature, (b) specific humidity, and (c) wind velocity.

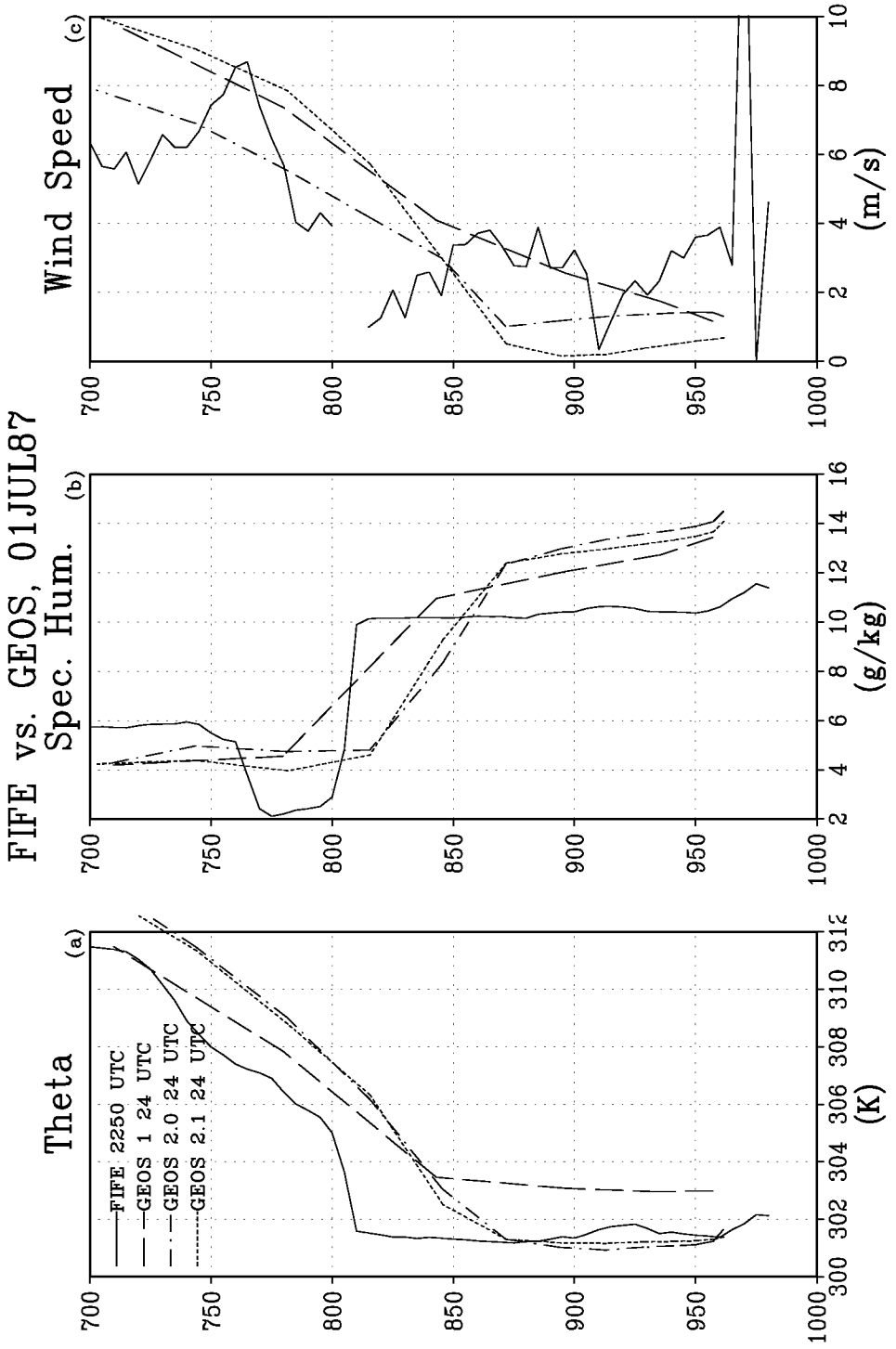

Figure 21: Vertical profiles near 00 UTC 02 JUL for FIFE PBL observations (the legend indicates launch time) and GEOS PBL profiles of (a) potential temperature, (b) specific humidity, and (c) wind velocity (note that 24 UTC equates to 00 UTC of the following day).

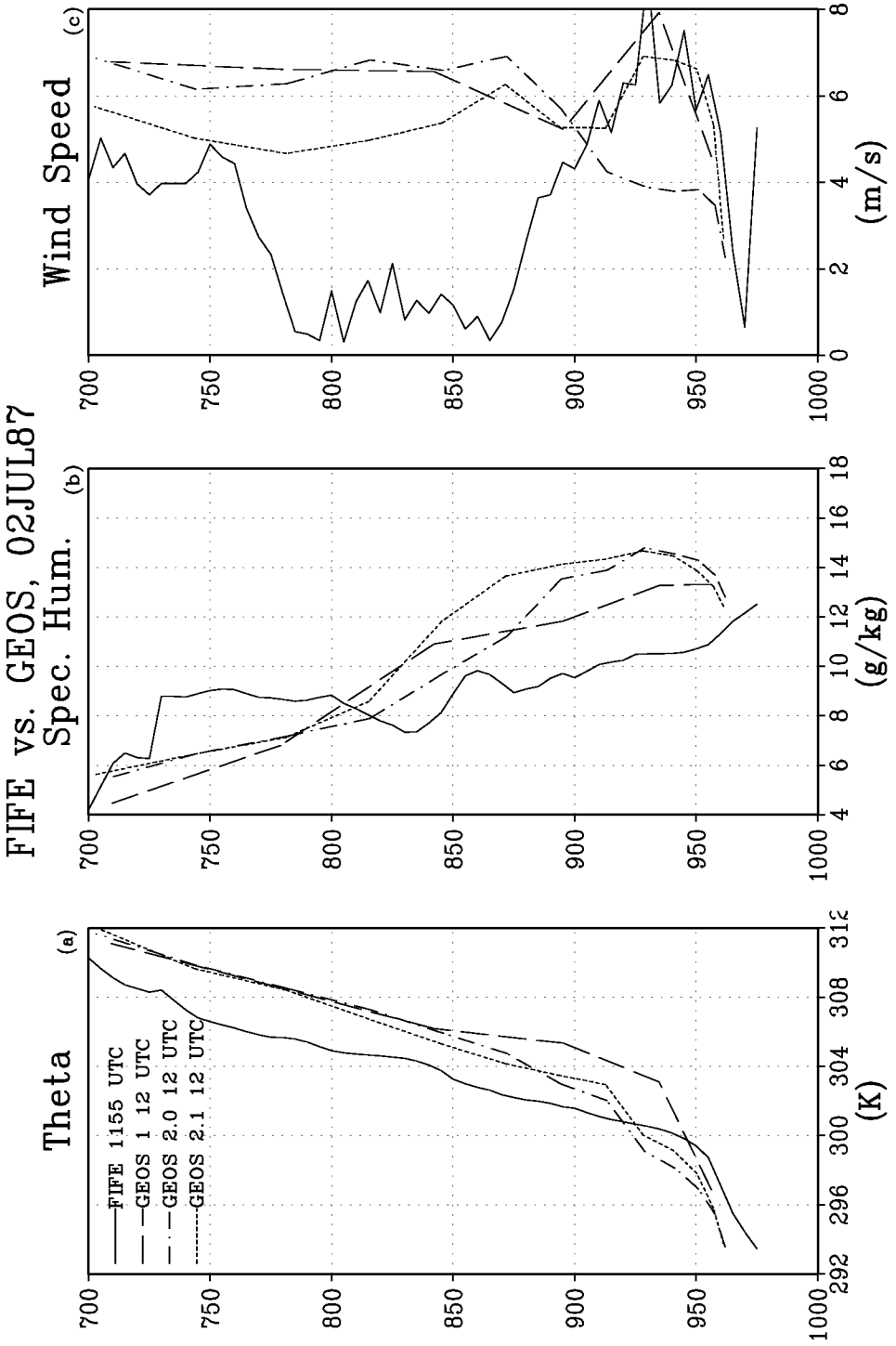

Figure 22: Vertical profiles for 12 UTC 02 JUL for FIFE PBL observations (the legend indicates launch time) and GEOS PBL profiles of (a) potential temperature, (b) specific humidity, and (c) wind velocity.

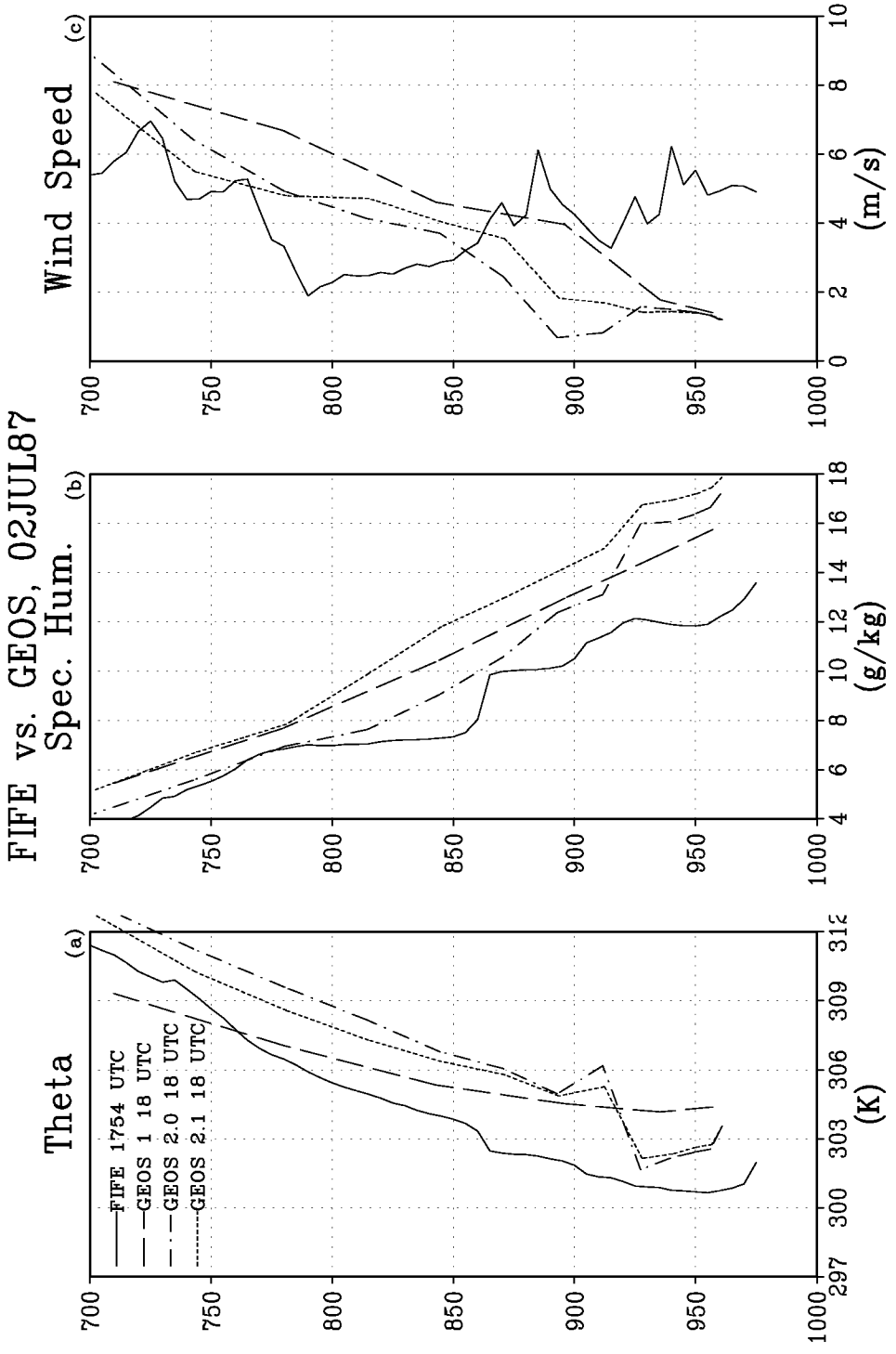

Figure 23: Vertical profiles for 18 UTC 02 JUL for FIFE PBL observations (the legend indicates launch time) and GEOS PBL profiles of (a) potential temperature, (b) specific humidity, and (c) wind velocity.

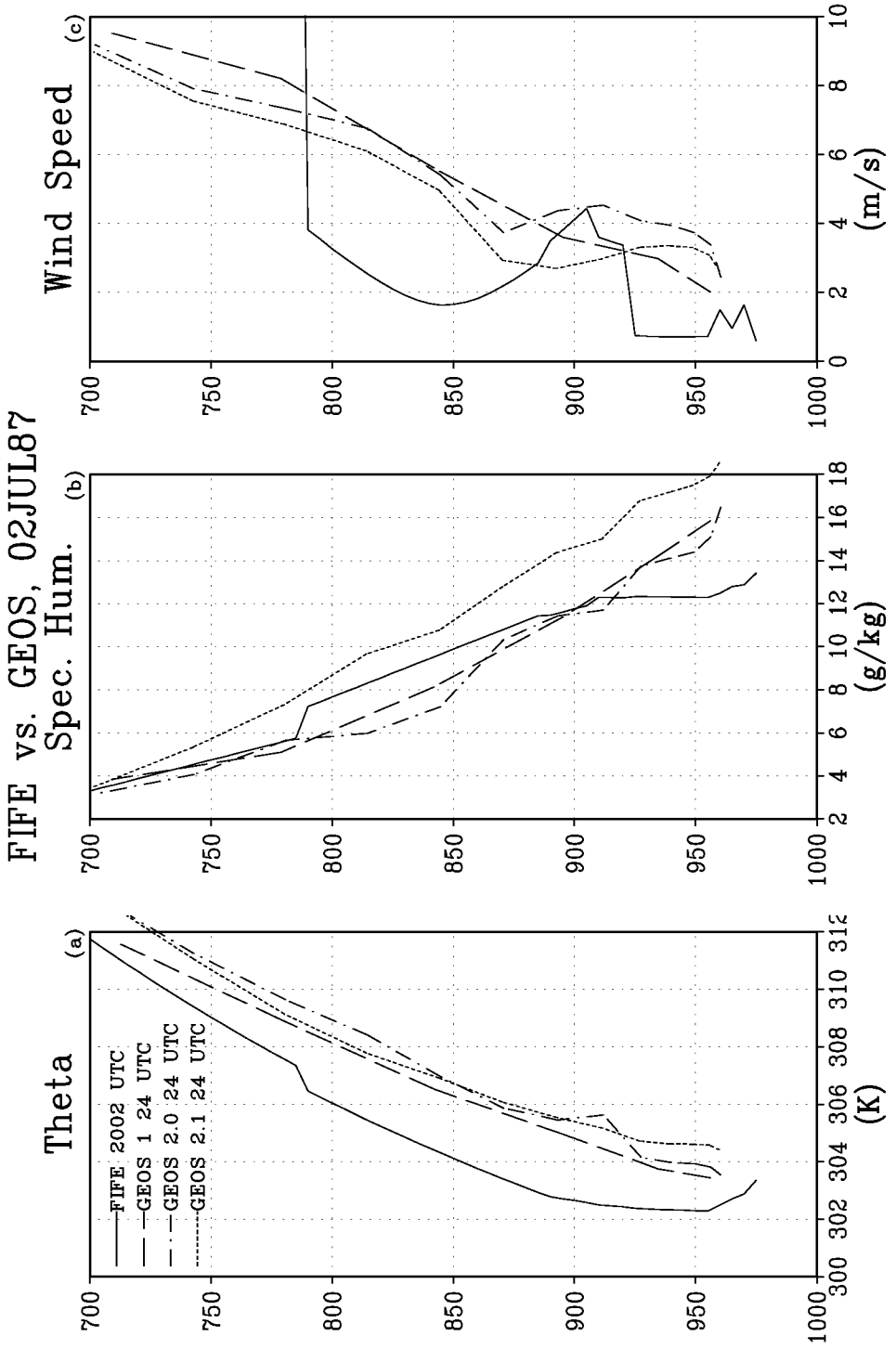

Figure 24: Vertical profiles near 00 UTC 03 JUL for FIFE PBL observations (the legend indicates launch time) and GEOS PBL profiles of (a) potential temperature, (b) specific humidity, and (c) wind velocity (note that 24 UTC equates to 00 UTC of the following day).

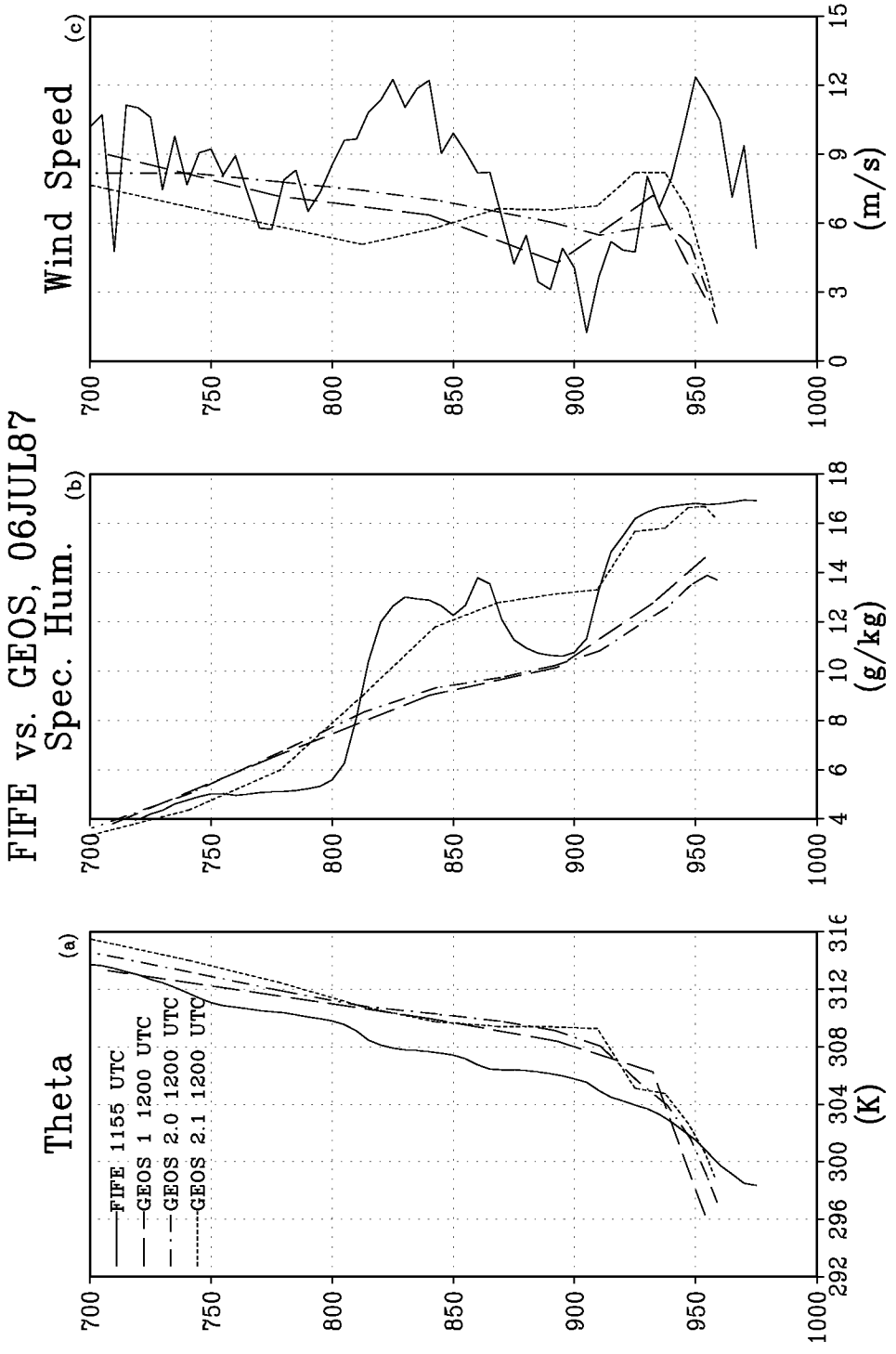

Figure 25: Vertical profiles for 12 UTC 06 JUL for FIFE PBL observations (the legend indicates launch time) and GEOS PBL profiles of (a) potential temperature, (b) specific humidity, and (c) wind velocity.

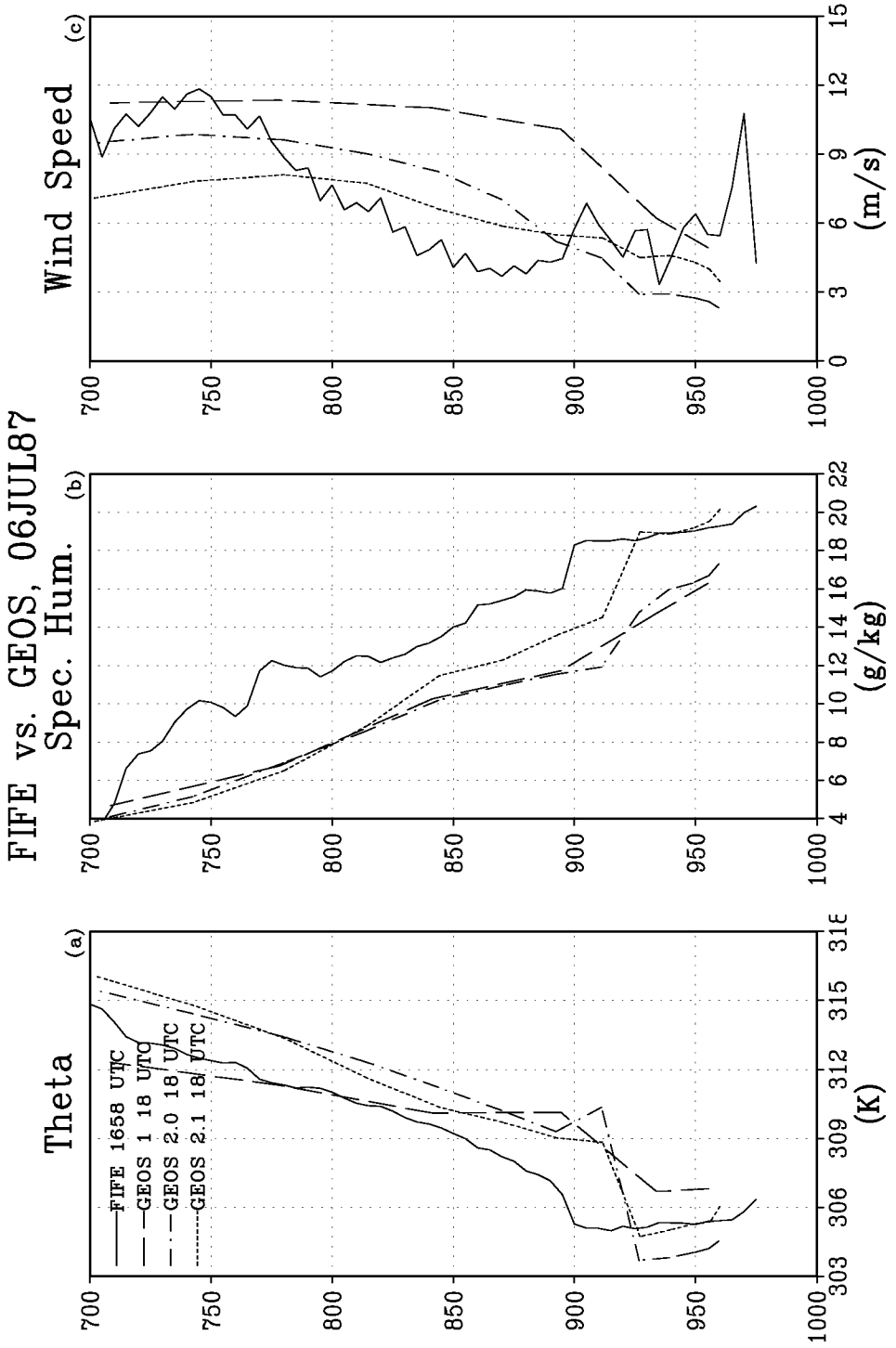

Figure 26: Vertical profiles for 18 UTC 06 JUL for FIFE PBL observations (the legend indicates launch time) and GEOS PBL profiles of (a) potential temperature, (b) specific humidity, and (c) wind velocity.

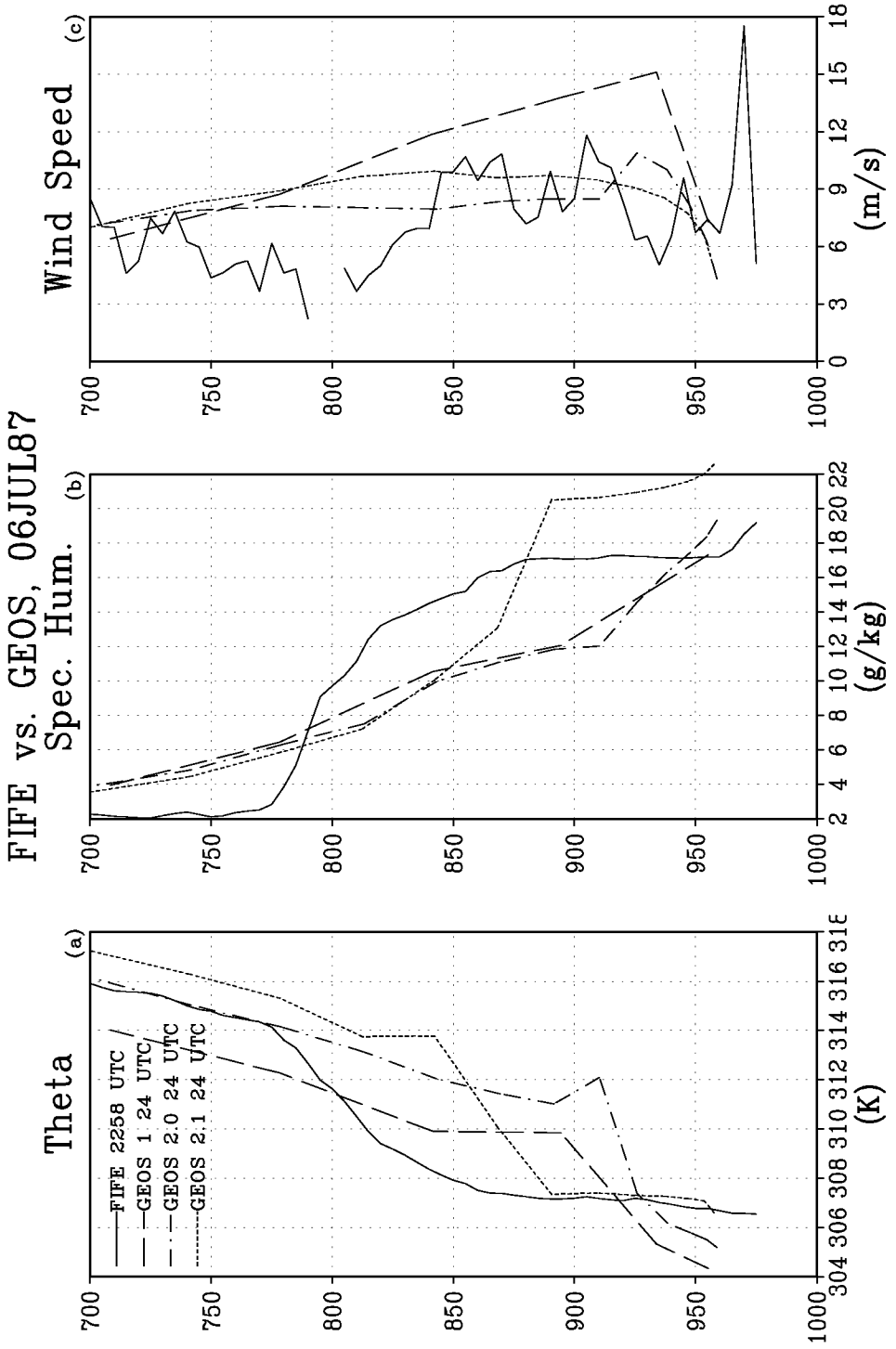

Figure 27: Vertical profiles near 00 UTC 07 JUL for FIFE PBL observations (the legend indicates launch time) and GEOS PBL profiles of (a) potential temperature, (b) specific humidity, and (c) wind velocity (note that 24 UTC equates to 00 UTC of the following day).

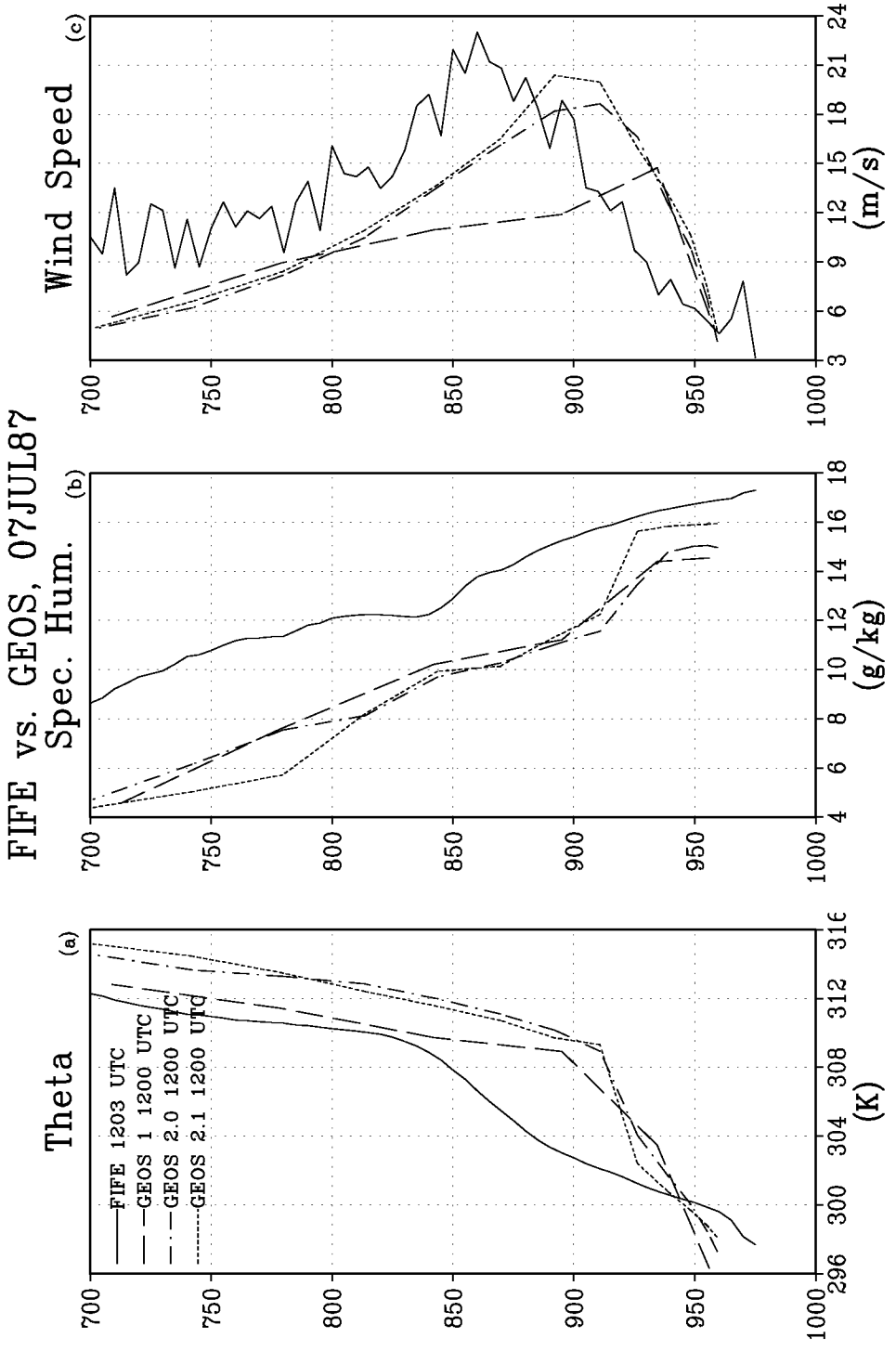

Figure 28: Vertical profiles for 12 UTC 07 JUL for FIFE PBL observations (the legend indicates launch time) and GEOS PBL profiles of (a) potential temperature, (b) specific humidity, and (c) wind velocity.

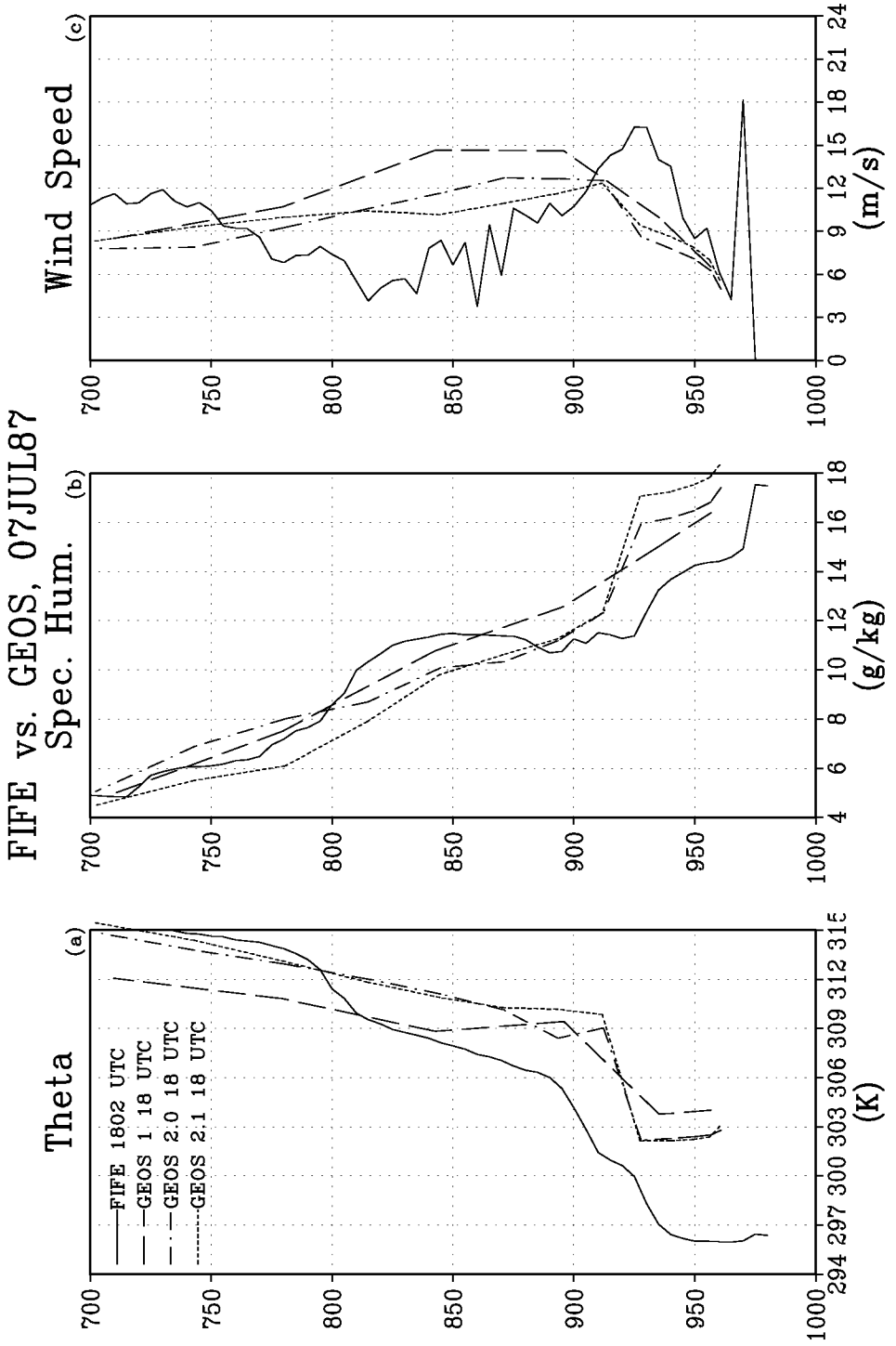

Figure 29: Vertical profiles for 18 UTC 07 JUL for FIFE PBL observations (the legend indicates launch time) and GEOS PBL profiles of (a) potential temperature, (b) specific humidity, and (c) wind velocity.

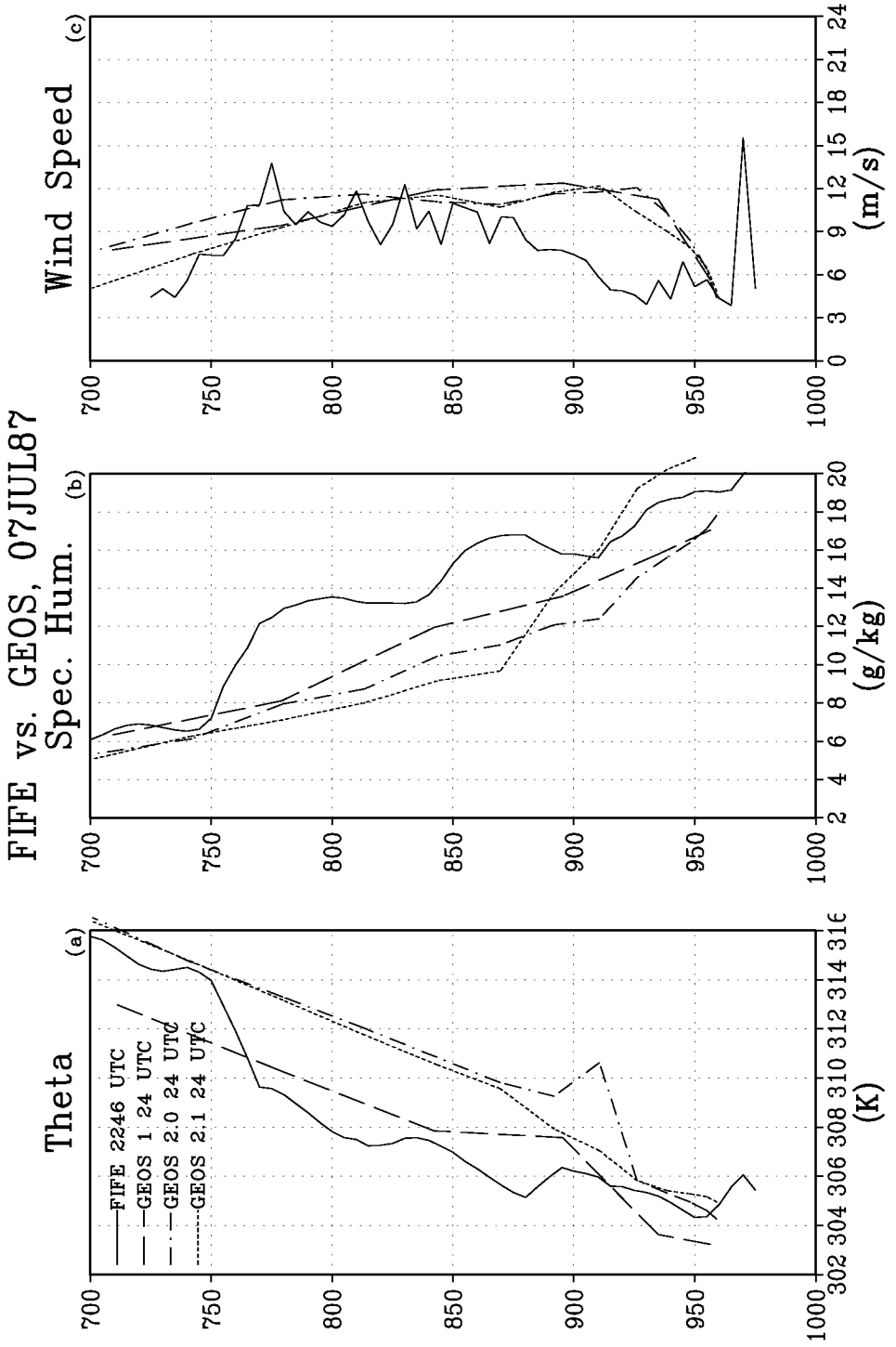

Figure 30: Vertical profiles near 00 UTC 08 JUL for FIFE PBL observations (the legend indicates launch time) and GEOS PBL profiles of (a) potential temperature, (b) specific humidity, and (c) wind velocity (note that 24 UTC equates to 00 UTC of the following day).

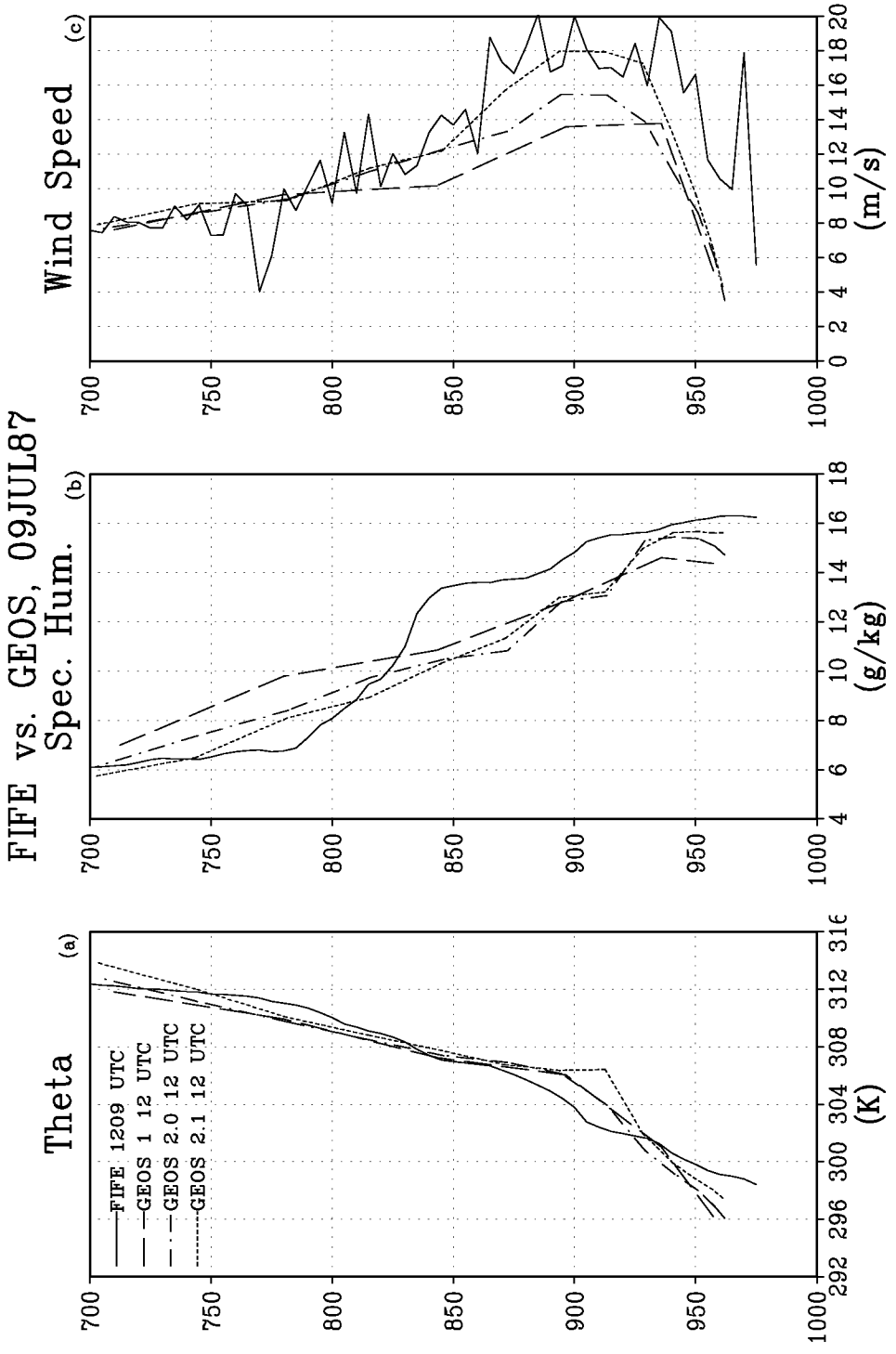

Figure 31: Vertical profiles for 12 UTC 09 JUL for FIFE PBL observations (the legend indicates launch time) and GEOS PBL profiles of (a) potential temperature, (b) specific humidity, and (c) wind velocity.

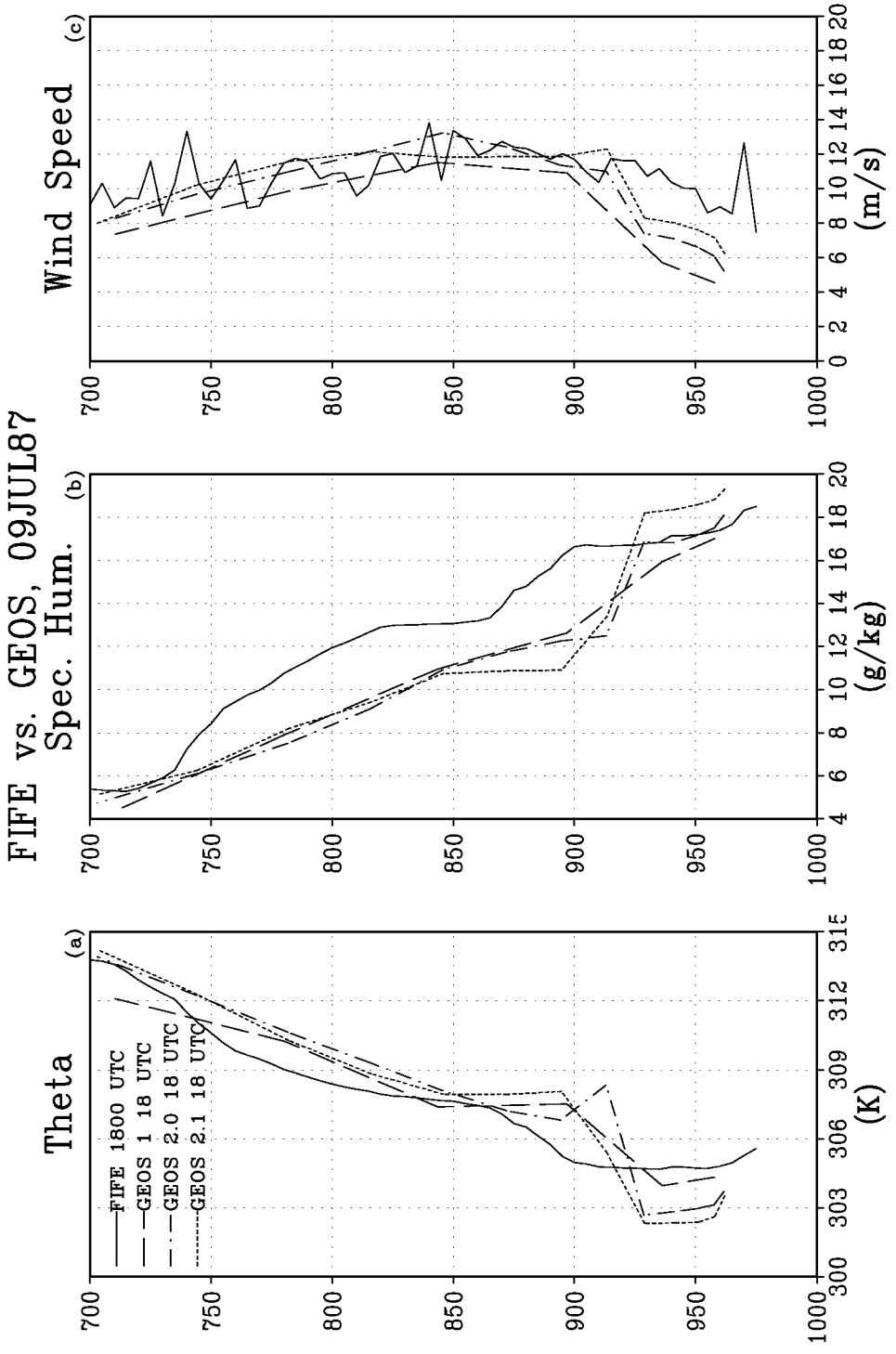

Figure 32: Vertical profiles for 18 UTC 09 JUL for FIFE PBL observations (the legend indicates launch time) and GEOS PBL profiles of (a) potential temperature, (b) specific humidity, and (c) wind velocity.

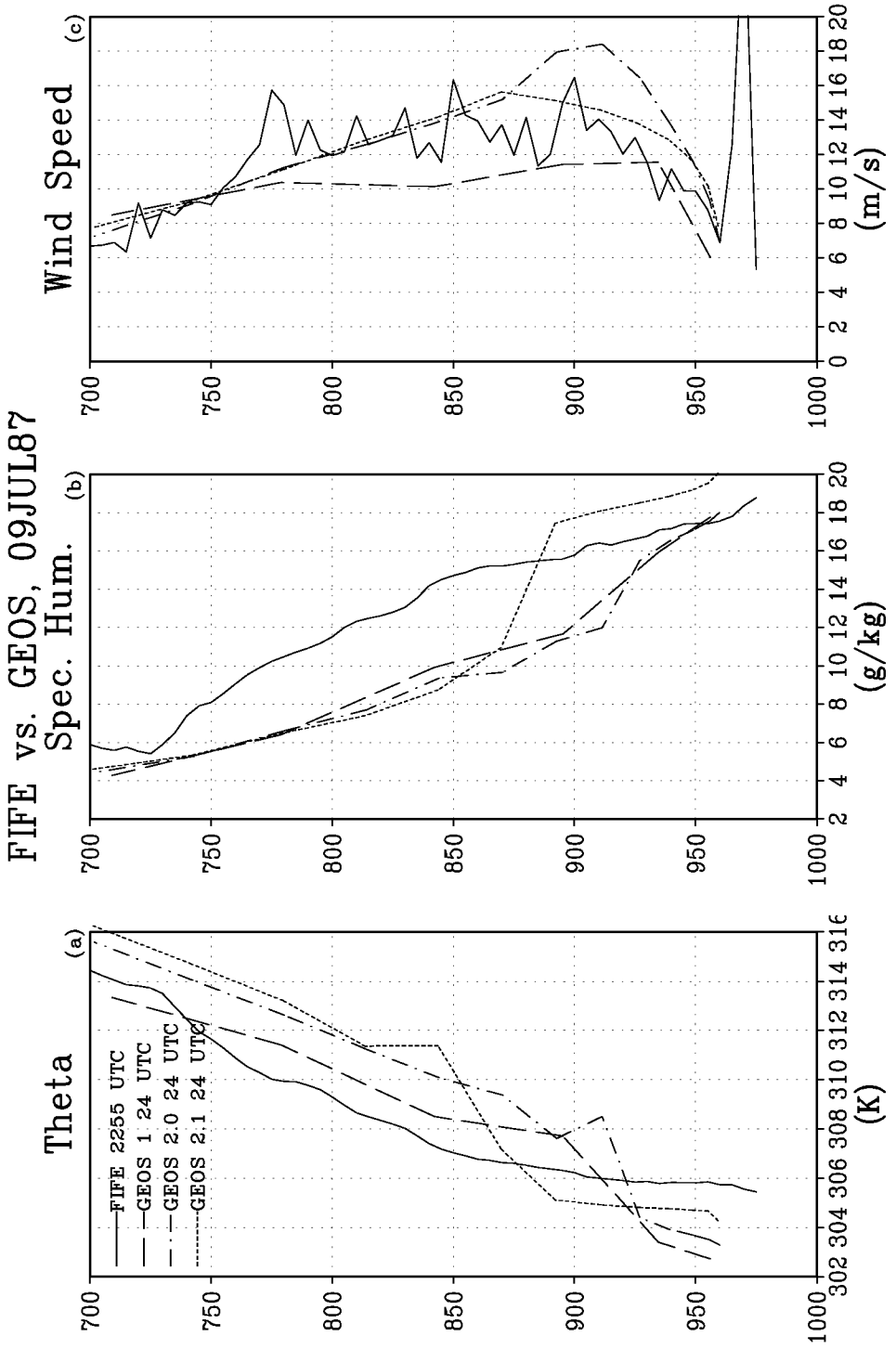

Figure 33: Vertical profiles near 00 UTC 10 JUL for FIFE PBL observations (the legend indicates launch time) and GEOS PBL profiles of (a) potential temperature, (b) specific humidity, and (c) wind velocity (note that 24 UTC equates to 00 UTC of the following day).

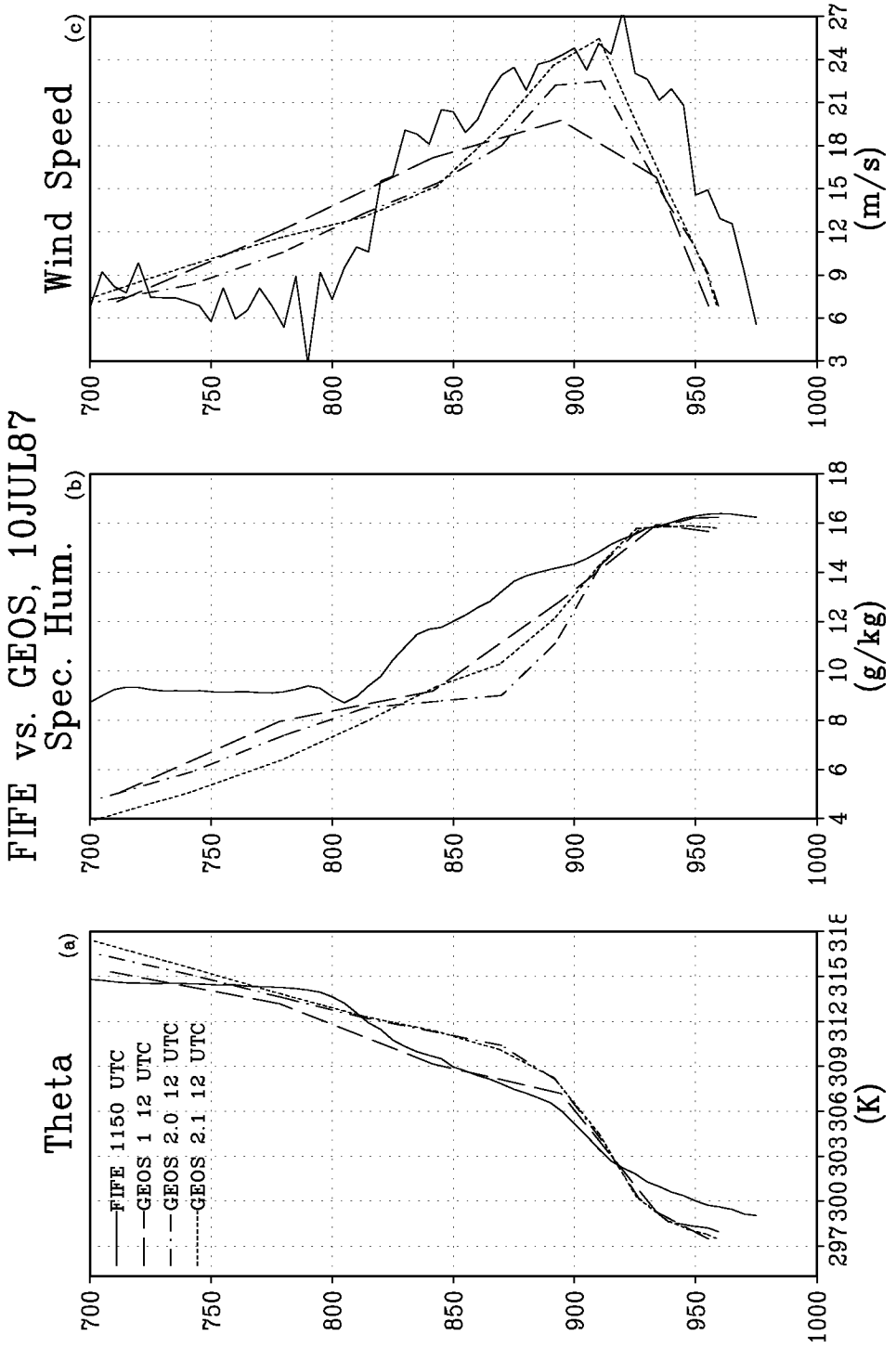

Figure 34: Vertical profiles for 12 UTC 10 JUL for FIFE PBL observations (the legend indicates launch time) and GEOS PBL profiles of (a) potential temperature, (b) specific humidity, and (c) wind velocity.

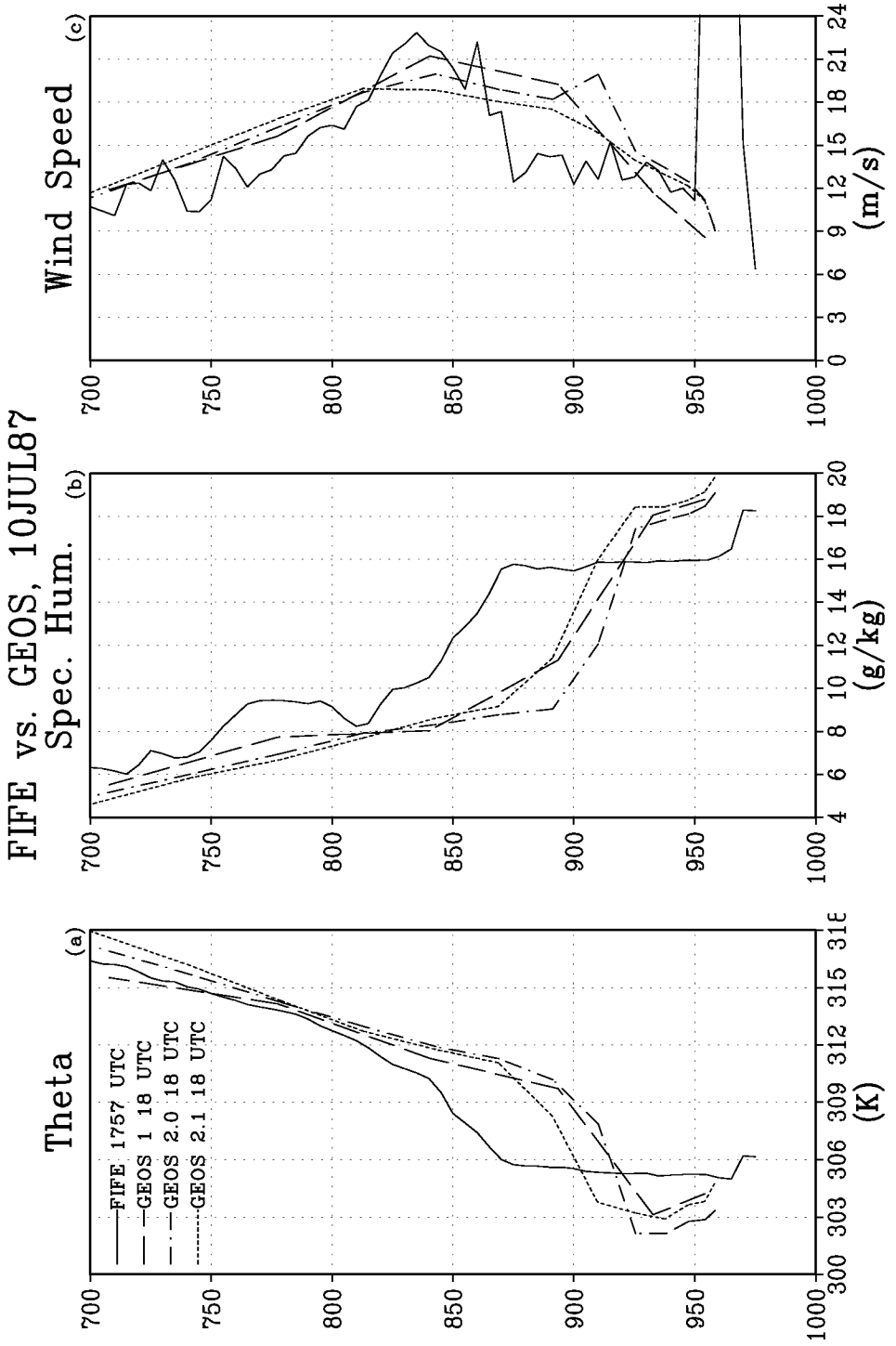

Figure 35: Vertical profiles for 18 UTC 10 JUL for FIFE PBL observations (the legend indicates launch time) and GEOS PBL profiles of (a) potential temperature, (b) specific humidity, and (c) wind velocity.

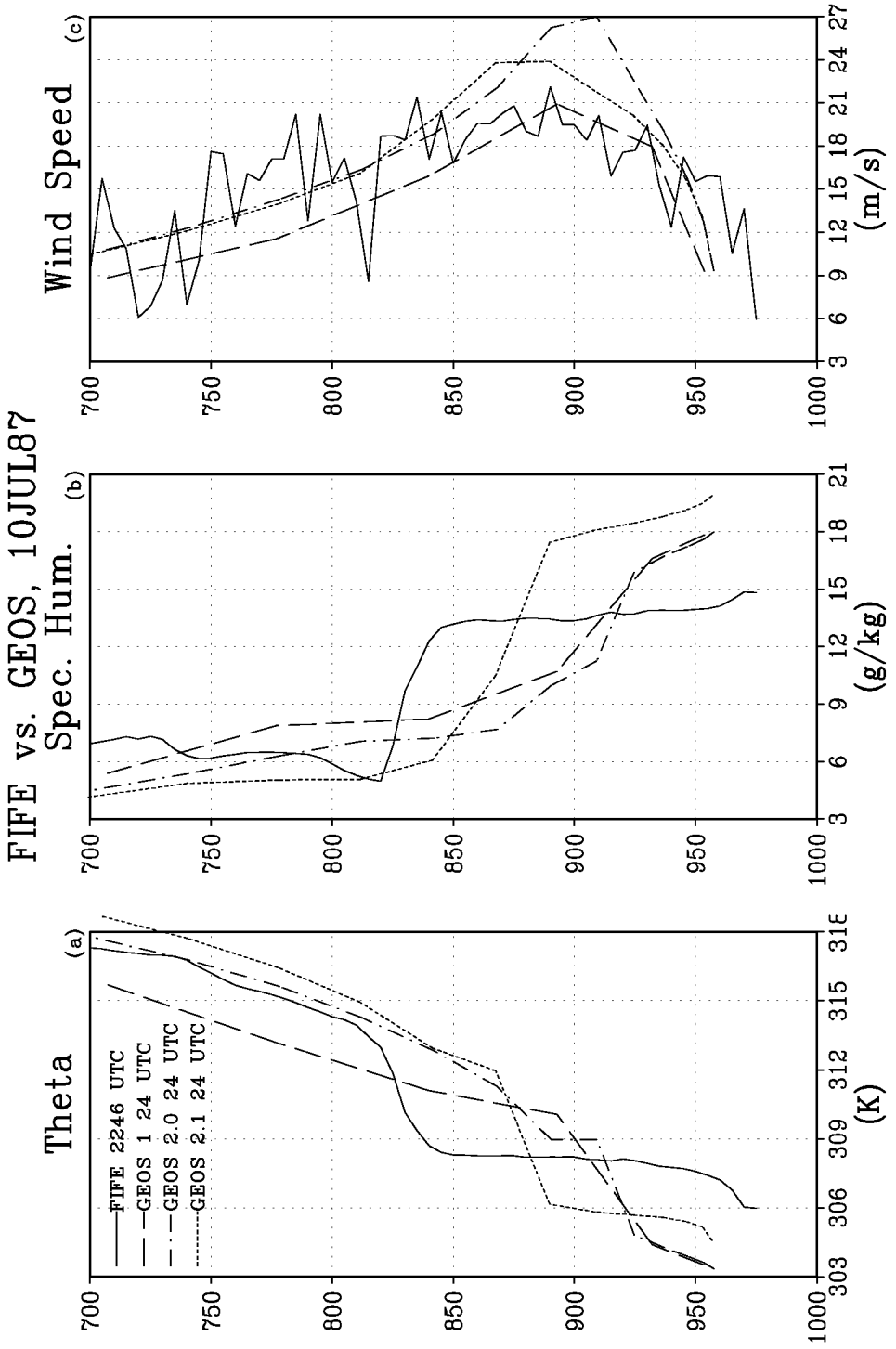

Figure 36: Vertical profiles near 00 UTC 11 JUL for FIFE PBL observations (the legend indicates launch time) and GEOS PBL profiles of (a) potential temperature, (b) specific humidity, and (c) wind velocity (note that 24 UTC equates to 00 UTC of the following day).

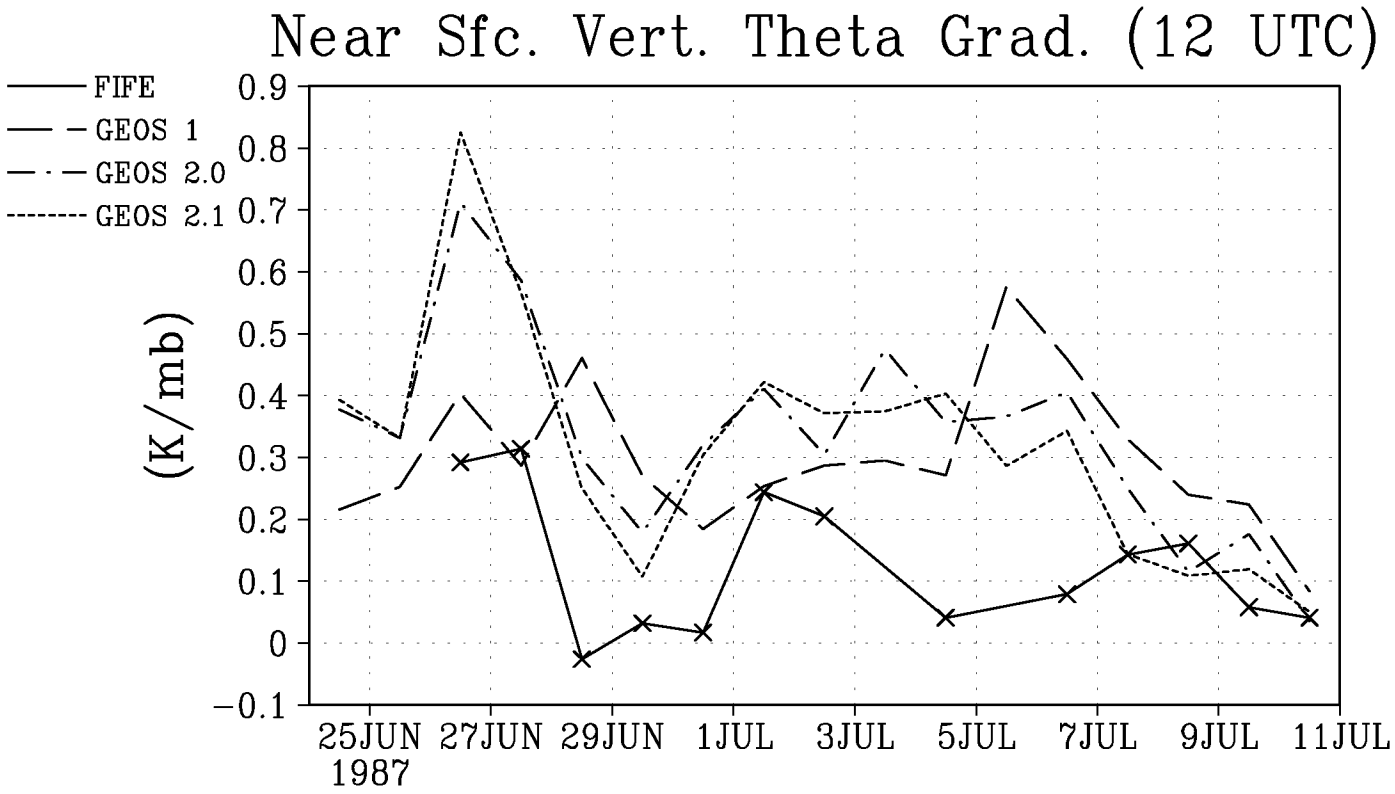

Figure 37: Vertical potential temperature gradient ($-\Delta\theta/\Delta p$) near the surface at 12 UTC. FIFE data is computed in the lowest 10 mb. GEOS-1 data is computed over the lowest two sigma levels (Δp=-22 mb). GEOS 2.0 and 2.1 are computed over the lowest three sigma levels (Δp=-11 mb).

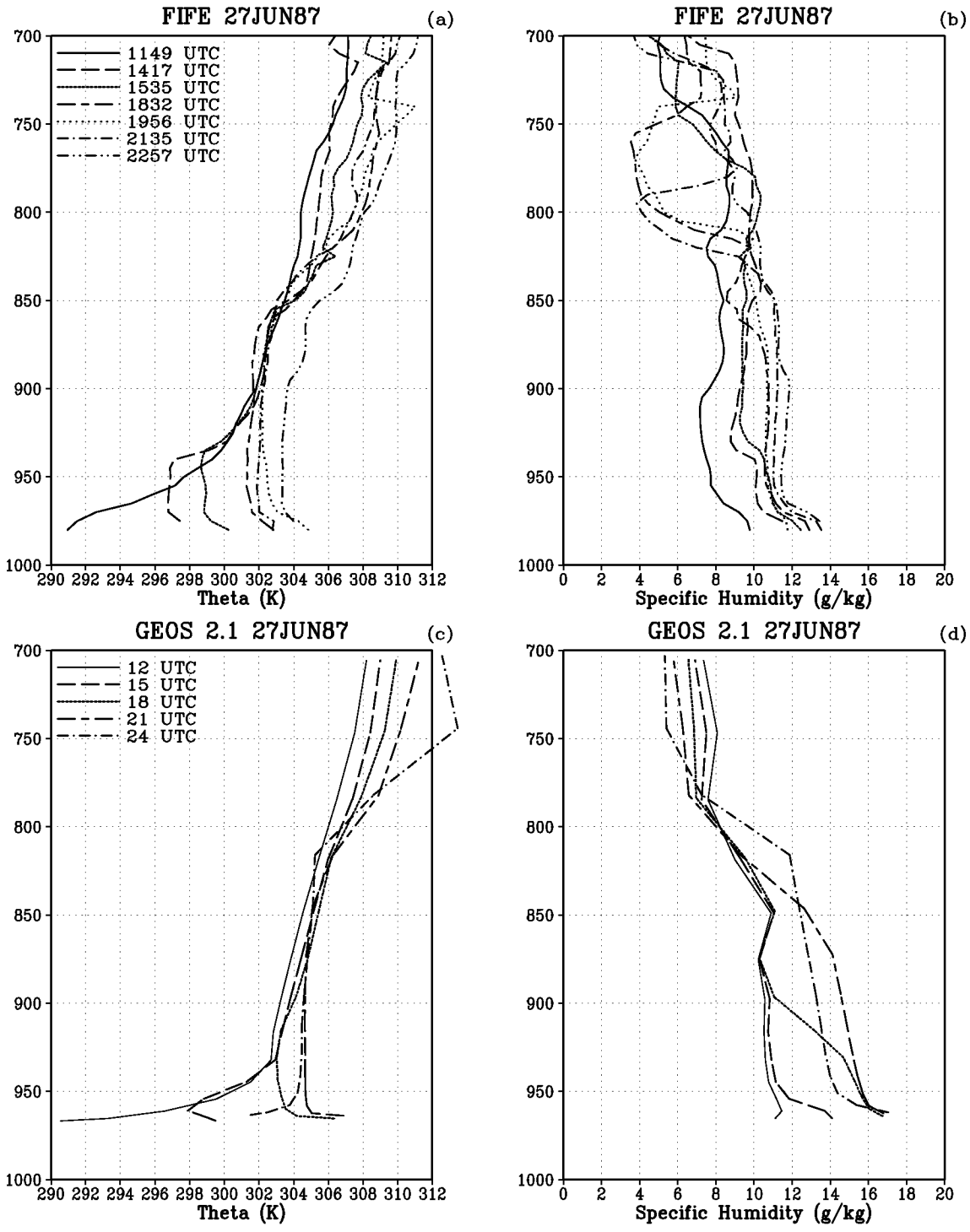

Figure 38: FIFE PBL observations for 27 JUN 87 of (a) potential temperature and (b) specific humidity. GEOS 2.1 PBL profiles for 27 JUN 87 of (c) potential temperature and (d) specific humidity.

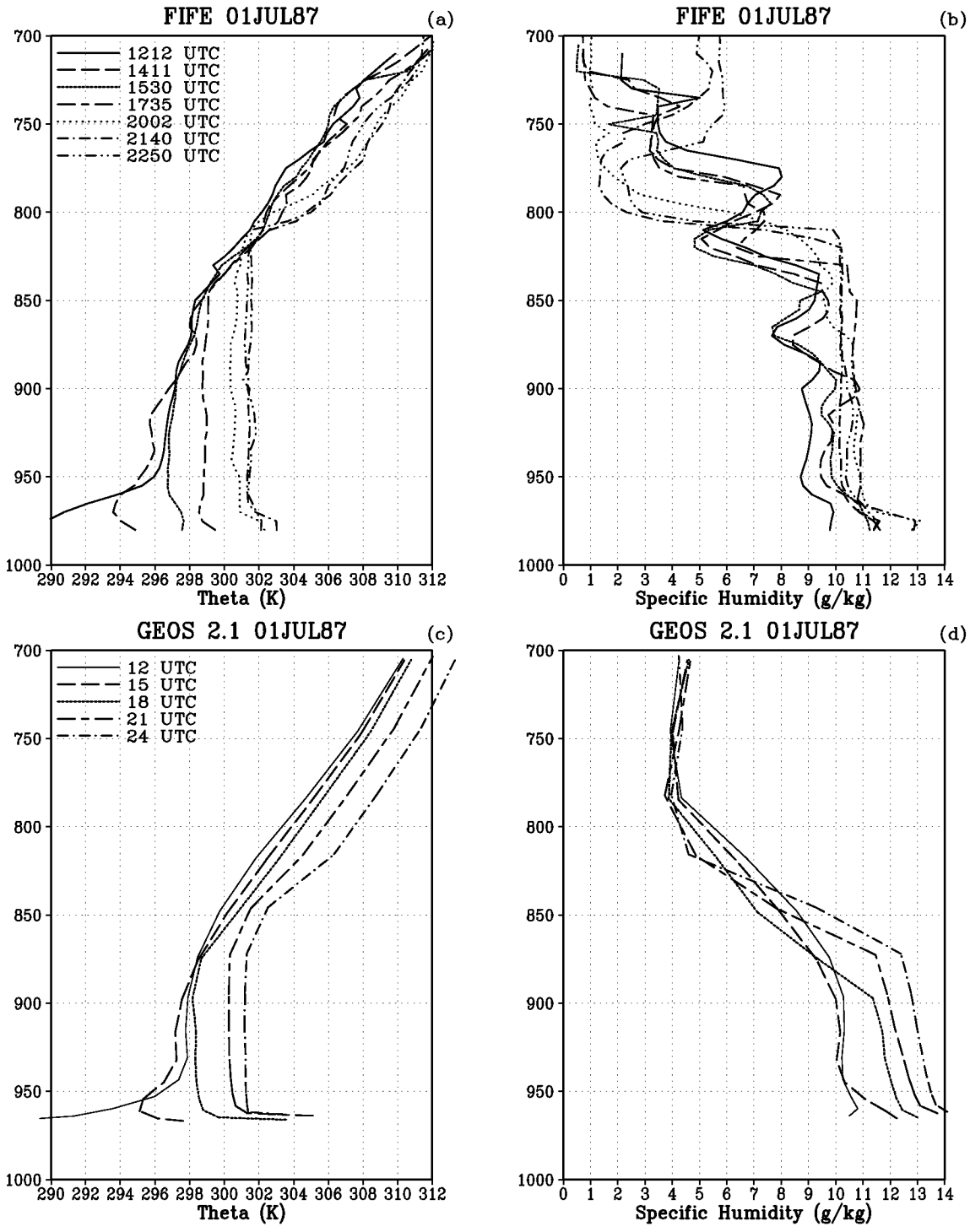

Figure 39: FIFE PBL observations for 01 JUL 87 of (a) potential temperature and (b) specific humidity. GEOS 2.1 PBL profiles for 01 JUL 87 of (c) potential temperature and (d) specific humidity.

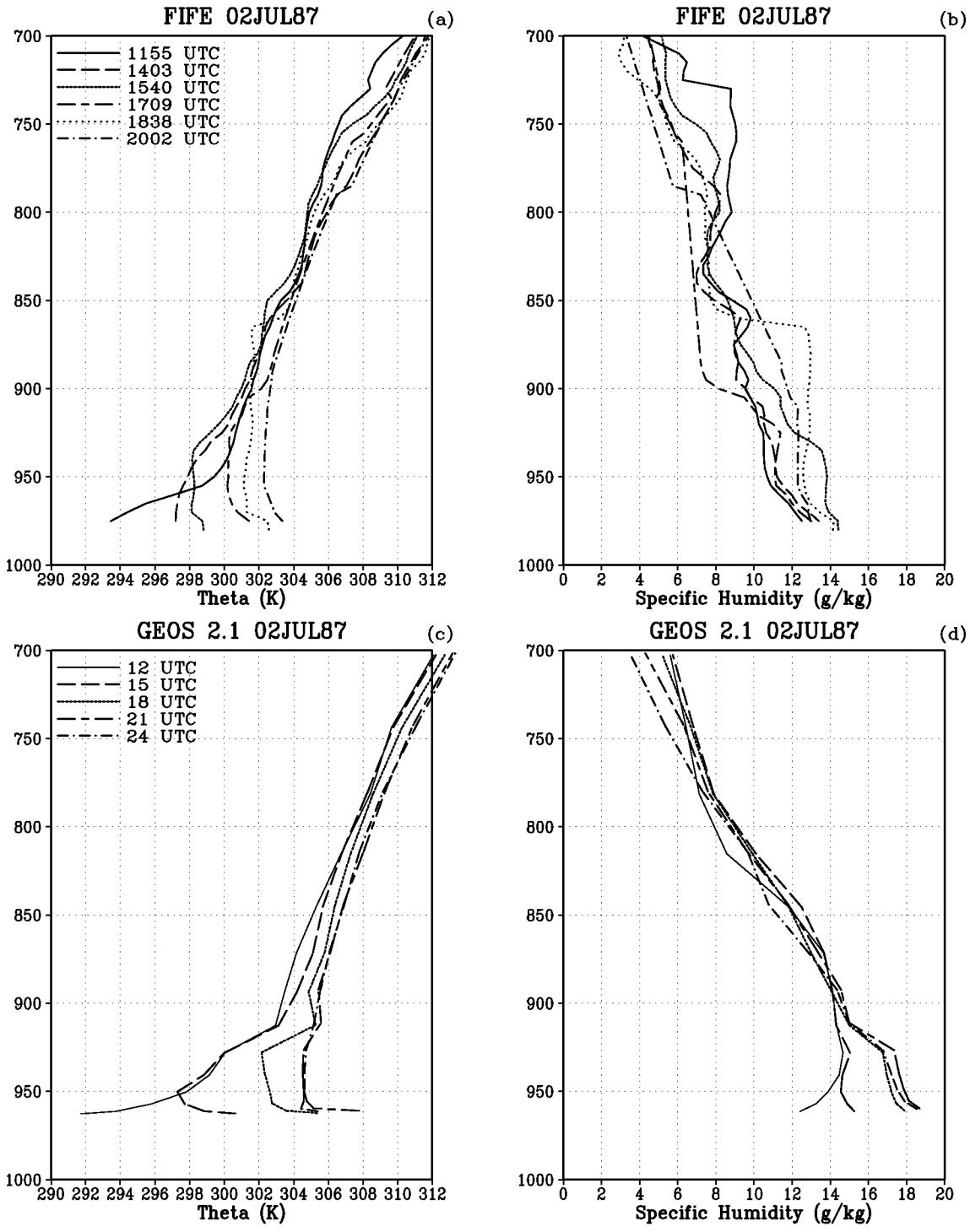

Figure 40: FIFE PBL observations for 02 JUL 87 of (a) potential temperature and (b) specific humidity. GEOS 2.1 PBL profiles for 02 JUL 87 of (c) potential temperature and (d) specific humidity.

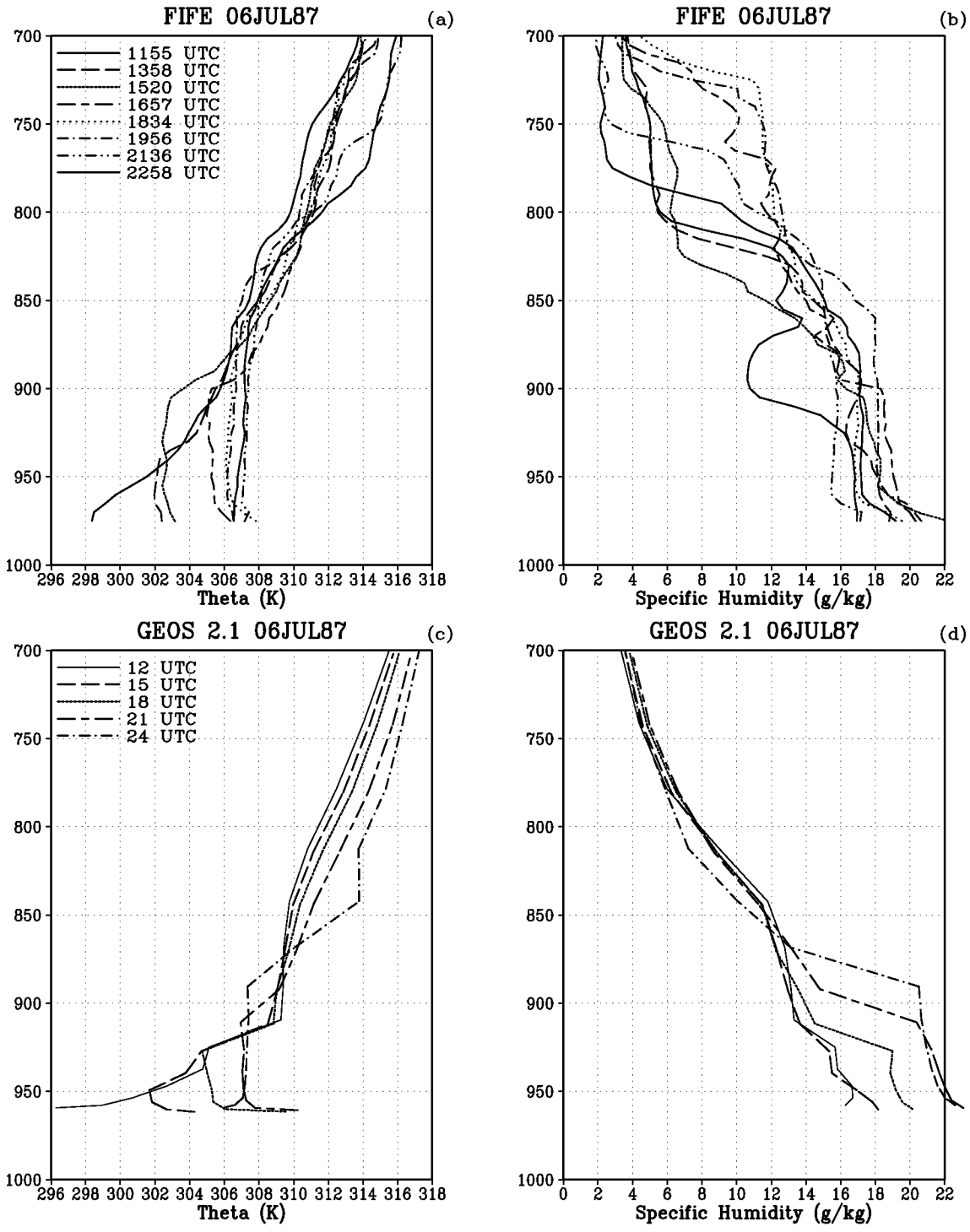

Figure 41: FIFE PBL observations for 06 JUL 87 of (a) potential temperature and (b) specific humidity. GEOS 2.1 PBL profiles for 06 JUL 87 of (c) potential temperature and (d) specific humidity.

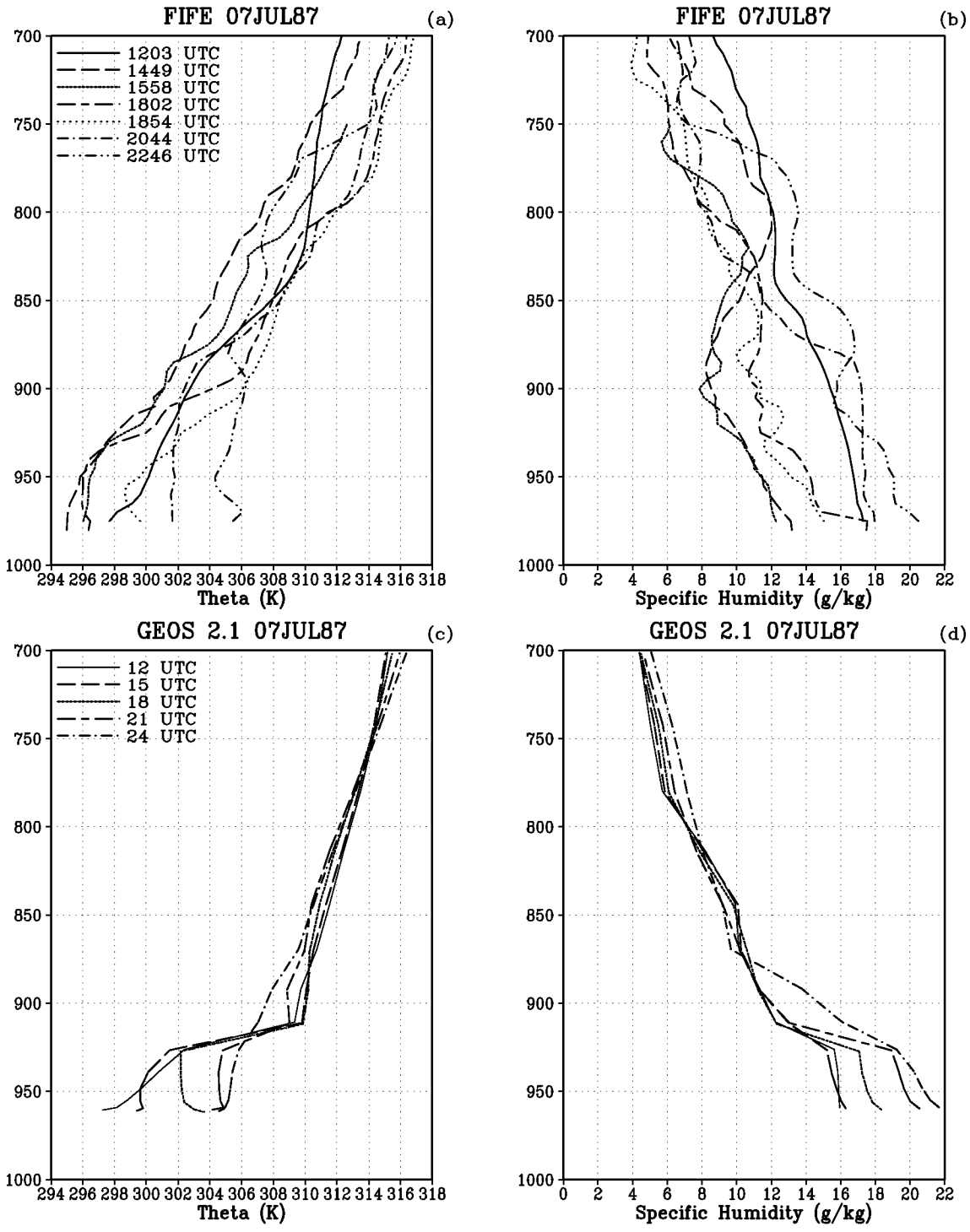

Figure 42: FIFE PBL observations for 07 JUL 87 of (a) potential temperature and (b) specific humidity. GEOS 2.1 PBL profiles for 07 JUL 87 of (c) potential temperature and (d) specific humidity.

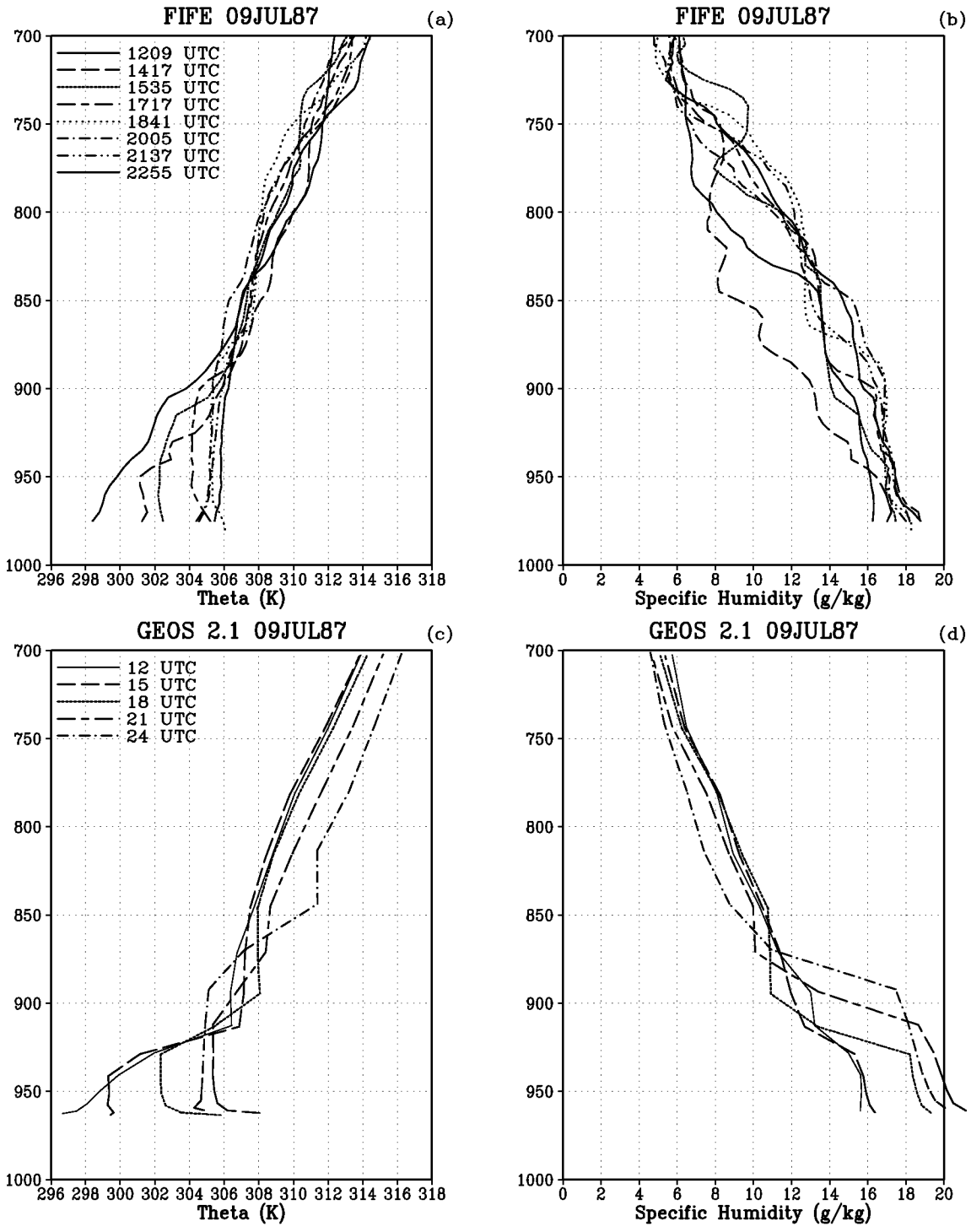

Figure 43: FIFE PBL observations for 09 JUL 87 of (a) potential temperature and (b) specific humidity. GEOS 2.1 PBL profiles for 09 JUL 87 of (c) potential temperature and (d) specific humidity.

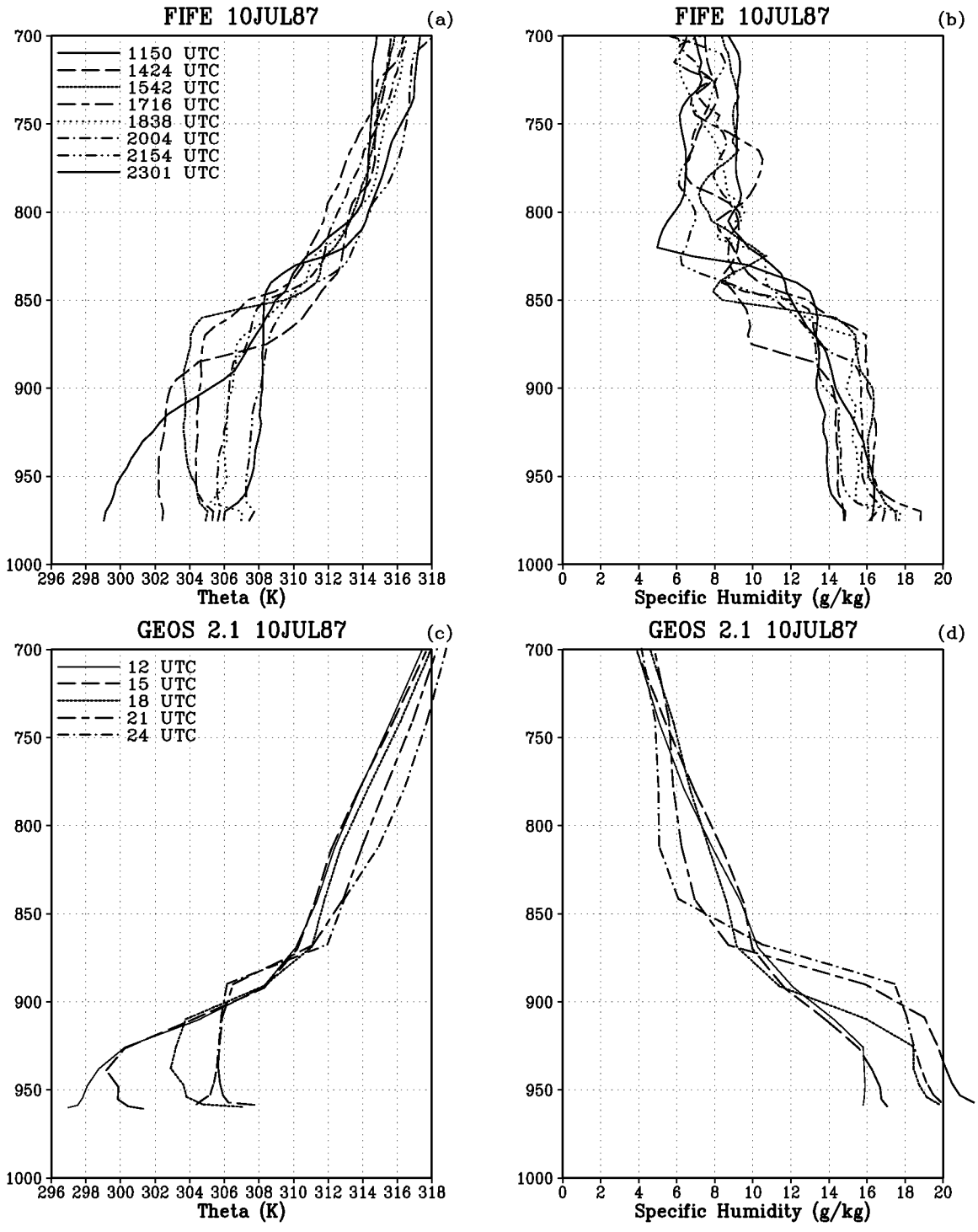

Figure 44: FIFE PBL observations for 10 JUL 87 of (a) potential temperature and (b) specific humidity. GEOS 2.1 PBL profiles for 10 JUL 87 of (c) potential temperature and (d) specific humidity.

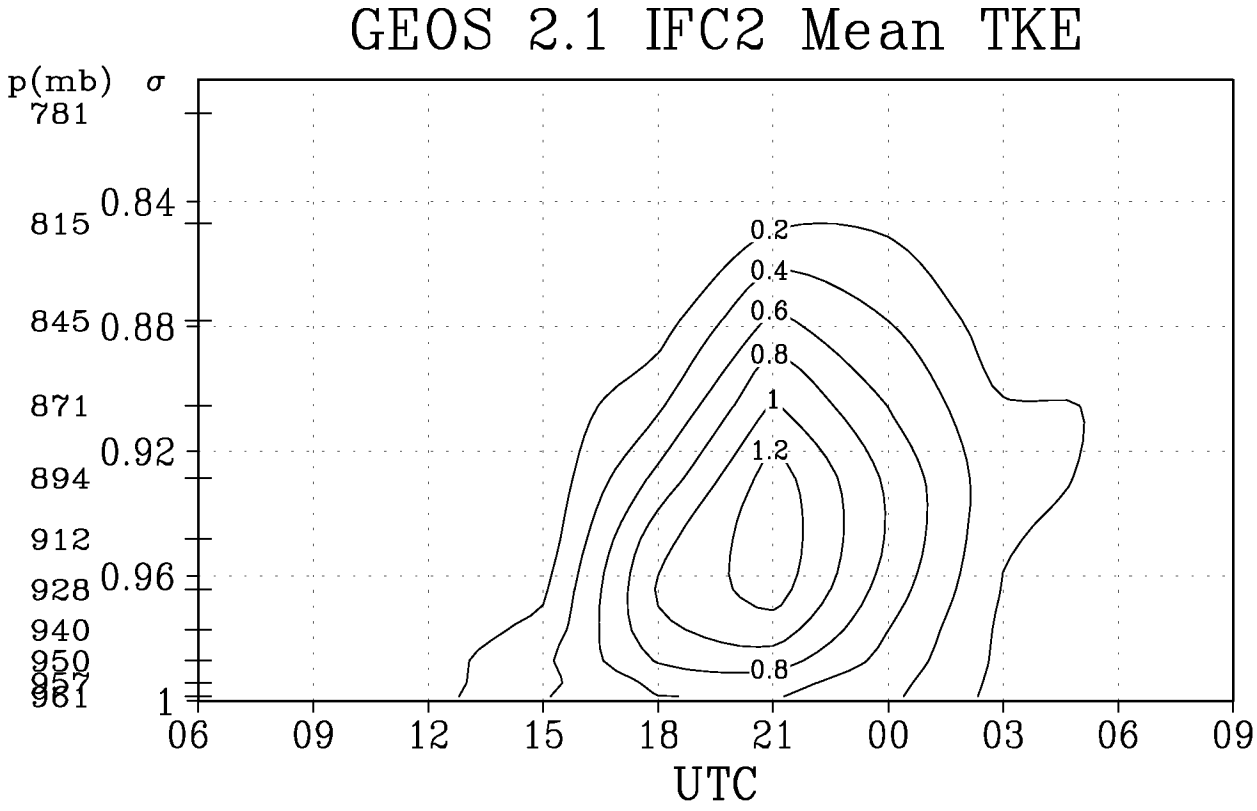

Figure 45: GEOS 2.1 IFC2 mean diurnal cycle of turbulent kinetic energy ($m^2 s^{-2}$). Plot is in model sigma coordinates, with mean pressure for each sigma level labeled on the left.

2.5 1988 Summer (June and July)

GEOS 2.0 and 2.1 validation experiments were also performed for the summer of 1988, specifically June and July. These were going to be included in the previous discussions on the daily mean and diurnal cycles. Analysis of the data, however, yielded some substantially different results compared to that of IFC2. It is important to note that the quantity of FIFE observations during the summer of 1988 is lower than 1987 or 1989. There were no IFCs or PBL observations during 1988. The fewer number of stations during likely influence the site-averages. We note that the the central United States experienced severe drought conditions during the spring and summer of 1988 with especially dry conditions during May and June.

During the analysis of the 1988 GEOS assimilations, a significant difference was identified in the monthly mean June and July energy budgets. The differences are quite apparent in the time series of daytime mean (from 12 UTC - 00 UTC) evaporative fraction (Fig. 46, where $EF = LE/(LE + H_s)$). During June of 1988, the magnitude of GEOS daytime mean EF resembles that of the observations. However, the observed EF maintains a steady magnitude into July, while the GEOS EF continues a downward trend (see also table 2). Closer examination of the turbulent fluxes shows that the GEOS sensible heating is slightly larger than FIFE in June, and increases dramatically in July (Fig. 47). The GEOS latent heat flux, on the other hand, is too large during June, and smaller in July (Fig. 48). This affects the near surface atmospheric temperature so that it is too cold in June (especially at night) and too warm during July, especially during the day (Fig. 49).

Table 2: June and July 1988 monthly mean evaporative fraction and soil wetness for GEOS and FIFE. Note that FIFE soil wetness is in volumetric units ($m^3 m^{-3}$), while the GEOS wetness is the fraction of potential evapotranspiration.

EF	June	July
FIFE	0.77	0.78
GEOS 2.1	0.76	0.54
GEOS 2.0	0.75	0.55
GEOS 1	0.76	0.54
Wetness		
FIFE	0.21	0.24
GEOS	0.26	0.076

The differences between the GEOS monthly mean energy budgets corresponds to variations in the monthly mean prescribed soil wetness. FIFE gravimetric observations of soil water

(Betts and Ball, 1998) indicate only a slight increase from June to July (table 2). This is consistent with the small variation of FIFE monthly mean EF. GEOS soil wetness, however, undergoes a sharp reduction of soil wetness from June to July, not only at this grid point, but across the whole region. This is consistent with the contrasting June and July monthly mean temperature, sensible heat and latent heat. It is interesting to note that as the GEOS soil wetness becomes very small, the latent heat flux does decrease, but is still quite large. Even though the July latent heat is only slightly less than observations, the surface layer specific humidity is still quite large (Fig. 50). We must conclude that the overestimate of GEOS specific humidity is not entirely related to the surface latent heat. These results and the similarity between each GEOS system demonstrate the effect that prescribed soil water has on the GEOS surface processes.

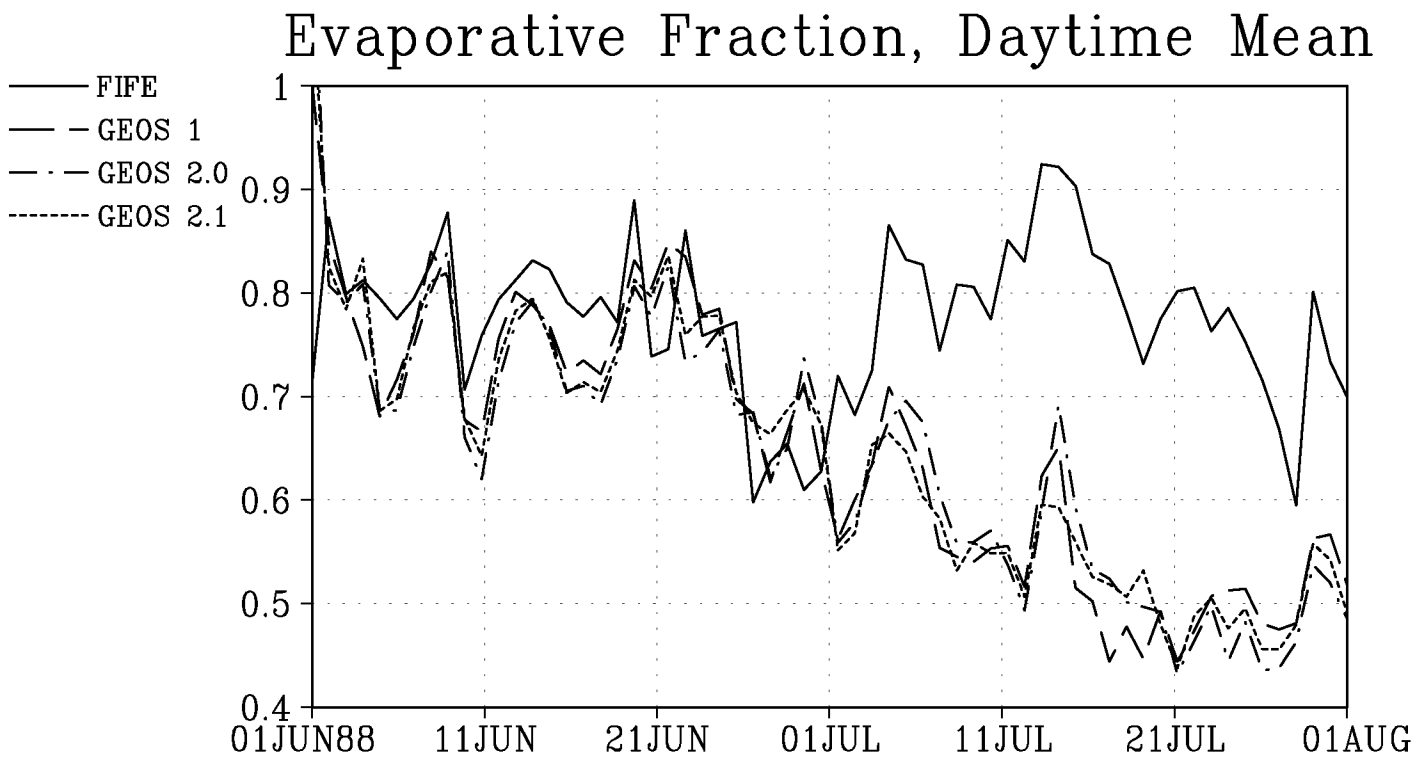

Figure 46: Daytime mean evaporative fraction for June and July 1988 (EF, defined in the text). Daytime mean is from 12 UTC to 00 UTC.

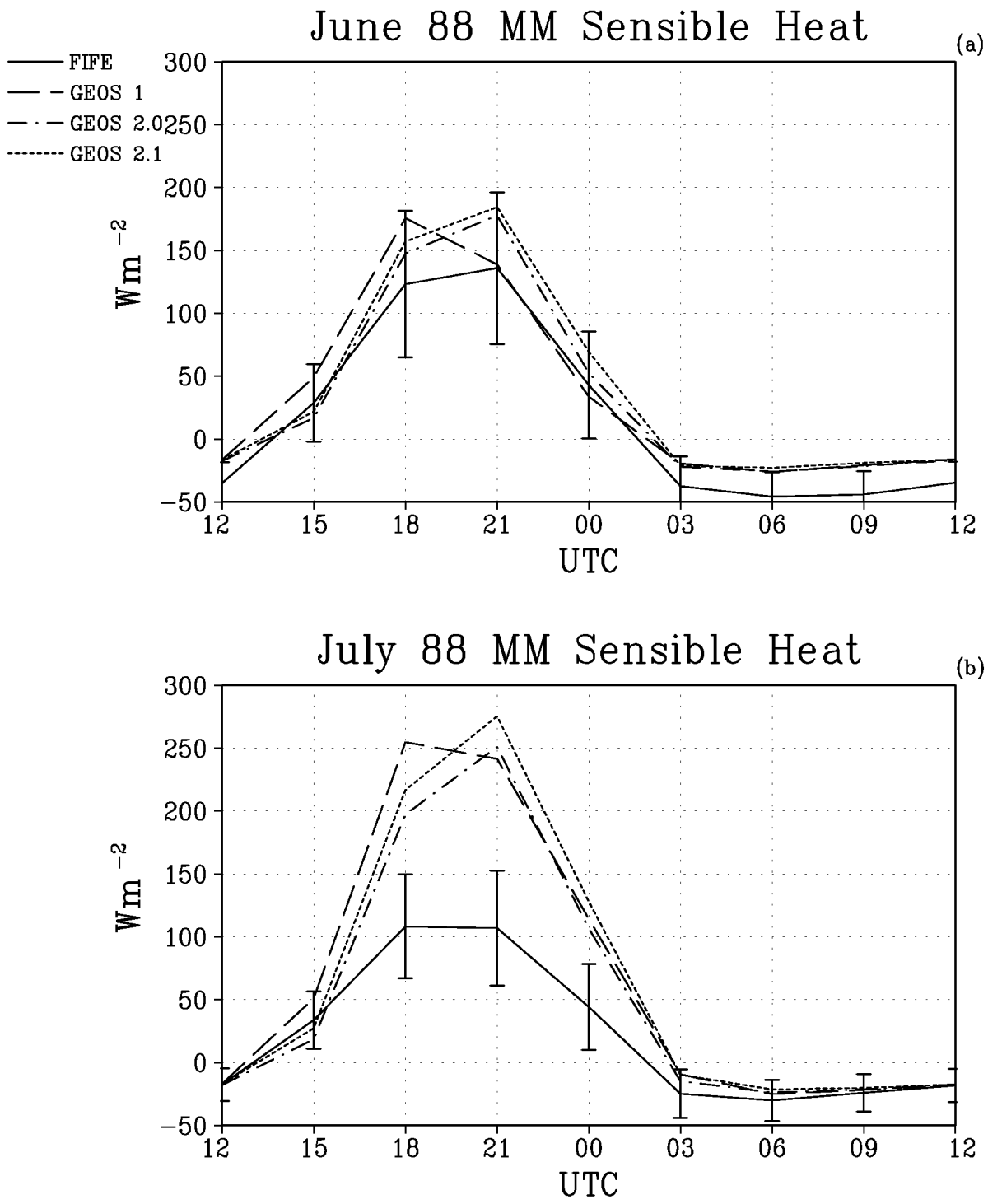

Figure 47: Mean diurnal cycle of sensible heat flux for (a) June 1988, and (b) July 1988.

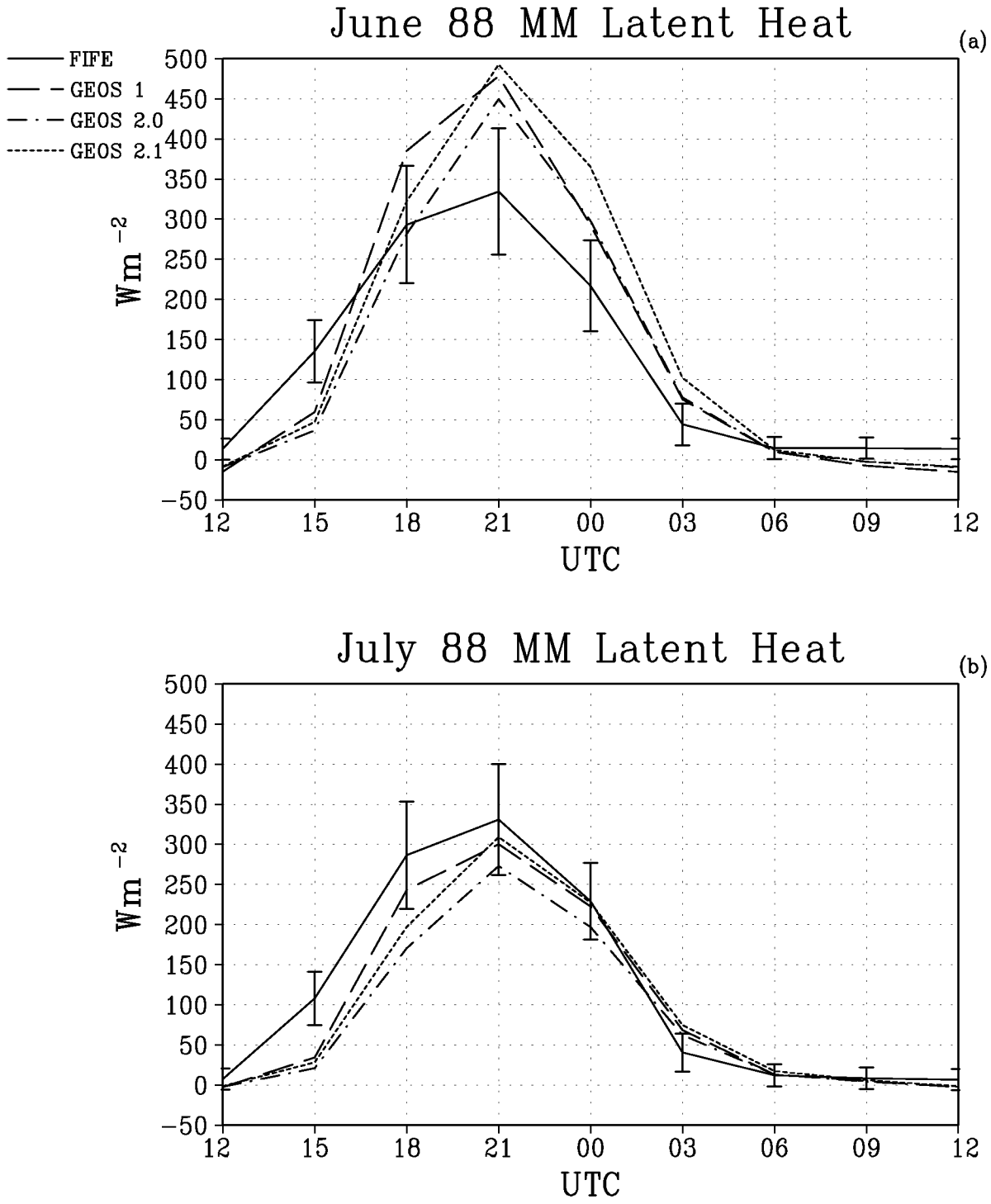

Figure 48: Mean diurnal cycle of latent heat flux for (a) June 1988, and (b) July 1988.

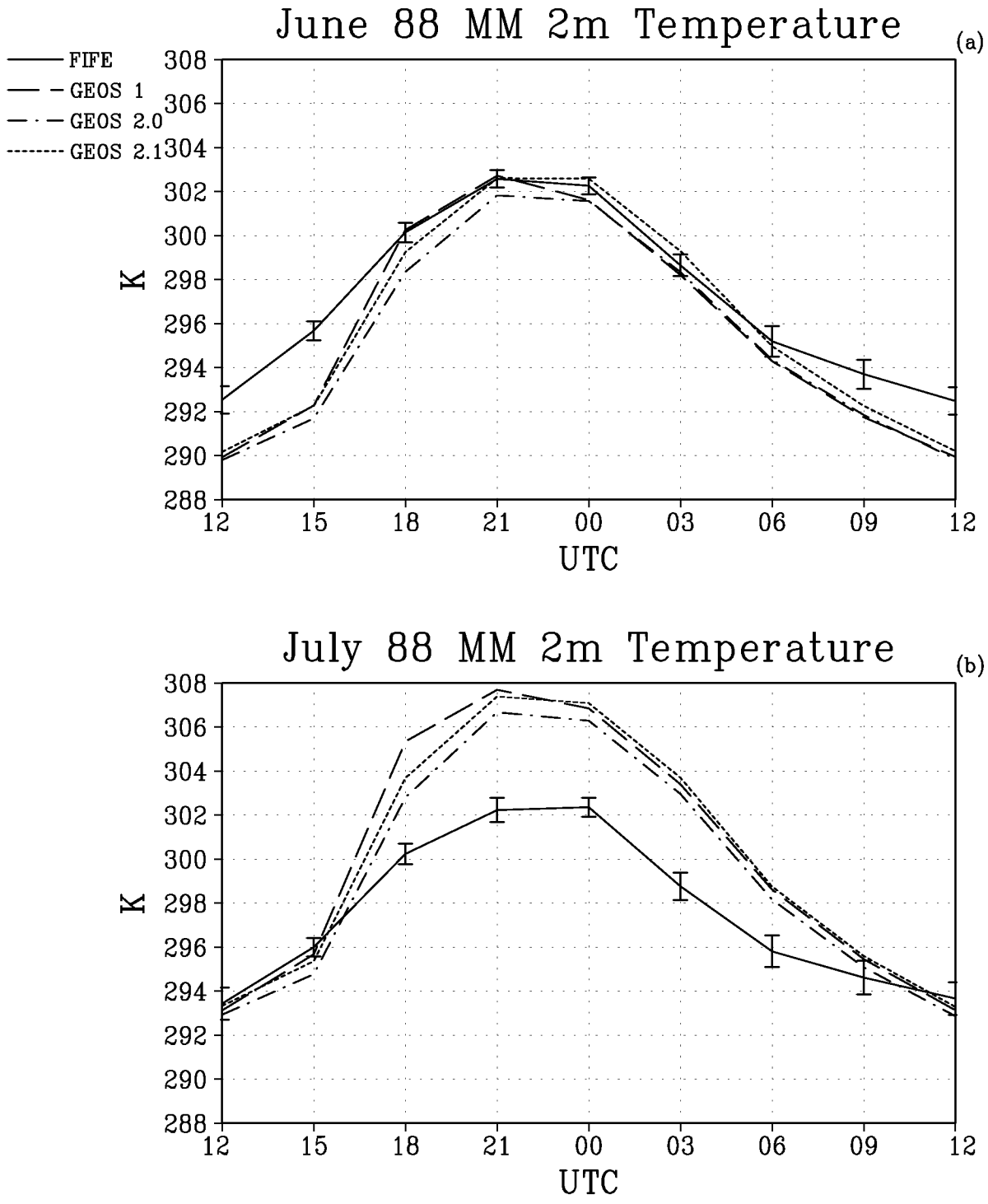

Figure 49: Mean diurnal cycle of two meter temperature for (a) June 1988, and (b) July 1988.

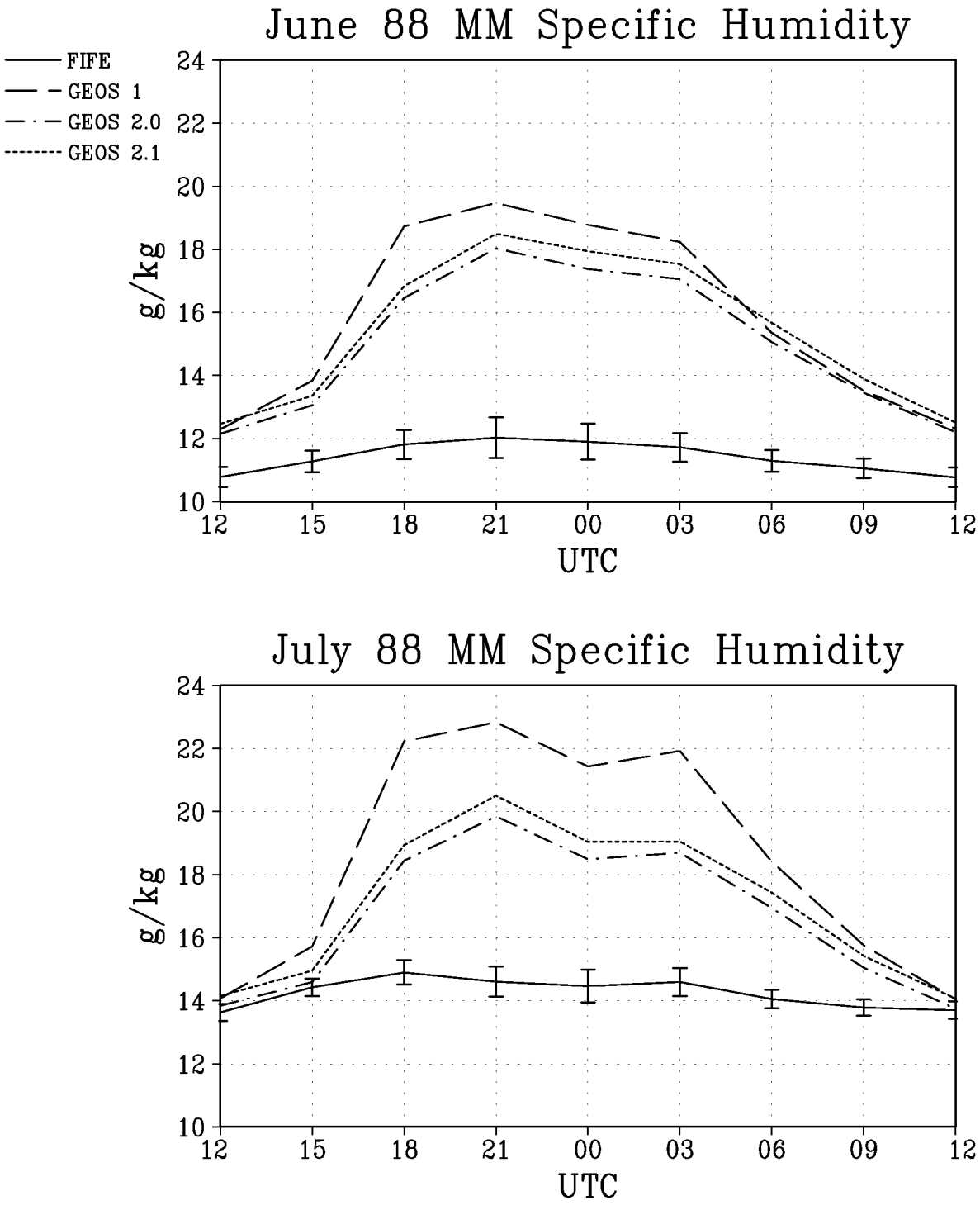

Figure 50: Mean diurnal cycle of two meter specific humidity for (a) June 1988, and (b) July 1988.

2.6 GEOS Grid Point Variability

Betts et al. (1996) and Betts et al. (1998) justify the use of a single point from the reanalysis system because the larger, synoptic scale fields are smoothly varying over GCM grid spaces. Therefore, comparing any one of the nearby grid points with FIFE would lead to the same conclusions. This should be acceptable; however, any horizontal variations of surface properties (eg. soil wetness, roughness or albedo) could cause a mean bias in the results. Here, we examine the variability of the surface and PBL data of GEOS 2.1 during IFC2 for the four grid points nearest the FIFE site.

In the present analysis, the GEOS grid point at 38°N, 97.5°W is compared with FIFE observations. This point was chosen because its surface pressure corresponded more closely to the observed surface pressure than any of the other grid points. Furthermore, the surface type in GEOS is prescribed as grassland which corresponds to the observed FIFE vegetation cover.

Table 3: IFC2 mean data from GEOS 2.1. Horizontal averages and standard deviations are computed for the four grid points closest to the FIFE site. These are then averaged in time, for 21 UTC data only.

Variable		
t2m	301.00 ± 0.77	K
q2m	19.48 ± 1.01	g kg^{-1}
ps	967.02 ± 8.61	mb
preacc	6.23 ± 6.72	mm dy^{-1}
pbl	98.82 ± 15.35	mb
cldfrc	0.490 ± 0.138	
hflux	72.35 ± 27.48	W m^{-2}
eflux	511.99 ± 80.05	W m^{-2}
radlwg	96.43 ± 12.36	W m^{-2}
radswg	678.18 ± 87.94	W m^{-2}
tg	302.71 ± 1.38	K
U	1.87 ± 0.69	m s^{-1}

We have analyzed the surface data at each of the grid points near the FIFE site (many figures not included). In general, the results presented in this report do hold for each grid point and the grid point mean. For example, the diurnal cycles of the ground heat flux, specific humidity and net shortwave radiation all show similar patterns at each grid point. The diurnal maxima and minima have some variability, but not enough to drastically alter

the conclusions. Table 3 presents the IFC2 mean data from GEOS 2.1 at 21 UTC (generally the diurnal maximum for many of the variables). The area average of the four closest grid points and the standard deviation were computed then time averaged for 21 UTC.

The grid point variability seems reasonable considering that this is area averaged over four $2° \times 2.5°$ grid points. The latent heat flux variability seems large, but even the smallest values are still somewhat larger than the observations. Also, one of the gridpoints is prescribed to be forest (38°N, 95°W) while the rest are grassland. Notice that precipitation variability is very large. The mean diurnal cycle of precipitation tends to be similar for each point, but the timing and magnitude on each day may vary.

The grid point variability of the PBL is more difficult to ascertain. Problems arise from the topography and its impact on data at sigma level coordinates. Each grid point will vary in pressure similar to that at the surface. This is demonstrated in Figure 51. The effects of the topography are very apparent within the PBL. Also, at this time, a substantial horizontal temperature gradient exists above (and likely, within) the PBL. While there may be some substantial variation between each grid point at any given time, the general conclusions discussed in this report should be applicable at each nearby grid point. The global generality of these conclusions will be addressed in future studies.

3 Summary and Discussion

First ISLSCP Field Experiment (FIFE) observations have been used to validate the surface properties of various versions of the Goddard Earth Observing System (GEOS) Data Assimilation System. This work follows that of Betts et al. (1996 and 1998) for the NCAR/NCEP and ECMWF reanalysis projects. The primary assumption is that we can learn something of the global system's surface parameterization from comparing point observations with gridpoint data. Two issues must be carefully considered when interpreting the results of this study. First, the GCM grid space area is much larger than the FIFE site area. This could lead to differences in local boundary conditions, such as albedo, surface roughness and soil wetness that lead to differences between the assimilation data and observations. Second, the results may depend on the regional climate and may not apply to other regions of the globe.

Results indicate several potential systematic problems in the surface properties of GEOS. First, the surface layer specific humidity is generally too large, especially during the daytime. This occurs even when the latent heat flux is slightly underestimated (July 1988). The result is a lifted condensation level that is too low compared with observations. While the large latent heating in some cases contributes to the specific humidity bias, the PBL is likely not entraining enough dry free atmosphere. The improper dirunal cycle of specific humidity could influence the diurnal cycle of precipitation (Betts et al. 1996).

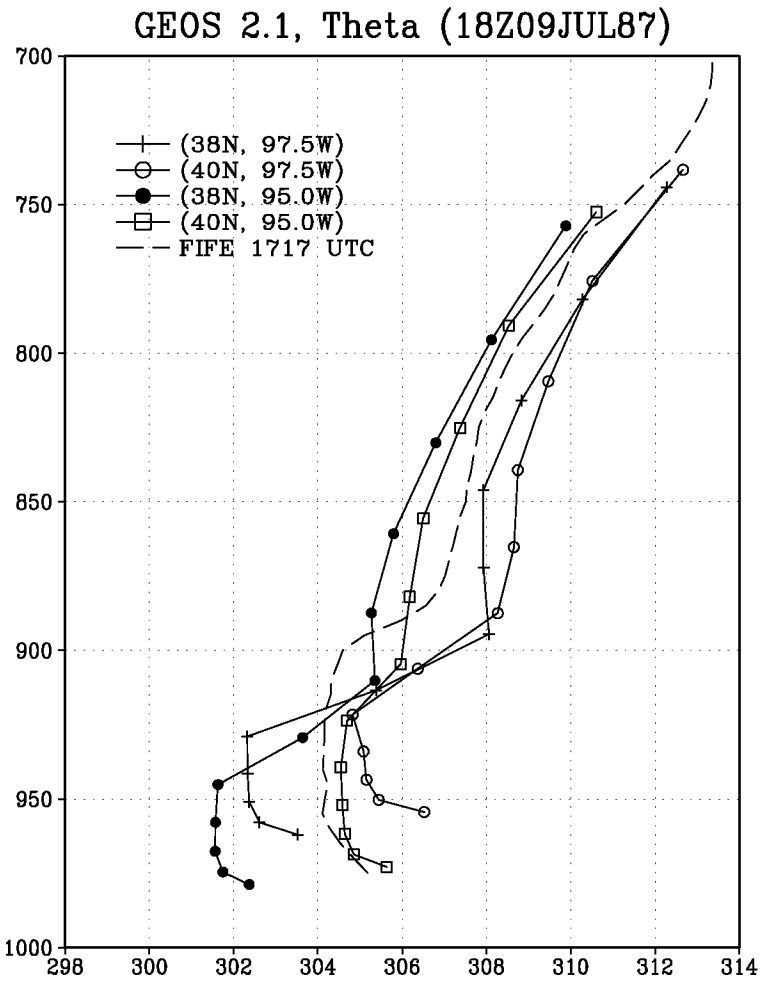

Figure 51: Vertical profiles of potential temperature at each of the closest grid points to the FIFE site.

The analysis of PBL and surface data has identified two factors that affect the development of the assimilated mixed layer. First, the surface sensible heat flux is consistently underestimated between 12 and 15 UTC. The lack of heat from the surface allows the stable surface layer to stay in place longer than observed. Secondly, the observed profiles indicate that the surface layer stability is too strong in the assimilation system or may include an elevated layer that is more stable than observed. The stable layer could be related to the slightly cooler surface temperatures, and too much net upward longwave radiation. As these factors are overcome by the diurnal heating of the surface, the GEOS 2.1 PBL can develop quickly, but too late in the diurnal period to catch up with observations.

The comparison of GEOS data to FIFE IFC2 seems mostly favorable. However, the June and July 1988 comparison demonstrates that soil wetness has substantial control over the surface energy budget. Likewise, this explains the relatively close correlation of each GEOS system (at the surface), but may also imply that the IFC2 comparison is favorable because the GEOS soil wetness happens to be comparable to FIFE.

As discussed previously, Betts et al. (1993, 1996 and 1998) have had considerable success in evaluating NCEP's and ECMWF's reanalyses products with FIFE observations. There appear to be several similarities between their comparisons and the present study.

Betts et al. (1996) compare the FIFE observation with the NCEP/NCAR forty year reanalysis (Kalnay et al. 1996). This reanalysis has a horizontal spectral resolution of T-62 and 28 vertical layers. The surface parameterization includes two interactive soil layers and transpiration (Pan 1990).

For both clear and cloudy conditions, shortwave radiation appears too large in the NCEP / NCAR data. The model clouds were updated every three hours leading to significant problems in the surface energy budget. The GEOS system has had several adjustments to the radiation parameterization, but a similar bias seems to exist. In GEOS, it is related in part to the albedo and in part to the representation of cloud.

Summertime precipitation amounts produced by the NCEP/NCAR reanalysis are larger than observation. Betts et al. (1996) results suggest a feedback between too much evaporation and too low Lifted Condensation Level (LCL) pressure, and the interaction with the PBL development. The GEOS system clearly exhibits too much surface layer specific humidity which reduces the LCL. While several scientific modifications have partially ameliorated the problem, the system still produces too much precipitation in the central United States.

Betts et al. (1996) indicate that the daytime development of the NCEP/NCAR system's convective PBL is within reason. The entrainment at the top of the PBL, however, was too small. The depth of the PBL tended to be lower than observed. This is also noted in the analysis of the GEOS assimilations. Similarly, the NCEP Eta operational model, which also uses a level 2.5 turbulence parameterization, has very limited PBL top entrainment

(Betts et al. 1997).

Betts et al. (1996) point out that by underestimating the entrainment of dry air from above the PBL, near surface specific humidity can be too large. The NCEP / NCAR diurnal cycle of near surface specific humidity, particularly the daytime maximum in summer, is larger than observed in FIFE. The biases were especially strong during June 1987, similar to the GEOS assimilations.

Further analysis of the NCEP assimilation shows that the surface layer vertical temperature gradient tended to be smaller than FIFE, possibly a result of too large roughness length. The near surface (2 meter) temperature data was used to determine the gradient. In GEOS, we find that the early morning near-surface vertical temperature gradients tend to be too stable. However, the winds in GEOS also appear to be too low (close to the surface).

Betts et al. (1993) used 48 hour forecasts from the ECMWF global model (T-106, 19 levels, Cycle 39) to compare with FIFE. These experiments provided a preliminary evaluation of the ECMWF surface and boundary layer parameterizations. Betts et al. (1998) updated the results for the ECMWF global reanalysis (Gibson et al. 1997). The model used T-106 horizontal resolution and 31 vertical layers. The years 1979 - 1993 were assimilated. One important component of the ECMWF reanalyses is that the soil water prognostic equation includes a nudging term, based on the near surface atmospheric specific humidity.

In ECMWF's reanalysis, the diurnal temperature maximum was comparable to observation, but the minimum temperature was too low. This was related to a low bias of incoming long-wave radiation. The low morning temperature corresponded to a strong surface inversion. These factors slowed the development of the convective PBL. The lag of the diurnal cycle of surface temperature in ECMWF was related to the thick soil layer (Betts et al. 1993 and 1997). The GEOS DAS exhibits similar features, except that an unrealistic phase of surface heating compounds the problems.

Similar to both NCEP and GEOS, the development of ECMWF's PBL affects the bias of near-surface specific humidity. The diurnal cycle of ECMWF's specific humidity improved drastically, however, due to the inclusion of nudging in the soil water content. The summertime bias of mixing ratio was only $+0.5$ g kg^{-1}. Without soil water nudging in the GCM simulations, the diurnal cycle of the surface layer specific humidity was too large. Interestingly, ECMWF's June evaporation was too low.

The GEOS comparison to FIFE yields conclusions similar to those for both ECMWF's and NCEP's reanalyses. Some of the underlying processes, however, show subtle differences. The limited representation of the GEOS surface parameterization may degrade the comparison with these observations; however, the PBL turbulence parameterization seems to improve the comparison. Regardless, the results do indicate several areas where improvements in the parameterization are needed.

While the results presented in this report are generally consistent with previous analyses of the GEOS DAS, some effort must be taken to make them more robust. Several possibilities exist that may improve future experiments and analyses of the surface and PBL parameterizations. First, field experiment data from a variety of regions will help to generalize some of these results. This will better help identify model deficiencies. Secondly, future versions of the GEOS DAS will include the Mosaic LSM. This surface parameterization incorporates grid space heterogeneity. This will allow the comparison of the appropriate land type to the observations, as well as provide an estimate of grid box variability.

4 Appendix: FIFE Datasets at DAO

For this report, surface data of Betts and Ball (1998) and PBL data from the FIFE CD-ROM (Strebel et al. 1994) were used. Both data sets have been converted into a binary format for use in Grads because the GEOS data is readily available in that format.

Betts and Ball's data has also been time averaged in order to compare with the GEOS output. In particular, a monthly mean data set is available as well as a 3 hourly mean data set. The standard output of the GEOS DAS surface data is in a 3 hourly backward mean. Therefore, the data at 03 UTC is the average of data from 00 - 03 UTC. For further discussion, see Schubert et al. (1995). Betts and Ball's data files and their Grads equivalent are available at 15 and 45 minutes past the hour (30 minute centered means).

There are two sets of radiation data. The portable area mesonet (PAM) stations recorded net radiation and several component radiation terms, while flux stations recorded all radiation terms in addition to the turbulent heat fluxes. The flux station data is only available during the summers, and the radiation data from the flux station is preferable to the PAM radiation data. There is a bias that exists between the two radiation measurements which can be very large during the daytime (see Smith et al. 1992; Betts and Ball 1998; Bosilovich and Sun 1998).

A typical FIFE surface table file includes:

```
sfcp      Surface Pressure (mb)
ta        Atmospheric Temperature at 2 m (C)
tw        Wet Bulb Temperature at 2 m (C)
prec      Rain Rate (mm/3 hr)
u         East-West Wind Component 5.4 m (m/s)
v         North-South Wind Component 5.4 m (m/s)
tsurf     Radiometric Surface Temp (C)
ts10      10 cm deep soil temperature (C)
ts50      50 cm deep soil temperature (C)
rsdn      Incoming Shortwave Radiation (W/m2)
rsup      Reflected Shortwave Radiation (W/m2)
rnet      Net Radiation (W/m2)
rldn      Incoming IR Radiation (W/m2)
q         Atmospheric Mixing Ratio (g/Kg)
tocl      Total Cloud cover (Eighths) (1987 only)
rnet2     Net Rad. (different from rnet) (W/m2)
LE        Latent Heat Flux (W/m2)
Hs        Sensible Heat Flux (W/m2)
```

```
Hg          Soil Heat Flux (W/m2)
rsdn2       Incoming Shortwave Radiation (W/m2)
rsup2       Reflected Shortwave Radiation (W/m2)
rldn2       Incoming IR Radiation (W/m2)
rlup2       Reflected IR Radiation (W/m2)
```

Note that all the variables up to the total cloud cover (tocl) are from surface PAM stations, and are generally available for the whole period. The rest are flux station observations which were generally taken only during summer periods and IFCs. Also, Betts and Ball's flux station data in 1988 report the reflected shortwave radiation (rsup2) as a negative number, but positive in other years. This has been corrected in the Grads files.

The Grads PBL data files are defined between 1000 mb and 505 mb at 5 mb intervals. The data has been separated into one file for each day, because of the irregular time intervals of balloon launches.

Use the PBL data with caution. The time intervals that Grads will default to are likely not correct. This is due to the irregular launch time of the soundings. A time variable is included in the Grads data file. Check this variable for each profile used. Also, the wind variables tended to show some very unrealistically large values. In some of the profile, these were marked as undefined. All PBL data files, however, were not screened.

PBL data files include the following variables:

```
time        Decimal time (UTC) (Check this for each profile)
pres        Atmospheric Pressure (mb)
hgt         Balloon Height AGL (m)
ta          Atmospheric Temperature (C)
tw          Atmospheric Wet Bulb Temperature (C)
q           Atmospheric Mixing Ratio (g/Kg)
theta       Atmospheric Potential Temperature (K)
uwind       East-West Wind (m/s)
vwind       North-South Wind (m/s)
```

The raw FIFE data can be acquired through the Oak Ridge National Laboratory data archive, or from FIFE CD-ROM (Strebel et al. 1994). See Betts and Ball (1994) for information on the processing of the FIFE site-averaged data.

5 References

Allen, D.J., K. E. Pickering and A. Molod, 1997. An Evaluation of deep convective mixing in the Goddard Chemical Transport Model using International Satellite Cloud Climatology Project cloud parameters.*J. Geophys. Res.*, **102**, No. D21, 25467-25476.

Betts, A. K., and A. C. M. Beljaars, 1993: Estimation of effective roughness length for heat and momentum from FIFE data. *Atmos. Res.*, **30**, 251 - 261.

Betts, A., and J. H. Ball, 1998: FIFE surface climate and site-averaged dataset 1987 - 1989. *J. Atmos. Sci.*, **55**, 1091-1108.

Betts, A., J. H. Ball, and A. C. M. Beljaars, 1993: Comparison between the land surface response of the ECMWF model and the FIFE-1987 data. *Q. J. R. Meteorol. Soc.*, **119**, 975 - 1001.

Betts, A., S.-Y. Hong, and H.-L. Pan, 1996: Comparison of the NCAR-NCEP reanalysis with 1987 FIFE Data. *Mon. Wea. Rev.*, **124**, 1480 - 1498.

Betts, A., F. Chen, K. E. Mitchell, and Z. I. Janić, 1997: Assessment of the land surface and boundary layer models in two operational versions of the NCEP Eta model using FIFE data. *Mon. Wea. Rev.*, **125**, 2896 - 2916.

Betts, A., P. Viterbo, and A. C. M. Beljaars, 1998: Comparison of the land-surface interaction in the ECMWF reanalyses model with the 1987 FIFE data. *Mon. Wea. Rev.*, **126**, 186 - 198.

Blackadar, A.K.,1977: High Resolution Models of the Planetary Boundary Layer. *Advances in Environmental Science and Engineering, Vol 1* Editors Pfafflin and Zeigler, Gordon and Breach, Scientific Publishers.

Bloom, S.C., L.L. Takacs, A. M. da Silva, and D. Ledvina, 1991: Data assimilation using incremental analysis updates. *Mon. Wea. Rev.*, **124**, 1256-1271.

Bosilovich, M. G., and W.-Y. Sun, 1998: Monthly simulation of surface layer fluxes and soil properties during FIFE. *J. Atmos. Sci.*, **55**, 1170-1184.

Cohn, S. E., A. da Silva, J. Guo, M. Sienkiewicz and D. Lamich, 1998: Assessing the effects of data selection with the DAO Physical-space statistical analysis system. *Mon. Wea. Rev.*, **In Press.**

DAO 1996: Algorithm Theoretical Basis Document. Online: http://dao.gsfc.nasa.gov, NASA GSFC, Greenbelt MD.

Dorman, J. L., and P. J. Sellers, 1989: A global climatology of albedo, roughness length and stomatal resistance for atmospheric general circulation models as represented by the Simple Biosphere model (SiB). *J. Appl. Meteor.*, **28**, 833-855.

Gibson, J. K., P. Kallberg, S. Uppala, A. Hernandez, A. Nomura, and E. Serrano, 1997: ERA Description. ECMWF Re-Analyses Project Rep. Series 1, ECMWF Reading, United Kingdom, 72 pp.

Helfand, H. M., and J. C. Labraga, 1988: Design of a non-singular level 2.5 second-order closure model for the prediction of atmospheric turbulence. *J. Atmos. Sci.*, **45**, 113-132.

Helfand, H. M., and S. Schubert, 1995: Climatology of the simulated Great Plains low-level jet and its contribution to the continental moisture budget of the United States. *J. Climate*, **8**, 784-806.

Higgins, R. W., J. E. Janowiak and Y. Yao, 1996: A gridded hourly precipitation data base for the United States (1963 - 1993). NCEP/Climate Predictions Center ATLAS No. 1, 47 pp. [Available from NCEP/Climate Predictions Center, W/NP52, Washington, DC 20233.]

Kalnay, E. and Coauthors, 1996: The NCEP/NCAR 40-year reanalysis project. *Bull. Amer. Meteor. Soc.*, **72**, 437-472.

Koster, R. D., and M. J. Suarez, 1996: Energy and water balance calculations in the Mosaic LSM. NASA Tech. Memorandum 104606-Volume 9, NASA, Goddard Space Flight Center, Greenbelt, MD.

Molod, A., H. M. Helfand and L. Takacs, 1996. The Climatology of Parameterized Physical Processes in the GEOS-1 GCM and Their Impact on the GEOS-1 Data Assimilation System. *J. Climate*, **9**, No. 4, 764-785.

Pan, H.-L., 1990: A simple parameterization of evapotranspiration over land for the NMC medium range forecast model. *Mon. Wea. Rev.*, **118**, 2500 - 2512.

Pickering, K., A. M. Thompson, W. -K. Tao, R. B. Rood, D. P. McNamara, and A. Molod, 1995. Vertical Transport by Convective Clouds: Comparisons of Three Modeling Approaches. *GRL*, **22**, No. 9, 1089-1092.

Schemm, J., S. Schubert, J. Terry, and S. Bloom, 1992: Estimation of monthly mean soil moisture for 1979 - 1989. NASA Tech. Memo. No. 104571, Goddard Space Flight Center, Greenbelt, MD 20771.

Schubert, S. D., J. Pfaendtner, and R. Rood, 1993: An assimilated data set for Earth

Science applications. *Bull. Amer. Meteor. Soc.*, **74**, 2331 - 2342.

Pfaendtner, J. S. Bloom, D. Lamich, M. Seablom, M. Sienkiewicz, J. Stobie, and A. da Silva, 1995: Documentation of the Goddard Earth Observing System (GEOS) Data Assimilation System - Version 1. NASA Tech. Memo. No. 104606, Goddard Space Flight Center, Greenbelt, MD 20771.

Sellers, P. J., F. G. Hall, G. Asrar, D. E. Strebel, and R. E. Murphy, 1988: The First ISLSCP Field Experiment. *Bull. Amer. Meteor. Soc.*, **69**, 22 - 27.

Sellers, P. J., F. G. Hall, G. Asrar, D. E. Strebel, and R. E. Murphy, 1992: An overview of the First International Satellite Land Surface Climatology Project (ISLSCP) Field Experiment (FIFE). *J. Geophys. Rev.*, **97(D17)**, 18345 - 18371.

Smith, E. A., W. Crosson, and B. Tanner, 1992: Estimation of surface heat and moisture fluxes over a prairie grassland. 1: In situ energy budget measurements incorporating a cooled mirror dew point hygrometer. *J. Geophys.Res.*, **97(D17)**, 18577 - 18582.

Smith, E. A., M.-K. Wai, H. J. Cooper, M. T. Rubes and A. Hsu, 1994: Linking Boundary layer circulations and surface processes during FIFE 89. Part I: Observational analysis. *J. Atmos. Sci.*, **51**, 1497-1529.

Strebel, D. E., D. R. Landis, K. F. Hummerich, and B. W. Meeson, 1994: Collected data of the First ISLSCP Field Experiment. Vol. 1, *Surface observations and non-image data sets.* NASA Goddard Space Flight Center, Greenbelt, MD, CD-ROM.

Suarez, M. J., and L. L. Takacs, 1995: Documentation of the Aries/GEOS Dynamical Core Version 2, NASA Tech. Memorandum 104606-Volume 2, NASA, Goddard Space Flight Center, Greenbelt, MD.

Takacs, L. L., A. Molod, and T. Wang, 1994: Documentation of the Goddard Earth Observing System (GEOS) General Circulation Model - Version 1. NASA Tech. Memorandum 104606-Volume 1, NASA, Goddard Space Flight Center, Greenbelt, MD.

REPORT DOCUMENTATION PAGE

Form Approved
OMB No. 0704-0188

1. AGENCY USE ONLY *(Leave blank)*	2. REPORT DATE	3. REPORT TYPE AND DATES COVERED
	August 1998	Technical Memorandum

4. TITLE AND SUBTITLE
Technical Report Series on Global Modeling and Data Assimilation
Volume 14—A Comparison of GEOS Assimilated Data with FIFE Observations

5. FUNDING NUMBERS
Code 910.3/913

6. AUTHOR(S)
Michael G. Bosilovich and Siegfried D. Schubert
Max J. Suarez, Series Editor

7. PERFORMING ORGANIZATION NAME(S) AND ADDRESS (ES)
Data Assimilation Office
Climate and Radiation Branch
Goddard Space Flight Center
Greenbelt, Maryland

8. PEFORMING ORGANIZATION REPORT NUMBER
98B00068

9. SPONSORING / MONITORING AGENCY NAME(S) AND ADDRESS (ES)
National Aeronautics and Space Administration
Washington, DC 20546-0001

10. SPONSORING / MONITORING AGENCY REPORT NUMBER
TM–1998–104606, Vol. 14

11. SUPPLEMENTARY NOTES
Michael G. Bosilovich: Universities Space Research Association, Greenbelt, Maryland

12a. DISTRIBUTION / AVAILABILITY STATEMENT
Unclassified–Unlimited
Subject Category: 46
Report available from the NASA Center for AeroSpace Information,
7121 Standard Drive, Hanover, MD 21076-1320; (301) 621-0390.

12b. DISTRIBUTION CODE

13. ABSTRACT *(Maximum 200 words)*

First ISLSCP Field Experiment (FIFE) observations have been used to validate the near-surface properties of various versions of the Goddard Earth Observing System (GEOS) Data Assimilation System. The site-averaged FIFE data set extends from May 1987 through November 1989, allowing the investigation of several time scales, including the annual cycle, daily means and diurnal cycles. Furthermore, the development of the daytime convective planetary boundary layer is presented for several days. Monthly variations of the surface energy budget during the summer of 1988 demonstrate the affect of the prescribed surface soil wetness boundary conditions. GEOS data comes from the first frozen version of the assimilation system (GEOS-1 DAS) and two experimental versions of GEOS (v. 2.0 and 2.1) with substantially greater vertical resolution and other changes that influence the boundary layer.

This report provides a baseline for future versions of the GEOS data assimilation system that will incorporate a state-of-the-art land surface parameterization. Several suggestions are proposed to improve the generality of future comparisons. These include the use of more diverse field experiment observations and an estimate of gridpoint heterogeneity from the new land surface parameterization.

14. SUBJECT TERMS
data assimilation, GCM, FIFE, planetary boundary layer, land surface

15. NUMBER OF PAGES
80

16. PRICE CODE

17. SECURITY CLASSIFICATION OF REPORT	18. SECURITY CLASSIFICATION OF THIS PAGE	19. SECURITY CLASSIFICATION OF ABSTRACT	20. LIMITATION OF ABSTRACT
Unclassified	Unclassified	Unclassified	UL